PHASE TRANSITIONS IN INDUCED LATTICE GAUGE MODELS

by

MERVLYN MOODLEY

Submitted in partial fulfilment of the
requirements for the degree of
Master of Science
in the

Department of Physics,
University of Natal

Pietermaritzburg
1995

To my parents and to the memory of my dear aunt, Mrs. K. Govender.

Abstract

The present research is based on the study of the phase strncture of lattice models incorporating selfinteracting scalars and gauge background fields otherwise known as induced gauge models. Emphasis is placed on the effect the choice of the integration measure over the radial modes of the scalar fields have on the phase structure of these models. Both numerical simulations and analytical results based on the mean field approximations are presented.

In Chapter 1 an introduction to quantum field theory is given leading to the formulation of Euclidean quantum field theory.

In Chapter 2 global and local gauge invariance together with the mechanism of spontaneous symmetry breaking are discussed.

In Chapter 3 the formulation of quantum field theory on the lattice is introduced. The lattice regularization entails discretizing space and time and presents an elegant approach to studying certain phenomena of the continuum theory which are beyond the reach of standard perturbative analysis.

In Chapter 4 the Monte Carlo methods for evaluating the Euclidean Feynman path integral as applied to lattice gauge theory are discussed.

In Chapter 5 numerical studies of some lattice gauge models are presented. Both pure lattice gauge models and gauge-Higgs models are examined.

In Chapter 6 the Kazakov-Migdal model which presents an interesting approach to inducing QCD is discussed.

In Chapter 7 the mixed fundamental-adjoint induced model is introduced. This model succeeds in breaking the local Z_N symmetry of the Kazakov-Migdal model by adding to it scalar fields in the fundamental representation of the gauge group. The effect of the choice of the radial integration measure on the phase structure of a class

of Abelian induced models is studied.

Preface

The research on which this dissertation was based was carried out in the Department of Physics, University of Natal, Pietermaritzburg, from January 1993 to November 1995, under the supervision of Dr. Assen Ilchev.

These studies represent original work by the author and have not otherwise been submitted in any other form for any degree or diploma to any university. Where use has been made of the work of others it is duly acknowledged in the text.

Acknowledgements

I wish to express my gratitude to my supervisor, Dr. Assen Ilchev, for his expert guidance and also for inciting within me the same passion that he possesses for the subject. The interesting discussions with him were nothing less than inspirational. I will also like to thank my family for their continued support and encouragement especially my brother, Luwen, for assisting in the last minute preperations of the numerous diagrams. Last but not least I am deeply indebted to Sri Sai Baba for his spiritual guidance.

List of Contents

Chapter 1

Quantum Field Theory

1.1 Lagrangian Classical Mechanics

According to the Lagrangian formulation of classical mechanics the dynamics of a system with finite number of degrees of freedom is governed by the principle of least action.

Consider a system of n particles. The positions of all n particles are specified by a single point in an abstract $3n$-dimensional space known as the *configuration space*: a particular configuration of the system corresponds to a point $p(q_1, \ldots, q_{3n})$ in configuration space where q_i are called the (*generalised*) coordinates. To fully describe the mechanical state of the system one needs to specify alongside the (generalised) coordinates, the (generalised) velocities: $v_i = \dot{q}_i = \frac{dq_i}{dt}$. The $6n$ parameters, that is, the $3n$ (generalised) coordinates and the $3n$ (generalised) velocities, specify the mechanical state of the system. They can be considered as the coordinates of a point in an abstract $6n$-dimensional space known as the *phase space* of the system.

When the mechanical state of the system changes with time the point in the corresponding phase space, which describes the state of the system, will move along a

continuous curve. Each two accessible points A and B in the phase space of a mechanical system can be connected by different continuous curves which correspond to different *paths* or *histories* the system can follow in its evolution from state A to state B. In classical mechanics it is postulated that, given all interactions affecting a particular mechanical system, there is only one path it can follow between A and B. This is called the *classical trajectory* and is found as the solution of the equations of motion. The main problem of classical mechanics is to find this unique path in phase space along which the state of the system evolves under given conditions. The Lagrangian approach to solving this problem consists of defining a functional called the *action* which is a map of all continuous curves in phase space onto the field of (real)numbers. The central hypothesis of the Lagrangian formalism is the *Hamiltonian* or *least action principle* which states that the actual path in phase space which describes the evolution of the state of the system is the one for which the mentioned functional is a minimum. This reduces the main problem in classical mechanics to a problem from variational calculus. From a first glance this may seem as an unbridgeable difference in the approach from the one followed by Newton where the same problem was solved by means of differential equations. In fact this difference is not as big as it seems because a variational problem usually leads to a system of simultaneous differential equations known as the *Euler-Lagrange equations*.

The Lagrangian of the system,

$$L = L(q_i(t), \dot{q}_i(t)), \tag{1.1}$$

depends on the coordinates $q_i(t)$ and velocities $\dot{q}_1(t)$. The action functional S is defined as the time integral over the Lagrangian:

$$S([q_i(t)], t_1, t_2) = \int_{t_1}^{t_2} L(q_i, \dot{q}_i)\, dt, \tag{1.2}$$

were $[q_i(t)]$ denotes a functional relation with S. This means that for a given path parameterized by $q(t)$ and for $t_1 < t < t_2$ there corresponds a number S - the value

functional. When the action is so expressed it is convenient to write the Lagrangian as the difference between the kinetic energy and potential energy of the system:

$$L(q_i, \dot{q}_i) = T - V. \tag{1.3}$$

The minimum of the action corresponds to a stationary 'point' for which the variation of the action is zero:

$$\delta S = \delta \int_{t_1}^{t_2} L(q_i(t), \dot{q}_i(t))\, dt = 0. \tag{1.4}$$

The minimum action or stationary path is obtained by using the calculus of variation. Suppose the path is varied from $\bar{q}(t)$ by $\delta q(t)$ where $\delta q(t)$ is arbitrary for $t \neq t_1$ or t_2. The endpoints of $\bar{q}(t)$ are assumed to be fixed:

$$\delta q(t_1) = \delta q(t_2) = 0. \tag{1.5}$$

For $\bar{q}(t)$ to be an extremum of S the condition is

$$\delta S = S[\bar{q}(t) + \delta q(t)] - S[\bar{q}(t)] = 0 \tag{1.6}$$

to first order in $\delta q(t)$. Also, the variation in the Lagrangian is given as

$$\begin{aligned} \delta L &= L(q + \delta q, \dot{q} + \delta \dot{q}) \\ &= \delta q \frac{\delta L}{\delta q} + \delta \dot{q} \frac{\delta L}{\delta q}. \end{aligned} \tag{1.7}$$

Therefore from the definition in Eq. (1.2),

$$\begin{aligned} \delta S &= \int_{t_1}^{t_2} (\delta q \frac{\delta L}{\delta q} + \delta \dot{q} \frac{\delta L}{\delta \dot{q}})\, dt \\ &= \int_{t_1}^{t_2} \delta q \frac{\delta L}{\delta q}\, dt + \int_{t_1}^{t_2} \frac{\delta L}{\delta \dot{q}} \frac{d}{dt} \delta q\, dt \\ &= \int_{t_1}^{t_2} \delta q \frac{\delta L}{\delta q}\, dt + \delta q \frac{\delta L}{\delta \dot{q}} \Big|_{t_1}^{t_2} - \int_{t_1}^{t_2} \delta q \frac{d}{dt} \frac{\delta L}{\delta \dot{q}}\, dt \\ &= \int_{t_1}^{t_2} \delta q [\frac{\delta L}{\delta q} - \frac{d}{dt} (\frac{\delta L}{\delta \dot{q}})]\, dt, \end{aligned} \tag{1.8}$$

were $\delta q(t)$ vanishes at the endpoints t_1 and t_2. The function $q(t)$ which extremises the action is therefore a solution of the differential equation,

$$\frac{\delta L}{\delta q} - \frac{d}{dt}(\frac{\delta L}{\delta \dot{q}}) = 0, \tag{1.9}$$

which is referred to as the *Euler-Lagrange* equation.

If the generalised momentum p_i of the system is written as

$$p_i = \frac{\delta L}{\delta \dot{q}_i} \tag{1.10}$$

then the Hamiltonian of the system can be given as

$$H(q_i, p_i) = p_i \dot{q}_i - L(q_i, \dot{q}_i). \tag{1.11}$$

This is obtained by the Legendré transformation and conventions for the Einstein summation over repeated indices is understood. Now by differentiating seperately the two terms in the left hand side of Eq. (1.11) one obtains,

$$d(p_i \dot{q}_i(p,q)) = \dot{q}_i dp_i + \frac{\delta \dot{q}_j}{\delta p_i} p_j dp_i + \frac{\delta \dot{q}_j}{\delta q_j} p_j dq_i \tag{1.12}$$

and

$$dL(q_i, \dot{q}_i(p,q)) = \frac{\delta L}{\delta q_i} dq_i + \frac{\delta \dot{q}_i}{\delta p_i}\frac{\delta L}{\delta \dot{q}_j} dp_i + \frac{\delta \dot{q}_j}{\delta q_i}\frac{\delta L}{\delta \dot{q}_j} dq_i. \tag{1.13}$$

Combining Eqs. (1.12) and (1.13) and collecting terms it can be shown that

$$dH = [\dot{q}_i + \frac{\delta \dot{q}_j}{\delta p_j}(p_j - \frac{\delta L}{\delta \dot{q}_j})]dp_i + [-\frac{\delta L}{\delta q_i} - \frac{\delta \dot{q}_j}{\delta q_i}(\frac{\delta L}{\delta \dot{q}_j} - p_j)]dq_i \tag{1.14}$$

Substituting p_i from Eq. (1.10) in Eq. (1.14), the differential of the Hamiltonian has the final form,

$$dH = \dot{q}_i dp_i + \dot{p}_i dq_i. \tag{1.15}$$

Also,

$$dH = \frac{\delta H}{\delta p_i} dp_i + \frac{\delta H}{\delta q_i} dq_i \tag{1.16}$$

by differentiating with respect to q_i and p_i. By combining Eqs. (1.15) and (1.16) the Hamilton's form of the equations of motion is obtained:

$$\frac{\delta H}{\delta p_i} = \dot{q}_i \quad \text{and} \quad \frac{\delta H}{\delta p_i} = \dot{p}_i. \tag{1.17}$$

The above Hamilton's equations can also, in fact more elegently, be derived via the use of the principle of least action and variational calculus. This is done by first rewritting Eq.(1.11) in the form,

$$L(q_i, \dot{q}_j) = p_i \dot{q}_i(q_i, p_i) - H(q_i, p_i). \tag{1.18}$$

The action now becomes a functional of $2n$ independent functions, $q(t)$ and $p(t)$:

$$S([q_i, p_i], t_1, t_2) = \int_{t_1}^{t_2} (p_i \dot{q}_i - H(q_i, p_i))\, dt. \tag{1.19}$$

Now considering the independent variations in $\dot{q}_i$ and p_i the change in the action is calculated as follows:

$$\begin{aligned} \delta S &= \delta \int_{t_1}^{t_2} (p_i \dot{q}_i - H(q_i, p_i)\, dt \\ &= \int_{t_1}^{t_2} (\dot{q}_i \delta p_i + p_i \frac{d}{dt} \delta q_i)\, dt - \int_{t_1}^{t_2} (\frac{\delta H}{\delta p_i} \delta p_i + \frac{\delta H}{\delta q_i} \delta q_i)\, dt, \end{aligned} \tag{1.20}$$

and by collecting terms it can be shown that

$$\delta S = \int_{t_1}^{t_2} [(\dot{q}_i - \frac{\delta H}{\delta p_j}) \delta p_i - (\dot{p}_i + \frac{\delta H}{\delta q_i}) \delta q_i]\, dt. \tag{1.21}$$

By demanding that the action be stationary, that is by setting $\delta S = 0$, Eq. (1.17) is obtained from Eq. (1.21). This shows the equivalence of Lagrange's and Hamilton's equation.

1.2 Lagrangian Field Theory

Extending to field theory which describes a system with continuously distributed degrees of freedom, the field at each point in space is regarded as an independent

generalised coordinate. The field, $\phi_i = \phi_i(x,t)$, for $i = 1,2,\ldots,N$ is a function defined for each point in space-time.

For a field theory the analogue of the configuration space is an infinitely dimensional functional space. This is the fundamental difference between a discrete dimensional system and a field theory. The Lagrangian, which for a system of n particles is a function of time defined through the generalised coordinates and velocities, is replaced in a field theory by a Lagrangian density function. The Lagrangian density is a function of the field ϕ_i and its spatial and temporal derivatives $\partial_\mu \phi_i = \frac{\partial \phi_i}{\partial x_\mu}$:

$$\mathcal{L} = \mathcal{L}(\phi_i, \partial_\mu \phi_i). \tag{1.22}$$

In analogy with the Lagrangian formulation of classical mechanics in the previous section, the action for a field is written as,

$$S([\phi_i], \tau_1, \tau_2) = \int_{\tau_1}^{\tau_2} \mathcal{L}(\phi_i, \partial_\mu \phi_i)\, d^4x, \tag{1.23}$$

where d^4x is the four dimensional measure in Euclidean space and, τ_1 and τ_2 are the boundaries of integration that covers the physically relevant 3-dimensional Euclidean space. Now, for infinitesmal variation from ϕ_i to $\phi_i + \delta\phi_i$, the variation in the action is given by

$$\begin{aligned} \delta S &= \int_{\tau_1}^{\tau_2} d^4x \left(\frac{\partial L}{\partial \phi_i}\delta\phi_i + \frac{\partial L}{\partial(\partial_\mu \phi_i)}\delta(\partial_\mu \phi_i)\right) \\ &= \int_{\tau_1}^{\tau_2} d^4x \left(\frac{\partial L}{\partial \phi_i} - \partial_\mu \frac{\partial L}{\partial(\partial_\mu \phi_i)}\right)\delta\phi_i + \int_{\tau_1}^{\tau_2} d^4x \partial_\mu \left(\frac{\partial L}{\partial(\partial_\mu \phi_i)}\delta\phi_i\right), \end{aligned} \tag{1.24}$$

by using the definition $\delta(\partial_\mu \phi_i) = \partial_\mu \delta\phi_i$ and integrating by parts. The last term in Eq. (1.24) can be converted to a surface integral

$$\oint_\rho d\rho_\mu \frac{\partial L}{\partial(\partial \phi_i)}\delta\phi_i \tag{1.25}$$

by using Gauss's divergence theorem in four dimensions. Here ρ is the surface at the boundary and $d\rho_i$ the surface element. Usually it is required that $\delta\phi_i$ vanish on ρ.

So, by this requirement, the surface integral vanishes and the variation in the action is given by

$$\delta S = \int_{r_1}^{r_2} d^4x (\frac{\partial L}{\partial \phi_i} - \partial_\mu \frac{\partial L}{\partial(\partial_\mu \phi_i)}) \delta\phi_i. \tag{1.26}$$

For ϕ_i to extremise the action the sufficient condition, as before, is $\delta S = 0$. From this the Euler-Lagrange equations of motion for a field is obtained,

$$\frac{\partial L}{\partial \phi_i} - \partial_\mu \frac{\partial L}{\partial(\partial_\mu \phi_i)} = 0. \tag{1.27}$$

The similarity with Newton's technique of generating linear differential equations to describe the motion of particles becomes evident in field theory when the Lagrangian density is chosen to be of a quadratic form in the fields. This is so since a quadratic Lagrangian gives rise to a quadratic action which in turn, under the Lagrangian formalism, leads to a set of linear partial differential equations. Linear differential equations are important in field theory since they have the valuable property of allowing linear combinations of solutions to be solutions themselves(the *superposition principle*). This allows for the solution of the equations of motion by means of the Green function's method. It is for this reason that the quadratic Lagrangian densities are the most widely used choice for field theory.

1.2.1 The Scalar Field

The simplist of all fields is the scalar field $\phi(x)$ which describes particles with spin zero. The most general form of a quadratic Lagrangian density that contains a single real scalar field $\phi(x)$ is given by

$$\mathcal{L} = \frac{1}{2}[\partial_\mu \phi(x) \partial^\mu \phi(x) - m^2 \phi^2(x)] \tag{1.28}$$

where m is some constant with the dimensions of mass. Substituting this Lagrangian density in Eq. (1.27), it can be shown that

$$\frac{\partial \mathcal{L}}{\partial \phi} - \partial_\mu \frac{\partial \mathcal{L}}{\partial(\partial_\mu \phi)} = -(\partial_\mu \partial^\mu + m^2)\phi. \tag{1.29}$$

This gives the Euler-Lagrange equation for a scalar field in the form

$$(\Box - m^2)\phi = 0 \tag{1.30}$$

where $\Box = -\partial_\mu \partial^\mu$ is the d'Alembert operator. Eq. (1.30) is the *Klein-Gordon* equation. Solutions of this equation are given by a complete set of plane waves $\phi(x) = \phi^+(x) + \phi^-(x)$ where $\phi^+(x) = e^{ip\cdot x}$ and $\phi^-(x) = e^{-ip\cdot x}$. The general solution of the Klein-Gordon equation is therefore given by

$$\phi(x) = \int \frac{d^3p}{(2\pi)^2}\frac{1}{2p_\circ}\{a(p)e^{-ip\cdot x} + a^\dagger(p)e^{ip\cdot x}\} \tag{1.31}$$

where the four-vector p satisfies $p^2 = m^2$ and $p_\bullet = \sqrt{\boldsymbol{p}^2 + m^2}$. $a(p)$ and $a^\dagger(p)$ are respectively the annihilation and creation operators of particles with momentum p and rest-mass m.

For a complex scalar field the Lagrangian density is given by

$$\mathcal{L} = \frac{1}{2}[\partial_\mu \phi^*(x)\partial^\mu \phi(x) - m^2\phi^*(x)\phi(x)]. \tag{1.32}$$

The solution of the Klein-Gordon equation for a complex scalar field is analogous to Eq. (1.31) and contains operators $a^\dagger$, a, $b^\dagger$ and b. The $a^\dagger$ and a create and annihilate particles whereas the $b^\dagger$ and b create and annihilate antiparticles.

1.3 From Minkowski to Euclidean Field Theory

1.3.1 Minkowski Field Theory

In the Minkowski description of quantum field theory a system of coordinates is specified on a four-dimensional Minkowski manifold, $\mathcal{M}_4$. The Lorentz invariant product of two vectors x^μ and y^μ is defined as

$$x^\mu y_\mu = x_0 y_0 - \boldsymbol{x}\cdot\boldsymbol{y} \tag{1.33}$$

and the invariant interval as

$$ds^2 = dx^\mu dx_\mu. \tag{1.34}$$

Of specific interest in quantum field theory is the state of lowest energy or the ground state. This state is known as the vacuum $\mid \Omega >$ and it has a unique feature in that it is left invariant under unitary transformation of the Poincaré group,

$$U_p \mid \Omega >= \mid \Omega >. \tag{1.35}$$

where the unitary representation of the Poincaré group is usually written as

$$U_p = e^{i\mathbf{p}\cdot\mathbf{x}}. \tag{1.36}$$

A consequence of this invariance is the formal translational property of the field operator $\phi(x)$:

$$\phi(x) = e^{i\mathbf{p}\cdot\mathbf{x}}\phi(0)e^{-i\mathbf{p}\cdot\mathbf{x}} \tag{1.37}$$

The vacuum state $\mid \Omega >$ is essential in the fundamental concept of this theory since it leads to the construction of the vacuum expectation values of the Minkowski fields $\Phi_\mu(x_\mu)$. The importance of the vacuum expectation values becomes evident when taking into consideration the fact that they admit analytic continuation to imaginary time , unlike the Minkowski fields themselves.

In the Garding-Wightman axiomization [73], vacuum expectation values are taken of the products of field operators at different space-time points:

$$\mathcal{W}_n = < \Omega \mid \phi_1(x_1)\phi_2(x_2)\ldots\phi_n(x_n) \mid \Omega > . \tag{1.38}$$

These vacuum expectation values defined in Minkowski space are known as the *Wightman functions* [75]. Their properties give a complete description of the quantum field theory under consideration. By far the most important property of $\mathcal{W}_n$ is that it can be used to reconstruct the state of the system as well as the field operators. This is done by applying the *Wightman reconstruction* theorem. Since the vacuum state is

required to be translationally invariant by the uniqueness of the vacuum, $\mathcal{W}_n$ can be considered as just a function of the coordinate differences:

$$\mathcal{W}_n = \mathcal{W}_n(x_1 - x_2, x_2 - x_3, \ldots, x_{n-1} - x_n). \tag{1.39}$$

The idea behind Eq. (1.39) is given by the expression

$$\mathcal{W}_n = < \Omega \mid \phi(0) e^{i\mathbf{p}\cdot(x_2 - x_1)} \phi(0) \ldots e^{i\mathbf{p}\cdot(x_n - x_{n-1})} \phi(0) \mid \Omega > \tag{1.40}$$

which is obtained by substituting Eq. (1.37) in Eq. (1.38).

1.3.2 Euclidean Field Theory

Extending the Minkowski fields to incoorporate a complex four-vector:

$$x_j \rightarrow z_j = Re z_j + i Im z_j \quad j = 1, 2, \ldots n-1, \tag{1.41}$$

the coordinate differences are written as

$$z_j - z_{j+1} = x_j - x_{j+1} - i\kappa_j. \tag{1.42}$$

The Wightman function can therefore be given by

$$\mathcal{W}_n(x_1 - x_2, x_2 - x_3, \ldots, x_{n-1} - x_n) = \lim_{\kappa_1 \ldots \kappa_n \rightarrow 0} W_n(z_1, z_2, \ldots, z_n) \tag{1.43}$$

where W_n is the analytic continuation of $\mathcal{W}_n$ to the complex space of points z^μ. In the special case when $x^0 \rightarrow z^0 = ix^0$ and $x_i \rightarrow z^i = x^i$ for $i = 1, 2$ and 3 the metric of the complex space is Euclidean. The points $(z_1, z_2, \ldots, z_n)$ belong to a Euclidean space if each z_j has purely imaginary temporal components and real spatial components. They are parameterized such that $z_j = (ix_4, x)_j$ with the real variables $(x_j)_\mu$ written as a four-dimensional Euclidean vector $x_j(x, x_4)_j$. Furthermore, they possess an additional property whereby the coordinate difference $x_i - x_j$ is non-zero for all $i \neq j$. As such, the points $(z_1, z_2, \ldots, z_n)$ are called *non-coincident* points and are contained in a space-like region defined by

$$(x_i - x_j)^2 < 0, \qquad \text{for all } i \text{ and } j \tag{1.44}$$

called the *non-coincident Euclidean* region. It can be shown that that $\mathcal{W}_n$ is the boundary value of the function W_n, the latter being a function of only the differences of the non-coincident points $z_1 - z_2, \ldots, z_{n-1} - z_n$.

The Wightman functions in Euclidean space-time can be written as

$$S_n(x_1, x_2, \ldots, x_n) = W_n(z_1, z_2, \ldots, z_n) \tag{1.45}$$

which is the restriction of the analytic function W_n to a set of non-coincident Euclidean points. These are known as the *Schwinger functions* or the *Euclidean Green functions* and are given by the expectation value

$$S_n(x_1, x_2, \ldots, x_n) = < \Omega \mid \Phi_1(x_1), \Phi_2(x_2), \ldots, \Phi_n(x_n) \mid \Omega > \tag{1.46}$$

where $\Phi_i(x_i)$ are the Euclidian counterparts of the Minkowski fields. The Schwinger functions and the Wightman functions are just different branches of the same analytical function. The properties of the S_n are layed out in the Osterwalder-Schrader axioms[73] and these properties are sufficient to reconstruct the Garding-Wightman theory. Of particular importance is the property of analyticity which states that there is no discontinuity associated with the ordering of the complex variable z_j. Associated with this property is the total commutativity between the field operator:

$$[\Phi_i(x_i), \Phi_j(x_j)]_{\pm} = 0, \tag{1.47}$$

throughout the Euclidean space-time. Therefore S_n are the continuations of the time-ordered vacuum expectation values

$$S_n(x_1, x_2, \ldots, x_n) = < \Omega \mid \mathcal{T}\Phi_1(x_1)\Phi_2(x_2)\ldots\Phi_n(x_n) \mid \Omega > \tag{1.48}$$

where the time-ordering operator $\mathcal{T}$ orders the field operators from left to right according to descending time.

The physical significance of the above argument is that the Minkowski fields can be analtytically continued to Euclidean space-time and vise versa without affecting the

physics of the theory. This entails replacing the real Minkowski space with a complex space and obtaining $\mathcal{M}_4$ for real time and $\mathcal{E}_4$ for imaginary time. This technique is called the *Wick rotation.*

The time-ordered vacuum expectation values given by Eq.(1.48) are however not measurable quantities. In order to get any physical significance from them it is pertinent to reorganize them in such a way that it is possible to extract relevant information about the physical observables contained within them. This method of reorganization of the Euclidean Green functions is called *quantization.*

1.4 Quantization: The Path Integral Approach

Quantization of field theories is based on the canonical quantization procedure and the Feynman path integral(FPI) approach. In canonical quantization the dynamical variables which are the quantum fields $\phi_i(x)$ of the system are considered as operators in Fock space. These operators satisfy certain commutation relations and together with the Lagrangian density are used to construct the transition amplitude of the quantum system as it evolves with time. This method is fairly successful in its description of real processes. It does however have its limitations due to the fact that canonical quantization is defined only in the context of perturbation theory. The practical value of perturbation theoretical results is questionable when the expansion parameter is not small. This leaves beyond the reach of the theory such important aspects of quantum physics as for instance quark confinement in hadrons.

The Feynman path integral approach allows the transition amplitudes to be expressed as a weighted sum over all possible histories(paths) the system could follow during its evolution between an initial and a final state. The 'sum' involves an integration in the (infinitely dimensional)space of all field configurations $[\Phi]$. It is still an open question whether the measure of integration $D[\Phi]$ exists in this space. Feynman

has postulated that these weights are proportional to $exp\{-\frac{i}{\hbar}S[\Phi]\}$ where $S[\Phi]$ is the classical action for the field configuration $[\Phi]$:

$$Z = \int e^{-\frac{i}{\hbar}S[\Phi]}\, D[\Phi]. \tag{1.49}$$

For real values of the action S, the intergrand in the above integral is a rapidly oscillating function since S can be much larger than $\hbar$. As a result, for a very long time, the Feynman path integral was considered just as a compact expression from which one could derive the perturbation theory expansion. It was later realized that it was possible to transform this integral to one that is restricted to a Gaussian type integral which is prevalent in statistical systems. This is done by performing a Wick rotation to Euclidean space-time which eliminates any complex characteristics possessed by the integral. Thus the Feynman path integral can be written as a partition function:

$$Z = \int e^{-\frac{S_E[\Phi]}{\hbar}}\, D[\Phi], \tag{1.50}$$

which is an analytic continuation into Euclidean space-time and where S_E is the Euclidean action. The advantage of this approach is that it involves computations of only ordinary functions rather than operators which makes analytic treatments very much simpler. This results in Z being interpreted as the partition function of a classical statistical system in four-dimensions:

$$\sum_{\Phi} e^{-\frac{S[\Phi]}{\hbar}}, \tag{1.51}$$

where the sum is over all configurations Φ of the fields. This allows the expectation value of an observable $O(\Phi)$ to be written as a statistical average over all configurations:

$$< \mathcal{O} >= \sum_{\Phi} \mathcal{O}(\Phi) P(\Phi), \tag{1.52}$$

where $P(\Phi)$ is the probability with which the configuration Φ will occur in the space of all possible configurations.

1.4.1 The Feynman Path Integral in Quantum Field Theory

In this section the functional integral approach of Feynman is discussed for a Euclidean field theory using the Euclidean Green functions as discussed earlier. The Feynman path integral in field theory is defined as a sum over all field configurations in the four-dimensional Euclidean space-time. Each field configuration is considered as a point in an (infinitely dimensional)space - the space of the field configurations. The vacuum expectation value of the time ordered product of the field operators is given by the Euclidean Green function

$$\mathcal{G}(x_1, x_2, \ldots, x_n) = < \Omega \mid \mathcal{T}\Phi_1(x_1), \ldots, \Phi_n(x_n) \mid \Omega > . \tag{1.53}$$

The functional integral representation of this function is postulated as

$$\mathcal{G}(x_1, x_2, \ldots, x_n) = \mathcal{N} \int D[\Phi]\Phi(x_1) \ldots \Phi(x_n) exp\{-\frac{S[\Phi]}{\hbar}\} \tag{1.54}$$

where $D[\Phi]$ is the integration measure in the space of the field configurations and

$$S[\Phi(x)] = \int dx^4 \mathcal{L}(\Phi(x_i)\partial^\mu \Phi(x_i)) \tag{1.55}$$

is the corresponding action. N is the normalization factor:

$$\frac{1}{\mathcal{N}} = \int D[\Phi] exp\{-\frac{S[\Phi(x)]}{\hbar}\}. \tag{1.56}$$

If the system is now coupled to an external source $J(x)$, a new action

$$S'[\Phi, J] = \int dx^4 \mathcal{L}'(\Phi, J) \tag{1.57}$$

where $\mathcal{L}'(\Phi, J) = \mathcal{L}(\Phi) + \Phi(x)J(x)$ can be defined together with a generating functional

$$Z[J] = \mathcal{N} \int D[\Phi] exp\{-\frac{S'[\Phi, J]}{\hbar}\}. \tag{1.58}$$

Differentiating $Z[J]$ in the corresponding functional space with respect to the external source $J(x)$ it can be shown that

$$\frac{\delta^n Z[J]}{\delta J(x_1) \ldots \delta J(x_n)} = \mathcal{N} \int D[\Phi]\Phi(x_1) \ldots \Phi(x_n) exp\{-\frac{S'[\Phi, J]}{\hbar}\} \tag{1.59}$$

where $\delta^n/\delta J(x_1)\ldots\delta J(x_n)$ are variational derivatives (or functional derivatives).

It can be seen that when $J(x) = 0$, Eq.(1.59) reduces identically to Eq. (1.54). As a result the Euclidean Green functions are given by the functional derivatives of the generating functional $Z[J]$ evaluated at $J(x) = O$:

$$\mathcal{G}(x_1, \ldots, x_n) = \frac{\delta}{\delta J(x_1)} \cdots \frac{\delta}{\delta J(x_n)} \, |_{J=0} \, Z[J]. \tag{1.60}$$

It should be noted at this point that the path integrals defining the Green functions are not well defined in the continuum space-time. This is due to the fact that field theory corresponds to an infinite number of degrees of freedom which does not allow for a consistent definition of the integration measure over the field of configurations. This problem is resolved by defining the path integral on a discretized space-time (a lattice).

Chapter 2

Gauge Theory

The first gauge theory was formulated in 1864 by Maxwell. In this theory of (classical) electrodynamics the subsequent freedom of choice of potentials to describe the same electromagnetic field has layed the foundation for what is known as *gauge invariance*. Gauge theories have since then evolved to play an important part in physics. In fact, it is believed that all fundamental interactions are described by some form of gauge theory. In quantum field theory, gauge transformations affect the phases of the fields and as such, a gauge theory is defined as a quantum field theory which is invariant under gauge transformations.

2.1 Global and Local Gauge Invariance

2.1.1 Abelian Gauge Theory

To illustrate the features of a gauge theory, consider the Lagrangian density of a single complex scalar field $\phi(x)$,

$$\mathcal{L}(\phi(x), \partial^\mu\phi(x)) = \partial_\mu\phi^*\partial^\mu\phi + V(\phi, \phi^*), \tag{2.1}$$

where $V(\phi, \phi^*)$ (the 'potential') is usually taken as

$$V(\phi, \phi^*) = m^2(\phi\phi^*) + \lambda(\phi\phi^*)^2 \tag{2.2}$$

The parameters m and λ are associated respectively with the mass and the self-interaction strength of the field. This Lagrangian is invariant under the transformation generated by the group $U(1)$. Let g be an element of $U(1)$: $g = e^{i\alpha}$, where α is an arbitrary real constant satisfying $0 \leq \alpha < 2\pi$. With each element of $U(1)$ one associates a phase transformation (gauge transformation):

$$\begin{aligned} \phi \quad &\rightarrow \phi' \quad = e^{i\alpha}\,\phi, \\ \phi^* \quad &\rightarrow \phi^{*'} \quad = e^{-i\alpha}\,\phi^*. \end{aligned} \tag{2.3}$$

This transformation leaves the Lagrangian unchanged:

$$\begin{aligned} \mathcal{L}(\phi', \partial^\mu\phi') &= \partial_\mu(e^{-i\alpha}\,\phi^*)\partial^\mu(e^{i\alpha}\,\phi) + m^2(e^{-i\alpha}\,\phi^*)(e^{i\alpha}\,\phi) + \lambda[(e^{-i\alpha}\,\phi^*)(e^{i\alpha}\,\phi)]^2 \\ &= \partial_\mu\phi^*\partial^\mu + m^2(\phi\phi^*) + \lambda(\phi^*\phi)^2. \end{aligned} \tag{2.4}$$

This gauge transformation is called *global* in the sense that the phase shift it producers affects the field at all space-time points in the same way. This theory is said to exhibit a *global gauge invariance* under the group $U(1)$.

The question now arises whether it is possible to generalise these transformations such that the gauge transformation at each point of space and time are different and independent of each other? This can be done, but at the price of adding a new field to the theory. The gauge symmetry in this case is said to be *local*, that is, α is a function of space and time: $\alpha = \alpha(x^\mu)$. The *local gauge transformations* of the fields under the group U(1) look like

$$\begin{aligned} \phi(x^\mu) \quad &\rightarrow \phi'(x^\mu) \quad = e^{i\alpha(x^\mu)}, \\ \phi^*(x^\mu) \quad &\rightarrow \phi^{*'}(x^\mu) \quad = e^{-i\alpha(x^\mu)}\phi^*(x^\mu). \end{aligned} \tag{2.5}$$

The derivatives of the fields are however not covariant under the local gauge transformations and acquire an extra term:

$$\begin{aligned}
\partial_\nu\phi(x^\mu) \quad &\rightarrow [\partial_\nu\phi(x^\mu)]' \quad = \partial_\nu(e^{i\alpha(x^\mu)}\ \phi(x^\mu)) \\
&\qquad\qquad = e^{i\alpha(x^\mu)}\ \partial_\nu\phi(x^\mu) + [i\partial_\nu\alpha(x^\mu)]e^{i\alpha(x^\mu)}\ \phi(x^\mu), \\
\partial_\nu\phi^*(x^\mu) \quad &\rightarrow [\partial_\nu\phi^*(x^\mu)]' \quad = \partial_\nu(e^{-i\alpha(x^\mu)}\ \phi^*(x^\mu)) \\
&\qquad\qquad = e^{-i\alpha(x^\mu)}\ \partial_\nu\phi^*(x^\mu) - [i\partial_\nu\alpha(x^\mu)]e^{-i\alpha(x^\mu)}\ \phi^*(x^\mu). \quad (2.6)
\end{aligned}$$

A consequence of the non-covariance of the operator ∂_ν is the non-invariance of the kinetic term $\partial_\mu\phi^*\partial^\mu\phi$ and thus the Lagrangian. To make the theory locally gauge invariant it is necessary to replace $\partial^\mu\phi(x^\mu)$ by a generalization that transforms in the same manner as the fields. What is required is a gauge covariant derivative, D_μ, that replaces ∂_μ and allows the derivatives of the fields to be invariant:

$$D_\mu\phi(x^\mu) \rightarrow [D_\mu\phi(x^\mu)]' = e^{i\alpha(x^\mu)}\ D_\mu\phi(x^\mu). \quad (2.7)$$

This is achieved by introducing a new field $A_\mu(x^\mu)$ into the Lagrangian which compensates for the unwanted terms $\pm e^{\pm i\alpha(x^\mu)}[i\partial_\nu\alpha(x^\mu)]\phi(x^\mu)$ and gives the form of the covariant derivative as

$$D_\mu = \partial_\mu + A_\mu(x^\mu). \quad (2.8)$$

To satisfy the above conditions, the new field $A_\mu(x^\mu)$ must be a Lorentz-vector which must also transform in a non-trivial way under the gauge transformation:

$$A_\mu(x^\mu) \rightarrow A'_\mu(x^\mu) = A_\mu(x^\mu) + \delta A_\mu(x^\mu). \quad (2.9)$$

Now substituting Eq. (2.9) in Eq. (2.8), the gauge transformation of the covariant derivative of the field is

$$\begin{aligned}
D_\mu\phi \rightarrow [D_\mu\phi]' &= (\partial_\mu + A_\mu + \delta A_\mu)e^{i\alpha}\phi \\
&= \partial_\mu(e^{i\alpha}\phi) + e^{i\alpha}A_\mu\phi + e^{i\alpha}(\delta A_\mu)\phi \\
&= e^{i\alpha}(\partial_\mu\phi) + e^{i\alpha}(i\partial_\mu\alpha)\phi + e^{i\alpha}A_\mu\phi + e^{i\alpha}(\delta A_\mu)\phi
\end{aligned}$$

$$= e^{i\alpha}(\partial_\mu + A_\mu) + e^{i\alpha}(i\partial_\mu\alpha + \delta A_\mu)\phi$$
$$= e^{i\alpha}D_\mu\phi + e^{i\alpha}(i\partial_\mu\alpha + \delta A_\mu)\phi. \quad (2.10)$$

So, for $D_\mu\phi$ to be gauge invariant the requirement is that $\delta A_\mu = -i\partial_\mu\alpha(x^\mu)$. $A_\mu(x^\mu)$ is called a *gauge field* and its complete transformation under the local gauge transformation is

$$A_\mu(x^\mu) \rightarrow A'_\mu(x^\mu) = A_\mu(x^\mu) - i\partial_\mu\alpha(x^\mu). \quad (2.11)$$

To make this gauge field a dynamical variable it is necessary to add a term to the Lagrangian that involves the derivatives $\partial_\nu A_\mu$ of the gauge fields. This term enters the Lagrangian via the tensor $F_{\mu\nu}$ which, in the case of $U(1)$ gauge symmetry, is defined as

$$F_{\mu\nu} = \partial_\mu A_\nu - \partial_\nu A_\mu. \quad (2.12)$$

$F_{\mu\nu}$ is the field strength tensor and is invariant under the local gauge transformations. To include this into the Lagrangian, a scalar field must be produced from $F_{\mu\nu}$. The simplest such scalar in four space-time dimensions is $F_{\mu\nu}F^{\mu\nu}$ and it leads to a gauge invariant Lagrangian density:

$$\mathcal{L}(\phi(x^\mu), A_\mu(x^\mu)) = D_\mu\phi^* D^\mu\phi + V(\phi, \phi^*) - \frac{1}{4}F_{\mu\nu}F^{\mu\nu}. \quad (2.13)$$

This combined scalar-vector Lagrangian density defines the classical Maxwell's theory of scalar electrodynamics. The quantum analogue is scalar quantum electrodynamics.

2.1.2 Multicomponent Gauge Transformations

Gauge transformations are generalized by considering a set of n-component scalar fields $\{\phi_1(x_1), \phi_2(x_2), \ldots, \phi_n(x_n)\}$ together with a set of phase factors $\{\alpha_1, \alpha_2, \ldots, \alpha_n\}$ that are unique for different components of the fields $\phi_i(x_i)$. The Lagrangian density for such a theory is

$$\mathcal{L}(\phi_i, \phi_2, \ldots, \phi_n) = \sum_i \{\partial_\mu\phi_i^*\partial^\mu\phi_i + \frac{m_i^2}{2}\phi_i^*\phi_i + \frac{\lambda_i}{4}(\phi_i^*\phi_i)^2\}. \quad (2.14)$$

It can be shown that this Lagrangian is invariant under the global gauge transformation

$$\phi_i(x) \rightarrow \phi_i'(x) = e^{i\alpha_i}\phi_i(x) \tag{2.15}$$

for $i = 1, 2, \ldots, n$.

2.1.3 Non-Abelian Gauge Theory

A further generalization of the gauge transformation can be obtained by considering groups of symmetry other than $U(1)$. The group $U(1)$ belongs to the class of the Abelian groups for which the group multiplication is commutative: for $e^{i\alpha} \in U(1)$ and $e^{i\beta} \in U(1)$,

$$\begin{aligned} e^{i\alpha}e^{i\beta} &= e^{i\beta}e^{i\alpha} \\ &= e^{i(\alpha+\beta)} \in U(1). \end{aligned}$$

Another, much larger and, as it turned out, physically even more important, is the class of the non-Abelian groups for which the group multiplication is not commutative. Let G be a non-Abelian Lie group. Consider now the complex scalar field as a column vector

$$\phi = \begin{pmatrix} \phi_1 \\ \vdots \\ \phi_n \end{pmatrix}, \tag{2.16}$$

in a n-dimensional complex vector space $\mathcal{V}$. Let T be an operator in this space such that

$$(T\phi)_i = \sum_{ij} (T)_{ij}\phi_j \tag{2.17}$$

where $(T)_{ij}$ are the matrix elements of T. Also, let the generalization of the phase factor be a vector $\alpha = (\alpha_1, \alpha_2, \ldots, \alpha_n) = \alpha_k$. Further, let L_k for $k = 1, 2, \ldots, n$ be the generators of a representation of G in $\mathcal{V}$. Then the group element governing the

local gauge transformation is written as

$$exp\{i\sum_{k=1}^{N}\alpha_k L_k\} = exp\{i\boldsymbol{L}\cdot\boldsymbol{\alpha}\} \tag{2.18}$$

and the transformation of the fields specified by n parameters become

$$\boldsymbol{\phi} \rightarrow \boldsymbol{\phi}' = exp\{i\boldsymbol{L}\cdot\boldsymbol{\alpha}\}\boldsymbol{\phi}. \tag{2.19}$$

In the non-Abelian case the operators T_k do not commute, that is, $T_kT_l \neq T_lT_k$. The generators L_k form an algebra, called the *Lie algebra* in which the multiplication of two operators is the commutator:

$$[T_k, T_l] = iC_{klm}T_m, \tag{2.20}$$

where the constant C_{klm} are real called *structure constants* and characterize the algebra. This algebra generates the factor $exp\{i\sum_{k=1}^{N}\alpha_k L_k\}$ which belongs to the considered representation of the *Lie group*.

In order for the Lagrangian to be invariant under the gauge transformation (Eq.(2.19)) it is required that all the masses $m_1, m_2, \ldots, m_n$ be equal and all the self-interaction strengths $\lambda_1, \lambda_2, \ldots, \lambda_n$ be equal. This is so since the operation in Eq. (2.17) mixes different components of $\boldsymbol{\phi}$. The Lagrangian invariant under global transformations of the form defined by Eq. (2.18) can therefore be written as

$$\mathcal{L}(\boldsymbol{\phi}\ \boldsymbol{\phi}^*) = \partial_\mu\boldsymbol{\phi}^*\cdot\partial^\mu\boldsymbol{\phi} + \frac{m^2}{2}\boldsymbol{\phi}^*\cdot\boldsymbol{\phi} + \frac{\lambda}{4}(\boldsymbol{\phi}^*\boldsymbol{\phi})^2. \tag{2.21}$$

To extend this theory to a local gauge theory the phase parameters $\boldsymbol{\alpha}$ needs to be considered as dependent on space and time: $\boldsymbol{\alpha}(x) = (\alpha_1(x), \ldots, \alpha(x)) = \alpha_k(x)$. By denoting $u(\boldsymbol{\alpha}) = exp\{i\boldsymbol{L}\cdot\boldsymbol{\alpha}(x)\}$ the gauge transformation can be written as

$$\boldsymbol{\phi} \rightarrow \boldsymbol{\phi}' = u(\boldsymbol{\alpha})\boldsymbol{\phi}. \tag{2.22}$$

By analogy with Eq. (2.6) the derivatives $\partial_\mu\boldsymbol{\phi}$ are not covariant and as a result a covariant derivative, D_μ, has to be defined:

$$D_\mu\boldsymbol{\phi} \rightarrow [D_\mu\boldsymbol{\phi}]' = u(\boldsymbol{\alpha})D_\mu\boldsymbol{\phi}. \tag{2.23}$$

D_μ is defined as

$$D_\mu = \partial_\mu - \imath \boldsymbol{L} \cdot \boldsymbol{A}_\mu \tag{2.24}$$

where the compensating fields $\boldsymbol{A}_\mu^k = (A_\mu^{(1)}, A_\mu^{(2)}, \ldots, A_\mu^{(n)})$ are called the gauge fields or the *Yang-Mills fields* and transform as

$$A_\mu^k \rightarrow A_\mu^{k'} = A_\mu^k + \delta A_\mu^k. \tag{2.25}$$

The derivatives of the $\boldsymbol{\phi}$-fields transform as,

$$\begin{aligned} D_\mu \boldsymbol{\phi} \rightarrow D'_\mu \boldsymbol{\phi}' &= (\partial_\mu - \imath \boldsymbol{L} \cdot \boldsymbol{A}'_\mu)(u(\boldsymbol{\alpha})\boldsymbol{\phi}) \\ &= u(\boldsymbol{\alpha})\partial_\mu \boldsymbol{\phi} + [\partial_\mu u(\boldsymbol{\alpha})]\boldsymbol{\phi} - \imath u(\boldsymbol{\alpha}) \boldsymbol{L} \cdot \boldsymbol{A}_\mu \end{aligned} \tag{2.26}$$

and by Eq. (2.23) as

$$\begin{aligned} D_\mu \boldsymbol{\phi} \rightarrow [D_\mu \boldsymbol{\phi}] &= u(\boldsymbol{\alpha})(\partial_\mu - \imath \boldsymbol{L} \cdot \boldsymbol{A}_\mu)\boldsymbol{\phi} \\ &= u(\boldsymbol{\alpha})\partial_\mu \boldsymbol{\phi} - \imath u(\boldsymbol{\alpha}) \boldsymbol{L} \cdot \boldsymbol{A}_\mu \boldsymbol{\phi}. \end{aligned} \tag{2.27}$$

Since Eq. (2.26) and Eq. (2.27) give the same transformation,

$$[\partial_\mu u(\boldsymbol{\alpha})]\boldsymbol{\phi} - \imath \boldsymbol{L} \cdot \boldsymbol{A}'_\mu u(\boldsymbol{\alpha})\boldsymbol{\phi} = -\imath u(\boldsymbol{\alpha}) \boldsymbol{L} \cdot \boldsymbol{A}_\mu \boldsymbol{\phi}, \tag{2.28}$$

which implies that

$$\boldsymbol{L} \cdot \boldsymbol{A}'_\mu u(\boldsymbol{\alpha})\boldsymbol{\phi} = u(\boldsymbol{\alpha}) \boldsymbol{L} \cdot \boldsymbol{A}_\mu \boldsymbol{\phi} - \imath [\partial_\mu u(\boldsymbol{\alpha})]\boldsymbol{\phi}. \tag{2.29}$$

Since this must he true for all $\boldsymbol{\phi}$(x), it can be shown that

$$\boldsymbol{L} \cdot \boldsymbol{A}'_\mu = u(\boldsymbol{\alpha}) \boldsymbol{L} \cdot \boldsymbol{A}_\mu u(\boldsymbol{\alpha})^{-1} - \imath [\partial_\mu u(\boldsymbol{\alpha})] u(\boldsymbol{\alpha})^{-1}. \tag{2.30}$$

In order to define the infinitesmal transformation δA_μ of the Young-Mills fields it is necessary to see the effect of the an infinitesmal change $\boldsymbol{\alpha}(x) \ll 1$,

$$exp\{\imath \boldsymbol{L} \cdot \boldsymbol{\alpha}(x)\} \simeq 1 - \imath \boldsymbol{L} \cdot \boldsymbol{\alpha}(x). \tag{2.31}$$

To first order in $\boldsymbol{\alpha}(x)$ it can be shown that

$$\begin{aligned} \boldsymbol{L}\cdot\boldsymbol{A}'_{\mu} &= \boldsymbol{L}\cdot\boldsymbol{A}_{\mu} - i\alpha_j A^k_{\mu}[L_j, L_k] - (\boldsymbol{L}\cdot\partial_{\mu}\boldsymbol{\alpha}) \\ &= \boldsymbol{L}\cdot\boldsymbol{A}_{\mu} + C_{ijk}L_i\alpha_j A^k_{\mu} - (\boldsymbol{L}\cdot\partial_{\mu}\boldsymbol{\alpha}). \end{aligned} \tag{2.32}$$

Using the fact that the L_k form a basis for the Lie algebra and they are linearly independent, Eq. (2.32) gives the complete transformation of the Yang-Mills fields under local gauge transformation:

$$A^{i\prime}_{\mu} = A^i_{\mu} + C_{ijk}\alpha_j(x)A^k_{\mu} - \partial_{\mu}\alpha_i(x). \tag{2.33}$$

To make the fields A^k_{μ} dynamical in analogy with the Abelian case a new generalized field tensor is defined which has a more complicated form the Eq. (2.12). This generalized field strength tensor is given by

$$F^i_{\mu\nu} = \partial_{\mu}A^i_{\nu} - \partial_{\nu}A^i_{\mu} + C_{ijk}A^j_{\mu}A^k_{\mu}. \tag{2.34}$$

With this a complete locally gauge invariant Lagrangian can be defined which describes the interaction between the gauge fields $\boldsymbol{A}^{\ k}_{\mu}$ and the scalar fields ϕ:

$$\mathcal{L}(\phi, \boldsymbol{A}_{\ \mu}) = D_{\mu}\phi^* D^{\mu}\phi + \frac{m^2}{2}\phi^*\phi + \frac{\lambda}{4}(\phi^*\phi)^2 - \frac{1}{4}F^i_{\mu\nu}F^{i\mu\nu}. \tag{2.35}$$

This is the Yang-Mills Lagrangian density for a scalar field theory. The Yang-Mills fields play a major part in the description of models of strong and weak interactions[77]. Yang and Mills considered the simplest non-Abelian group $SU(2)$ which deals with isospin.

2.2 Spontaneous Symmetry Breaking

Gauge theories are based on the assumption that all interactions are mediated by gauge bosons that have zero masses. In nature however, only the photons and the

gluons are massless but the $W^{\pm}$ and Z^0 bosons are certainly not. The addition of an arbitrary mass term for the gauge field might seem to elliviate the problem of masslessness, but this creates a more serious problem. It breaks the gauge invariance of the theory. Under the local transformations of the gauge group $U(1)$, the mass term for the A-field transforms as follows,

$$\begin{aligned} A_\mu A^\mu \rightarrow [A_\mu A^\mu]' &= A_\mu A^\mu + i(\partial_\mu \alpha) A^\mu + i A_\mu (\partial^\mu \alpha) \\ &= A_\mu A^\mu + 2i(\partial_\mu \alpha) A^\mu \\ &\neq A_\mu A^\mu \end{aligned}$$

in the Abeliau case and the mass term is also not gauge invariant in the non-Abelian case. The question now arises whether it is possible to accomodate for massive gauge fields and yet preserve the gauge invariance of the theory? This can be done, and the technique involves employing the mechanism of *spontaneous symmetry breaking*. The symmetry of a system is said to be *spontaneously broken* if the Lagrangian density is invariant under a certain symmetry group but the ground state (the vacuum) of the system is not. Examples of such phenomena are many in all branches of physics. Take for instance the case of a ferromagnet. Although the Hamiltonian describing the system is invariant under the rotation group, the ground state is not below the Currie point. This is so since the magnetic dipoles tend to align themselves along a specific direction giving a definite degenerate ground state. Another classical example is a thin plastic rod under axial pressure. This strip can buckle in any transverse arbitrary direction and as a result will break the symmetry of the direction it chooses to buckle. In this section spontaneous symmetry breaking is discussed for cases of global gauge invariance and local gauge invariance.

2.2.1 Global Gauge Invariance: The Goldstone Model

Consider the Lagrangian density

$$\mathcal{L} = \partial_\mu \phi^* \partial^\mu \phi - \mu^2 \phi^* \phi - \lambda(\phi^* \phi)^2, \tag{2.36}$$

where μ^2 is the (bare) mass such that $m^2 = -\mu^2$. It can be shown that $\mathcal{L}$ is invariant under the global gauge transformation,

$$\phi \rightarrow \phi' = e^{i\alpha}\phi. \tag{2.37}$$

Let ϕ_0 be a constant such that $\phi = \phi_0$ be a solution to the equations of motion of the system at ground state such that the potential

$$V(\phi\phi^*) = \mu^2 \phi^* \phi + \lambda(\phi^* \phi)^2 \tag{2.38}$$

is a minimum. If $\lambda < 0$ the Lagrangian has no lower bound and the theory will not exist. For $\lambda > 0$ a theory can be defined for two cases of μ^2, $\mu^2 > 0$ and $\mu^2 < 0$.

In the case of $\mu^2 > 0$, the minimum of V corresponds to a ground state $\phi_0 = 0$ which is invariant under Eq. (2.37). As a result there is no spontaneous symmetry breaking since the Lagrangian and the ground state possess the same symmetry.

For $\mu^2 < 0$ the potential V has a local maximum at $\phi_0 = 0$ and minima at

$$\phi_0 = \sqrt{\frac{-\mu^2}{2\lambda}} e^{i\sigma} \equiv \frac{\nu}{\sqrt{2}} e^{i\sigma} \tag{2.39}$$

where σ is the phase angle which defines a direction in the complex plane of ϕ. This corresponds to a whole circle of minimum V for $0 \leq \sigma < 2\pi$ with radius $\frac{\nu}{\sqrt{2}}$. Therefore there are infinitly many degenerate vacua each of which can have preference of being the ground state of the theory. As a result the symmetry is spontaneously broken. Consider now a specific case when $\sigma = 0$, that is, $\phi_0 = \frac{\nu}{\sqrt{2}}$. Let

$$\phi(x) = \frac{1}{\sqrt{2}}[\nu + \xi(x) + i\eta(x)] \tag{2.40}$$

where $\xi(x)$ and $\nu(x)$ are real fields which measure the shift or deviation of $\phi(x)$ from the ground state $\phi_0 = 0$. Substituting Eq.(2.40) in Eq.(2.36) the Lagrangian density becomes

$$\begin{aligned}\mathcal{L} = \quad & \tfrac{1}{2}(\partial_\mu \xi)^2 + \tfrac{1}{2}(\partial_\mu \eta)^2 - \tfrac{1}{2}\lambda\nu^2\xi^2 \\ & -\lambda\nu\xi(\xi^2+\eta^2) - \tfrac{1}{4}\lambda(\xi^2+\eta^2)^2, \end{aligned} \tag{2.41}$$

where all unimportant constant terms have been ignored. Since Eq. (2.36) and Eq. (2.41) are the same Lagrangian density with different fields, they should lead to the same quantum field theory. So since ξ and η are quantum fields (Klein-Gordon fields in this case) it can be expected as a postulate of Lagrangian field theory that the field $\eta(x)$ will possess no mass while the field $\xi(x)$ will have a mass $m = \sqrt{2\lambda\nu^2}$ corresponding to the mass term $-\frac{1}{2}\lambda\nu^2\xi^2$. The masslessness of $\eta(x)$ can be attributed to the degeneracy of the vacuum. Therefore it can be seen that when the global symmetry is spontaneously broken, massless bosons appear. This statement is known as the *Goldstone theorem* and the massless bosons are called *Goldstone bosons.*

2.2.2 Local Gauge Invariance: The Higgs Model

Consider the Lagrangian density

$$\mathcal{L} = (D_\mu\phi)^*(D^\mu\phi) - \mu^2\phi^*\phi - \lambda(\phi^*\phi)^2 - \frac{1}{4}F_{\mu\nu}F^{\nu\mu}, \tag{2.42}$$

where

$$\begin{aligned} D_\mu = \quad & \partial_\mu - igA_\mu, \\ F_{\mu\nu} = \quad & \partial_\mu A_\nu - \partial_\nu A_\mu. \end{aligned} \tag{2.43}$$

This Lagrangian density can be shown to be invariant under the local gauge transformation:

$$\begin{aligned} \phi(x) \rightarrow \quad & \phi'(x) = \quad e^{i\alpha(x)}\phi(x), \\ A_\mu(x) \rightarrow \quad & A'_\mu(x) = \quad A_\mu(x) - \frac{1}{g}\partial_\mu\alpha(x). \end{aligned} \tag{2.44}$$

Based on the same argument as for the Goldstone model it can be seen for $\lambda > 0$ that the case $\mu^2 < 0$ results in spontaneous symmetry breaking while the case $\mu^2 > 0$ does not. Proceeding in the same manner as for the Gladstone model, let

$$\phi(x) = \frac{1}{\sqrt{2}}[\nu + \xi(x) + i\eta(x)]. \tag{2.45}$$

In terms of the fields in Eq. (2.45), the Lagrangian density becomes,

$$\begin{aligned} \mathcal{L} &= \frac{1}{2}(\partial_\mu \xi)^2 + \frac{1}{2}(\partial_\mu \eta)^2 + \frac{1}{2}g^2\nu^2 A_\nu A^\nu \\ &\quad -\frac{1}{2}(2\lambda\nu^2)\xi^2 - g\nu A^\mu \partial_\mu \eta - \frac{1}{4}F_{\mu\nu}F^{\mu\nu}, \end{aligned} \tag{2.46}$$

where interaction terms have been omitted. From Eq. (2.46) it can be seen that η corresponds to the massless Goldstone boson and ξ to a massive boson with mass $\sqrt{2\lambda\nu^2}$. The most interesting feature of Eq. (2.46) is the presence of the term $\frac{1}{2}g\nu^2 A_\mu A^\mu$ which might be related to a massive gauge field. This interpretation cannot be justified directly due to the presence of the term $-g\nu A_\nu \partial^\nu \eta$ which seems to mix the gauge fields A_ν and the real scalar field η. Also, the Lagrangian in Eq. (2.46) seems to have gained an extra degree of freedom. This extra degree of freedon is only apparent since a change in variables in producing Eq. (2.46) should not affect the number of degrees of freedom. This problem is solved by choosing a special gauge such that the scalar field $\eta(x)$ is eluminated. This is done by requiring that the scalar field $\phi(x)$ transform as:

$$\phi(x) \rightarrow \phi'(x) = \frac{1}{\sqrt{2}}[\nu + \sigma(x)], \tag{2.47}$$

where $\sigma(x)$ is a real scalar field. The special gauge which allows for this kind of transformation is called a *unitary gauge*. Substituting this in Eq.(2.42), the transformed Lagrangian becomes,

$$\begin{aligned} \mathcal{L} &= \frac{1}{2}(\partial_\mu \sigma)^2 - \frac{1}{2}(2\lambda\nu^2)\sigma^2 - \frac{1}{4}\lambda\sigma^4 \\ &\quad + \frac{1}{2}g^2(A_\mu)^2(2\nu\sigma + \sigma^2) - \frac{1}{2}g^2\nu^2 A_\mu A^\mu - \frac{1}{4}F_{\mu\nu}F^{\mu\nu}, \end{aligned} \tag{2.48}$$

where the $F_{\mu\nu}$ and A_μ correspond to their transformed counterparts $F'_{\mu\nu}$ and A'_μ. This complete Lagrangian gives the interaction between a massive gauge field $A_\mu(x)$ with

mass $g\nu$ and a massive scalar field $\sigma(x)$ with mass $\sqrt{2\lambda\nu^2}$. The latter field is called a *Higgs field* and the phenomenon whereby the gauge field becomes massive without violating the invariance of the Lagrangian is called the *Higgs mechanism.* It should be noted that the Higgs mechanism does not give rise to a Goldstone boson as in the Goldstone model. Since the scalar field $\eta(x)$ was eliminated in this mechanism it is said to be a *would-be-Goldstone boson.*

Chapter 3

Lattice Gauge Theory

3.1 Introduction

The theory of elementary particles is dominated by the study of gauge field theory. In fact, the Standard Model (or the Glashow-Salam-Weinberg model) relies heavily on the concepts of local gauge invariance and spontaneous symmetry breaking. The theory corresponding to this model has been renormalized to give well defined mathematical interpretation. The theoretical predictions compare extremely well with that of experimental results. This however, was done mainly in the context of perturbation theory which exploits the presence of effectively weak coupling parameters. Nevertheless, there exists non-perturbative categories of phenomena which cannot be treated perturbatively. One such phenomenon is the confinement of quarks.

To show that the confinement of quarks is a strong coupling phenomenon consider the following qualitative argument. The qualitative ideas about the nature of quark confinement tend to picture the quarks as being coupled to a conserved *gluo-electric* flux. This idea is analogous to electromagnetism where the electric field lines between two opposite electric charges at a distance r, give rise to the inverse distance law Coulomb potential, $V(r) = \frac{e^2}{r}$. If the medium between the charges is such that

the electric field lines are compressed in a narrow flux tube then the force between two charges would be independent of the seperation r which corresponds to a linear (confining)potential: $V(r) = \sigma r$. This now becomes a phenomenon analogous to the ground state of a superconductor where paired electrons give rise to the Meisner effect which prevents the penetration of magnetic fields into the superconductor. However, if a hypothetical monopole and antimonopole is placed into the superconducter, the magnetic flux will be confined to a string-like configuration joining the pair of monopoles. Similarly, the gluo-electric flux forms into a confined tube of conserved flux. These flux tubes will only end on a quark or antiquark. Perturbative theory cannot explain this phemonenon and a new technique needs to be sought.

One possible approach to the above problem could be a direct evaluation of the Feynman path integral introduced in §1.4:

$$Z = \int D[\phi] exp\{-\frac{S[\phi]}{\hbar}\}, \tag{3.1}$$

where $D[\phi]$ is the integration measure in the space of all field configurations. However, it is not clear if such a measure, $D[\phi]$, exists. This throws the shadow of doubt on the possibility of a direct evaluation of Eq. (3.1). The main difficulty arises from the fact that a field is a system of infinitely many degrees of freedom. What is required is a regularization of $D[\phi]$ and renormalization that will lead back to the original theory after the regularization is lifted. This could be achieved by the introduction of a space-time *lattice*. The problem with the ill defined measure is now alleviated by replacing the existing infinite degrees of freedom of the field by a finite dimensional space of *lattice configurations*. In this way the continuum theory is redefined on a finite number of space-time lattice points and the bonds connecting neighbouring points. The path integral can now be replaced by a well defined multiple integral:

$$\int D[\phi] \rightarrow \int \ldots \int \prod_i d\phi_i, \tag{3.2}$$

where ϕ_i corresponds to the values accessible to the field at the lattice point i.

3.1.1 Lattice Regularization

The lattice formulation of quantum field theory as proposed by Wilson[76] is based on discretizing space and time in Euclidean space-time. Consider a hypercubical lattice with spacing a. The vertices or *sites* of the lattice are labelled by vectors $x_\mu = an_\mu$ where $n_\mu = (n_1, n_2, n_3, n_4)$. On every lattice site x there exists a field $\phi(x)$ denoted by ϕ_x. The bond joining two adjacent neighbouring sites called *links* are specified by the unit vector $\hat{\mu}$. Fields on these links are denoted by $U_{x,\hat{\mu}}$. The derivatives of the field $\partial_\mu \phi(x)$ are replaced by finite differences of neighbouring lattice sites:

$$\partial_\mu \phi(x) \rightarrow \frac{1}{a}(\phi_{x+\hat{\mu}} - \phi_x). \tag{3.3}$$

The greatest advantage of the lattice is that it drastically reduces the set of all possible field configurations. In the space-time continuum a change of the fields at any point leads to a new field configuration, while in the lattice formulation the fields can change only at the lattice points or links. This makes it possible to define the measure $D[\phi]$ for the integrals over the field configurations as the product of measures $d\phi_i$ at the sites and/or the links:

$$D[\phi] \rightarrow \prod_i d\phi_i. \tag{3.4}$$

In the renormalisation scheme of perturbation theory, it is necessary to regularize the Feynman integrals in momentum space in order to renormalize the Green functions. A momentum cutoff is then introduced which remedies the problem of the ultra-violet divergences. Such a cutoff is provided by the lattice regularization scheme in a natural way. To show this , Fourier transform techniques are used on the lattice[24,72]. Consider a complex field ϕ_x on the lattice. Its Fourier transform is given by

$$\phi(x) = \int_{-\infty}^{\infty} \frac{d^4k}{(2\pi)^4} e^{ik\cdot x} \phi(k). \tag{3.5}$$

If wavelengths only less than twice the lattice spacing are considered, then the integration is restricted to one Brillouin zone of the reciprocal lattice, $\mid k_\mu \mid \leq \frac{\pi}{a}$. The

transform is then written as

$$\phi(na) = \int_{-\frac{\pi}{a}}^{\frac{\pi}{a}} \frac{d^4k}{(2\pi)^4}\phi(k)e^{ikna}. \tag{3.6}$$

Inverting Eq. (3.6) and representing it by a Fourier series, $\phi(k)$ has the form

$$\phi(k) = a\sum_n \phi(na)e^{-ikna}. \tag{3.7}$$

Setting $\phi(na) = \frac{1}{(2\pi)^4}$, a Fourier series represention of the δ-function in the Brillouin zone can be obtained,

$$\delta(k) = \frac{a}{(2\pi)^4}\sum_n e^{-ikna}, \tag{3.8}$$

which is periodic in the four-dimensional lattice. The Dirac δ-function, $\delta(x-y)$, in momentum space, is then the Kronecker-δ on the lattice:

$$\frac{1}{a}\delta_{xy} = \int\int_{-\frac{\pi}{a}}^{\frac{\pi}{a}}\int\int \frac{d^4p}{(2\pi)^4}e^{ip(x-y)a}. \tag{3.9}$$

Therefore it can be seen that the lattice provides a momentum cutoff of the order of the inverse lattice spacing.

3.2 Scalar Fields on the Lattice

Consider the free scalar field $\phi(x)$. In the continuum Euclidean field theory the action has the form

$$S[\phi] = \int d^4x\{\frac{1}{2}(\partial_\mu\phi)^2 + \frac{m^2}{2}\phi^2\}. \tag{3.10}$$

The quantization of this action using the Feynman path integral approach as discussed earlier yields a Green function:

$$\begin{aligned} G(x_1, x_2, \ldots, x_n) &= Z^{-1}\int D\phi(\phi(x_1)\phi(x_2)\ldots\phi(x_n))e^{S[\phi]} \\ Z &= \int D\phi e^{-S[\phi]} \end{aligned} \tag{3.11}$$

Eq. (3.10) is transformed to an action on the lattice according to the lattice regularization described above,

$$S[\phi] = \sum_n \{\frac{a^2}{2} \sum_{x=1}^{4} (\phi_{x+\hat{\mu}} - \phi_x)^2 + a^4(\frac{m^2}{2}\phi_x^2)\}. \tag{3.12}$$

The partition function is now given by an ordinary integral over the fields on the lattice sites,

$$Z = \int \prod_x d\phi_x e^{-S}. \tag{3.13}$$

The structure of Eq. (3.12) is analogous to those of the Gaussian type prevalent in statistical physics. That is, the action has a form quadratic in the fields:

$$S = \frac{1}{2} \sum_{m,n} \phi_m M_{nm} \phi_n, \tag{3.14}$$

where M_{nm} is an $n \times n$ matrix. The integral in Eq. (3.13) is therefore a standard Gaussian integral given by

$$Z = (2\pi)^{\frac{1}{2}} (det\ M)^{-\frac{1}{2}} \tag{3.15}$$

In order to obtain the corresponding Greens function, it is convenient to generalise this action to incorporate an external source J_n coupled to the fields ϕ on the sites of the lattice:

$$S = \frac{1}{2} \sum_{m,n} \phi_m M_{nm} \phi_n - \sum_n J_n \phi_n. \tag{3.16}$$

A generating functional for this action is written as

$$Z[J] = \int \prod_n d\phi_n e^{-s}. \tag{3.17}$$

Since the integral in Eq. (3.17) is of the Gaussian type it can be shown that

$$Z[J] = e^{\frac{1}{2} \sum J_n M^{-1}_{mn} J_m} (det\ M)^{-\frac{1}{2}} (2\pi)^{\frac{1}{2}}. \tag{3.18}$$

Eq. (3.18) shows that the propagator is the inverse of the matrix M_{nm}. So the two point correlation function is given by

$$< \phi_m \phi_n >= M^{-1}_{mn}. \tag{3.19}$$

It can be shown (see Rothe[72] or Creutz[12]), using the Fourier transform of ϕ_n in momentum space as given previously that

$$M_{mn}^{-1} = \int \frac{d^4k}{(2\pi)^4} \frac{e^{ik\cdot(m-n)a}}{\frac{4}{a^2}\sum_\mu(\sin^2(\frac{k_\mu}{2}) + m^2)}. \tag{3.20}$$

The action in Eq. (3.12) can therefore be written as,

$$S[\phi] = \frac{1}{2}\int \frac{d^4k}{(2\pi)^4}\{\sum_\mu \frac{4}{a^2}\sin^2(\frac{ak_\mu}{2}) + m^2\}\phi(-k)\phi(k). \tag{3.21}$$

It should be noted that the term $(m^2 + k^2)$ which appears in the continuum theory (see §1.2.1) is replaced in the lattice regularization by

$$m^2 + \sum_\mu \frac{4}{a^2}\sin^2(\frac{ak_\mu}{2}). \tag{3.22}$$

It can be shown that in the continuum limit as $a \to 0$, Eq. (3.22) approaches (m^2+k^2), which recovers the continuum theory.

Thus far only the action for a free scalar field has been discussed. Eq. (3.10) is now extended to incorporate a self-interaction term: $\frac{1}{2}\lambda\phi_x^4$. The action on the lattice then becomes,

$$S[\phi] = \sum_x \{\frac{a^2}{2}\sum_{\mu=1}(\phi_{x+\hat{\mu}} - \phi_x)^2 + a^4(\frac{m^2}{2}\phi_x^2 + \frac{\lambda}{4}\phi_x^4)\}. \tag{3.23}$$

The fields ϕ are usually rescaled by the self-interaction constant λ:

$$\phi_x \to \phi'_x = \sqrt{\lambda}\phi_x. \tag{3.24}$$

This gives the lattice action as

$$S[\phi] = \frac{1}{\lambda}S'[\phi'], \tag{3.25}$$

where

$$S'[\phi'] = \sum_x \{\frac{a^2}{2}\sum_{\mu=1}(\phi'_{x+\mu} - \phi'_x)^2 + a^4(\frac{m^2}{2}\phi'^2_n + \frac{1}{4}\phi'^4_x)\}. \tag{3.26}$$

The Green function in terms of the rescaled fields ϕ' is given by

$$G(x'_1, x'_2, \ldots, x'_n) = \frac{1}{Z'} \int \prod_n [d\phi'] \phi'_1 \phi'_2 \ldots \phi'_n e^{-\frac{1}{\lambda} S'[\phi']}, \tag{3.27}$$

where,

$$Z' = \int \prod_n [d\phi'] e^{-\frac{1}{\lambda} S'[\phi']}. \tag{3.28}$$

The analogy with statistical mechanics now becomes evident if $\frac{1}{\lambda} = \beta$ where β is taken to be the inverse temperature in statistical mechanics.

3.3 Gauge Transformations on the Lattice

To construct physically relevent lattice models it is essential that the theory is invariant under certain gauge transformations generated by the gauge group G. Let G be the Abelian group $U(1)$ with element $g = e^{i\alpha}$. To illustrate gauge invariance on a lattice, consider the lattice action of a complex scalar field:

$$\begin{aligned} S[\phi_x] &= \sum_x \{\frac{a^2}{2} \sum_{\mu=1}^{4} (\phi_{x+\mu} - \phi_x)(\phi^\dagger_{x+\hat{\mu}} - \phi^\dagger_x) + a^2 \frac{m^2}{2} \phi^\dagger_x \phi_x + a^2 \frac{\lambda}{4} (\phi^\dagger_x \phi_x)^2\} \\ &= \sum_x \{\frac{a^2}{2} \sum_{\mu=1}^{4} (-\phi^\dagger_x \phi_{x+\hat{\mu}}) + (a^4 \frac{m^2}{2} + 4a^2) \phi^\dagger_x \phi_x + a^2 \frac{\lambda}{4} (\phi^\dagger_x \phi_x)^2\}. \end{aligned} \tag{3.29}$$

The scalar fields which are defined on the sites of the lattice transform under the global $U(1)$ gauge transformation as

$$\begin{aligned} \phi_x &\to g\phi_x, \\ \phi^\dagger_x &\to \phi^\dagger_x g^\dagger. \end{aligned} \tag{3.30}$$

The combination $\phi^\dagger_x \phi_x$ is gauge invariant:

$$\begin{aligned} \phi^\dagger_x \phi_x &\to \phi^\dagger_x g^\dagger g \phi_x \\ &= \phi^\dagger_x \phi_x. \end{aligned} \tag{3.31}$$

In fact, it can be shown that all powers of the combination $(\phi_x^\dagger \phi_x)$ are invariant under the global gauge transformation of $U(1)$. The combination $\phi_x^\dagger \phi_{x+\hat{\mu}}$, known as the *bilocal interaction*, transforms invariantly as

$$\begin{aligned} \phi_x^\dagger \phi_{x+\hat{\mu}} &\rightarrow \phi_x^\dagger g^\dagger g \phi_{x+\hat{\mu}} \\ &= \phi_x^\dagger \phi_{x+\mu}. \end{aligned} \tag{3.32}$$

Therefore it can be concluded that the action given by Eq. (3.29) is invariant under global gauge transformations of the group $U(1)$.

To consider local gauge transformations, the gauge group element must be dependent on the lattice sites. That is, $g_x = e^{i\alpha_x}$ where α_x is labelled by the lattice sites. It can be shown that all combinations of the scalar fields are invariant under the local gauge transformation except the bilocal interaction which transforms as follows:

$$\begin{aligned} \phi_x^\dagger \phi_{x+\hat{\mu}} &\rightarrow \phi_x^\dagger g_x^\dagger g_{x+\hat{\mu}} \phi_{x+\hat{\mu}} \\ &\neq \phi_x^\dagger \phi_{x+\mu}. \end{aligned} \tag{3.33}$$

This non-invariance is a consequence of the finite difference $(\phi_{x+\hat{\mu}} - \phi_x)$ which replaces the derivative $\partial_\mu \phi$ in the continuum theory. As in the continuum theory a gauge field must be introduced which will compensate for the non-invariance in Eq. (3.33). This is done by defining a covariant difference,

$$R_{x,\hat{\mu}} \phi_{x+\hat{\mu}} - \phi_x. \tag{3.34}$$

To satisfy the conditions of non-invariance the new field $R_{x,\hat{\mu}}$ must transform under the local gauge transformation as,

$$R_{x,\hat{\mu}} \rightarrow g_x R_{x,\hat{\mu}} g_x^\dagger, \tag{3.35}$$

and must satisfy the hermiticity condition

$$R_{x,\mu} = R^{-1}_{x+\hat{\mu},-\hat{\mu}}. \tag{3.36}$$

So, with the above conditions the bilocal interaction must be replaced by

$$\phi_x^\dagger R_{x,\hat{\mu}} \phi_{x+\hat{\mu}}, \tag{3.37}$$

in order to ensure the local gauge invariance of the action. It will be seen later that the field $R_{x,\hat{\mu}}$ is just the link fields of the lattice $U_{x,\hat{\mu}}$. Therefore a lattice action can be written which is invariant under the local gauge transformation of the Abelian group $U(1)$:

$$S[\phi, U] = \sum_x \{\frac{a^2}{2} \sum_{\mu=1}^{4} (-\phi_x^\dagger U_{x,\hat{\mu}} \phi_{x+\hat{\mu}}) + (a^4 \frac{m^2}{2} + 4a^2)\phi_x^\dagger \phi_x + a^2 \frac{\lambda}{4} (\phi_x^\dagger \phi_x)^2\} + \sum_{\square} S_{\square}[U] \tag{3.38}$$

where $S_{\square}[U]$ is the lattice action that corresponds to the term $F_{\mu\nu}F^{\mu\nu}$ in the continuum theory. $S_{\square}$ possess great physical significance and will be discussed in detail in §3.4.1.1.

The above argument is now extended to a theory that undergoes transformations under a non-Abelian gauge group, G. For a non-Abelian theory it is necessary to consider the complex scalar field on the lattice sites as a column vector:

$$\phi_x = \begin{pmatrix} \phi_x^1 \\ \vdots \\ \phi_x^n \end{pmatrix}. \tag{3.39}$$

In terms of these fields, the action in Eq. (3.29) becomes,

$$S[\phi_x] = \sum_x \{\frac{a^2}{2} \sum_{\mu=1}^{4} (-\phi_x^\dagger \phi_{x+\hat{\mu}}) + (a^4 \frac{m^2}{2} + 4a^2)\phi_x^\dagger \phi_x + a^2 \frac{\lambda}{4} (\phi_x^\dagger \phi_x)^2\}. \tag{3.40}$$

Let $g = exp(i\boldsymbol{L} \cdot \boldsymbol{\alpha})$ be an element of the the group $SU(N)$ where $\boldsymbol{L}$ belongs to the Lie algebra of G. The field then transforms under the global gauge transformation as,

$$\begin{aligned} \phi_x &\rightarrow g\phi_x, \\ \phi_x^\dagger &\rightarrow \phi_x^\dagger g. \end{aligned} \tag{3.41}$$

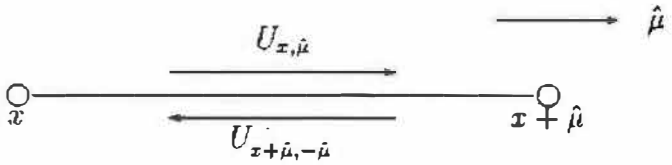

Figure 3.1: Gauge fields on the link showing orientation

It can be shown without difficulty that the action in Eq. (3.40) is indeed invariant under the global gauge transformation of $SU(N)$.

Consider now the case when the group element has the form, $g_x = exp(\boldsymbol{L} \cdot \boldsymbol{\alpha}_x)$. Following in the same manner as with local gauge transformations for Abelian groups it can be shown that the transformed action is

$$S[\phi, U] = \sum_x \{\frac{a^2}{2} \sum_{\mu=1}^{4} (-\phi_x^\dagger U_{x,\hat{\mu}} \phi_{x+\hat{\mu}}) + (a^4 \frac{m^2}{2} + 4a^2)\phi_x^\dagger \phi_x + a^2 \frac{\lambda}{4} (\phi_x^\dagger \phi_x)^2\} + \sum_\square S_\square[U] \tag{3.42}$$

where the link fields are now vectors:$\boldsymbol{U}_{x,\hat{\mu}}$.

3.4 Gauge Fields on the Lattice

In lattice models of gauge invariant field theories the gauge fields are placed on the links of the lattice. Let the gauge field on the link $(x, \hat{\mu})$ be $U_{x,\hat{\mu}}$ which is an element of the gauge group $\mathcal{G}$. The gauge fields on the lattice satisfy the relation (see Fig. (3.1)):

$$U_{x,\hat{\mu}} = U^{-1}_{x+\hat{\mu},-\hat{\mu}} \tag{3.43}$$

which follows from the unitarity of the gauge group. A gauge field A^c_μ in the continuum theory is related to $U_{x,\hat{\mu}}$ by the formal expression

$$U_{x,\hat{\mu}} = exp\{igA_\mu a\}. \tag{3.44}$$

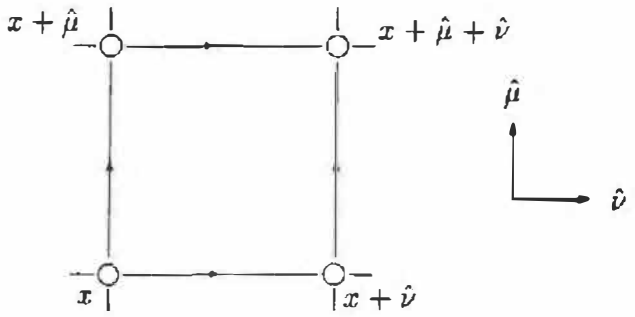

Figure 3.2: The plaquette defined in terms of the neighbouring sites and unit vectors.

A path γ traversed on the the lattice through the sites $x_1, x_2, \ldots, x_n$ is given by

$$U_\gamma = U_{x_1,\hat{\mu}} U_{x_2,\hat{\mu}}, \ldots, U_{x_n,\hat{\mu}} \tag{3.45}$$

which corresponds to a path ordered phase factor known as the *Schwinger line* integral,

$$U_\gamma = \mathcal{P}exp\{ig \int A^a_\mu \, dx^\mu\}, \tag{3.46}$$

of the continuum theory. The ordered path integral along a closed path is a gauge invariant. The simplest case of a closed path on the lattice is the path traversed along the elementary squares of the lattice. This path, called the *plaquette* or the *elementary Wilson loop* is denoted by "$\Box$" and is defined as

$$U_\Box = U_{x,\hat{\mu}} U_{x+\hat{\mu},\hat{\nu}} U^{-1}_{x+\hat{\nu},\hat{\mu}} U^{-1}_{x,\hat{\nu}} \tag{3.47}$$

Under the gauge transformation defined by the group G, the gauge fields transform according to

$$U_{x,\hat{\mu}} \rightarrow U'_{x,\hat{\mu}} = g_x U_{x,\hat{\mu}} g^{-1}_{x+\hat{\mu}}, \tag{3.48}$$

where g_x and $g_{x+\hat{\mu}}$ are the corresponding group elements of the sites x and $x+\hat{\mu}$.

3.4.1 Pure Lattice Gauge Theory

A pure lattice gauge theory is a theory that is constructed from the gauge fields (link fields) of the lattice alone without any matter (site) fields. In order to examine

the dynamics of such a theory an action $S[U]$ needs to be constructed. Wilson[76] proposed that this action should be the sum over all plaquette terms of the lattice:

$$S[U] = \sum_{\square} S_{\square}. \tag{3.49}$$

This is the minimal lattice action which leads to the continuum theory when the naive limit, $a \to \infty$, is taken('naive' here means that no renormalization is considered). On the other hand, there are many different approximations of the differentiation operator by means of the finite differences and so for one and the same continuum action many different lattice actions can be constructed. The question then arises, which of these actions is the correct one? The answer to this question lies in the concept of *universality*: if the thermodynamical limit is achieved at a critical point when the correlation length becomes infinite, the details of the lattice actions become irrelevent.

3.4.1.1 Abelian Lattice Gauge Theory

The local gauge transformation of a gauge field A_μ under the Abelian group $U(1)$ in the continuum theory is given by Eq. (2.11). The lattice version of this transformation is

$$A_{x,\hat{\mu}} \to A'_{x,\hat{\mu}} = A_{x,\hat{\mu}} - \frac{1}{a}(\alpha_{x,\hat{\mu}} - \alpha_x), \tag{3.50}$$

where the phase factor α_x is associated with the nearest neighbour lattice sites. The corresponding field strength tensor $F_{\mu\nu}$ describing the derivatives $\partial_\mu A_\nu$ of the gauge fields on the lattice has the form

$$F_{x,\mu\nu} = \frac{1}{a}(A_{x+\hat{\mu},\nu} - A_{x,\nu} - A_{x+\hat{\nu},\mu} + A_{x,\mu}), \tag{3.51}$$

which is defined around the plaquette on the lattice. Rescaling $A_{x,\mu}$ by the lattice spacing a and the electromagnetic charge g a new field

$$\Theta_{x,\mu} = agA_{x,\mu} \tag{3.52}$$

can be defined. With this a rescaled version of $F_{x,\mu\nu}$ can be defined in terms of $\Theta_{x,\mu}$:

$$\begin{aligned} f_{x,\mu\nu} &= a^2 g F_{x,\mu\nu} \\ &= \Theta_{x,\mu} + \Theta_{x+\hat{\mu},\nu} - \Theta_{x+\hat{\nu},\mu} - \Theta_{x,\nu}. \end{aligned} \tag{3.53}$$

The simplest action which preserves periodicity for such a system was proposed by Wilson[76] as

$$S[\Theta] = \frac{1}{2g^2} \sum_{x,\mu\nu} \Re e Tr e^{\imath f_{x,\mu\nu}}, \tag{3.54}$$

where the real part and the trace is taken so that the action is independent of the starting point and of the direction of the links that make up the plaquette. Due to its dependence on a^2, $f_{x,\mu\nu}$ will tend to zero in the continuum limit. So, for small lattice spacing a, the exponential in Eq. (3.54) can be expanded such that the action is written as

$$S[\Theta] = \frac{1}{2g^2} \sum_{x,\mu\nu} \Re e Tr(1 + \imath f_{x,\mu\nu} - \frac{1}{2} f^2_{x,\mu\nu} \ldots). \tag{3.55}$$

Now, the linear term $f_{x,\mu\nu}$ is zero since it is odd in the indices of μ and ν, and the higher order terms excluding $f^2_{x,\mu\nu}$ vanishes for $a \to 0$. So just leaving the quadratic term, the action can be written as,

$$S[\Theta] = \frac{1}{2} \sum_{x,\mu\nu} \Re e Tr(1 - \frac{1}{2} a^4 F^2_{x,\mu\nu}). \tag{3.56}$$

This action needs to be analagous to the continuum action in electrodynamics:

$$\frac{1}{4} \int d^4x F_{\mu\nu} F^{\mu\nu}. \tag{3.57}$$

That is, in the naive continuum limit as $a \to 0$, the action must have the form,

$$S \to \frac{1}{4} \sum_{x,\mu\nu} F^2_{x,\mu\nu}. \tag{3.58}$$

This is achieved by letting the proposed action defined in Eq. (3.54) to be

$$S[\Theta] = \frac{1}{g^2} \sum_{x,\mu\nu} \Re e Tr(1 - e^{f_{x,\mu\nu}}), \tag{3.59}$$

which is the sum over all the plaquettes on the lattice.

Defining the link fields as

$$U_{x,\hat{\mu}} = e^{i\Theta_{x,\mu}} \tag{3.60}$$

for $0 \geq \Theta_{x,\mu} < 2\pi$, the action in Eq.(3.59) can be shown to be

$$\begin{aligned} S[U] &= \frac{1}{g^2}\sum_{x,\mu\nu} \Re e Tr(1 - U_{x,\hat{\mu}}U_{x+\hat{\mu},\hat{\nu}}U^{-1}_{x+\hat{\nu},\hat{\mu}}U^{-1}_{x,\hat{\nu}}) \\ &= \frac{1}{g^2}\sum_{x,\mu\nu} \Re c Tr(1 - U_{\Box}). \end{aligned} \tag{3.61}$$

Since $\Theta_{x,\mu}$ acts as an angular variation for the link fields, the action is periodic in $\Theta_{x,\mu}$. So, taking the real part of the plaquette $U_{\Box}$, the action has the form

$$S[U] = \frac{1}{g^2}\sum_{x,\mu\nu} Tr\,(1 - \cos\Theta). \tag{3.62}$$

Eq. (3.62) gives the form of the action in a pure Abelian lattice gauge theory.

3.4.1.2 Non-Abelian Lattice Gauge Theory

As with gauge theories in the continuum theory, the extention from an Abelian theory to a non-Abelian theory on a lattice is not difficult. The action of a non-Abelian theory on a lattice is required to have as its continuum limit the Yang-Mills action as discussed earlier.

In analogy with the Abelian case, a rescaled version of $A_{x,\mu}$ (in the non-Abelian case this is given by a vector $\boldsymbol{A}_{x,\mu} = A^i_{x,\mu}$) needs to be defined:

$$\Theta_{x,\mu} = \frac{1}{2}ag\boldsymbol{L}\cdot\boldsymbol{A}_{x,\mu}, \tag{3.63}$$

where $\boldsymbol{L}$ are the generators of the gauge group. As with the Abelian case, letting

$$U_{x,\hat{\mu}} = e^{i\Theta_{x,\mu}}, \tag{3.64}$$

leads to an action,

$$S[U] = \frac{1}{g^2}\sum_{x,\mu\nu} \Re eTr(1 - U_{x,\hat{\mu}}U_{x+\hat{\mu},\hat{\nu}}U^{-1}_{x+\hat{\nu},\hat{\mu}}U^{-1}_{x,\hat{\nu}}). \tag{3.65}$$

To see what happens in the continuum limit the plaquette

$$\begin{aligned} U_{\Box} &= U_{x,\hat{\mu}}U_{x+\hat{\mu},\hat{\nu}}U^{-1}_{x+\hat{\nu},\hat{\mu}}U^{-1}_{x,\hat{\nu}} \\ &= e^{\imath\Theta_{x,\mu}}e^{\imath\Theta_{x+\hat{\mu},\nu}}e^{-\imath\Theta_{x,\hat{\nu},\mu}}e^{-\imath\Theta_{x,\nu}} \end{aligned} \tag{3.66}$$

is calculated explicitly. This is done by Taylor expanding the $\Theta_{x,\mu}$ on the different links of the plaquette with respect to the spacing, a:

$$\Theta_{x+\hat{\mu},\nu} \cong \Theta_{x,\nu} + a\partial_\mu\Theta_{x,\nu} + \ldots, \tag{3.67}$$

$$\Theta_{x+\hat{\nu},\mu} \cong \Theta_{x,\mu} + a\partial_\nu\Theta_{x,\mu} + \cdots. \tag{3.68}$$

The higher powers $a^2, a^3, \ldots$ have been ignored since one seeks the leading nontrivial order in a. Substituting this in Eq. (3.66),

$$U_{\Box} = exp\{\imath\Theta_{x,\mu}\}exp\{\imath(\Theta_{x,\nu} + a\partial_\mu\Theta_{x,\nu})\}exp\{\imath(\Theta_{x,\mu} + a\partial_\nu\Theta_{x,\mu})\}exp\{\imath\Theta_{x,\nu}\}. \tag{3.69}$$

Using the Baker-Hausdorff formula,

$$e^a e^b = e^{(a+b+\frac{1}{2}[a,b]+\ldots)}, \tag{3.70}$$

Eq. (3.69) becomes,

$$\begin{aligned} U_{\Box} &\cong exp\{\imath(\Theta_{x,\mu} + \Theta_{x,\nu} + a\partial_\mu\Theta_{x,\nu}) - \frac{1}{2}[\Theta_{x,\mu}, \Theta_{x,\nu}]\} \\ &\quad \times exp\{-\imath(\Theta_{x,\mu} + \Theta_{x,\nu} + a\partial_\nu\Theta_{x,\mu} - \frac{1}{2}[\Theta_{x,\mu}, \Theta_{x,\nu}]\} \\ &= exp\{\imath a(\partial_\mu\Theta_{x,\nu} - \partial_\nu\Theta_{x,\mu}) - [\Theta_{x,\mu}, \Theta_{x,\nu}]\}. \end{aligned} \tag{3.71}$$

Now since Eq. (3.52) and Eq. (3.63) give the same rescaled $A_{x,\mu}$:

$$\frac{1}{2}ag\boldsymbol{L}\cdot\boldsymbol{A}_{x,\mu} = agA_{x,\mu}, \tag{3.72}$$

which implies that

$$A_{x,\mu} = \frac{1}{2}\boldsymbol{L} \cdot \boldsymbol{A}_{x,\mu}. \tag{3.73}$$

Therefore,

$$\begin{aligned} U_{\square} &= exp\{ia^2 g(\partial_\mu A_{x,\nu} - \partial_\nu A_{x,\mu} + ig[A_{x,\mu}, A_{x,\nu}])\} \\ &= exp(ia^2 g F_{x,\mu\nu}) \end{aligned} \tag{3.74}$$

where,

$$F_{x,\mu\nu} = \partial_\mu A_{x,\nu} - \partial_\nu A_{x,\mu} + ig[A_{x,\mu}, A_{x,\nu}] \tag{3.75}$$

is the field strength tensor for the Yang-Mills theory. Now expanding the exponential and taking the trace of Eq. (3.74):

$$\begin{aligned} Tr\ U_{\square} &\cong Tr\ (1 + ia^2 g F_{x,\mu\nu} - \frac{1}{2}a^4 g^2 F^2_{x,\mu\nu} + \ldots) \\ &= Tr\ 1 + ia^2 g Tr\ F_{x,\mu\nu} - \frac{1}{2}a^4 g^2 Tr\ F_{x,\mu\nu} + \ldots \\ &= Tr\ 1 - \frac{1}{2}a^4 g^2 Tr\ F_{x,\mu\nu} + \ldots, \end{aligned} \tag{3.76}$$

since $Tr\ F_{x,\mu\nu} = 0$. Using Eq. (3.75) and the fact that $[T_i, T_j] = 2iC_{ijk}T_k$,

$$Tr\ F^2_{x,\mu\nu} = \frac{1}{2}(\partial_\mu A^i_{x,\nu} - \partial_\nu A^i_{x,\mu} - gC_{ijk}A^j_{z,\mu}A^k_{x,\nu})^2 \tag{3.77}$$

Finally the non-Abelian action on the lattice can be written as,

$$S \cong \frac{1}{2g^2}\sum_{x,\mu\nu} a^4 g^2 \frac{1}{2}(\partial_\mu A^i_{x,\nu} - \partial_\nu A^i_{x,\mu} - gC_{ijk}A^j_{x,\mu}A^k_{x,\nu})^2 \tag{3.78}$$

which in the continuum limit reproduces the Euclidean action for the Yang-Mills theory:

$$S \to \frac{1}{2}\int d^4x (F^i_{\mu\nu})^2. \tag{3.79}$$

3.5 Order Parameters

In analogy with the continuum theory, the observables on the lattice are defined by averages over the field configurations:

$$< O >= Z^{-1} \sum_{x,\mu\nu} O(U_{x,\hat{\mu}}) exp\{-S[U_{x,\hat{\mu}}]\}. \tag{3.80}$$

It is evident in lattice gauge theory that the observable $< O >$ exhibits different characteristic behaviours depending on certain external parameters. (coupling constants, masses, etc) These different behaviours are known as *phases*. As the external parameters are varied, it is possible that the system will go from one phase to another. This transition from one phase to another is called a *phase transition* and takes place at some critical values of the parameters. Let $< O >$ be a function of a parameter p. If at some point p_1, $< O >$ is discontinuous, that is, if

$$\lim_{p \to p_1 - \epsilon} < O > \neq \lim_{p \to p_1 + \epsilon} < O > \tag{3.81}$$

then the system is said to undergo a *first order* phase transition at $p = p_1$ (see Fig. 3.3(a)).

If at some other point p_2, $< O >$ is continuous but its first derivative is discontinuous, that is, if

$$\frac{d < O >}{dp} |_{p=p_2-\epsilon} \neq \frac{d < O >}{dp} |_{p=p_2+\epsilon} \tag{3.82}$$

then the system undergoes a *second order* phase transition at $p = p_2$ (see Fig. 3.3(b)).

Of particular interest are the average observables that can vary between zero and some non-zero average values. One of the characteristic features of gauge theories is that only gauge invariant observables can have non-zero average values. This statement is known as the *Elitzur's theorem*[25]. The exact statement of this theorem is: The average value of any non-zero invariant observable is identically zero for all values of the external observables. Therefore the only observables that need to be

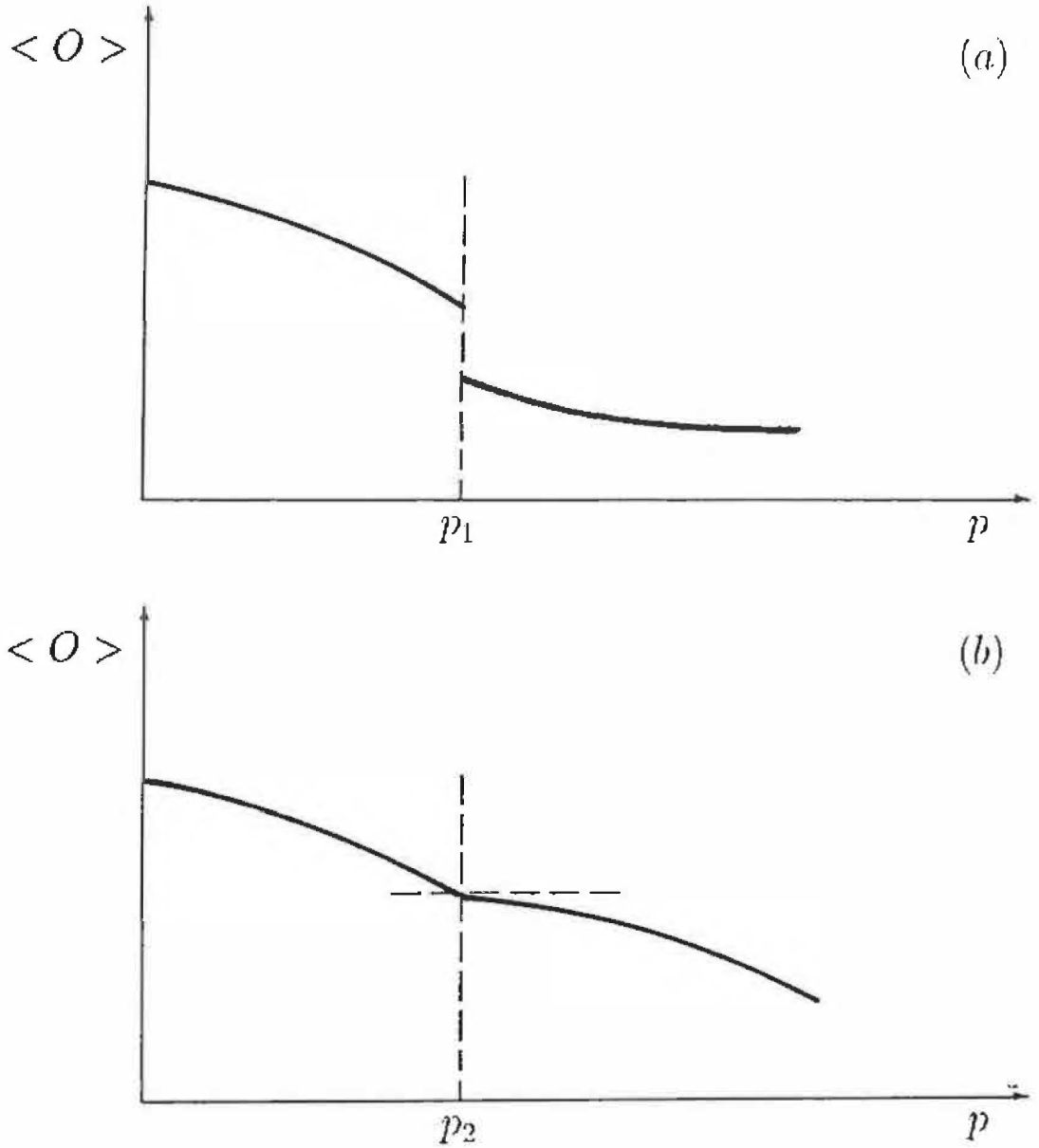

Figure 3.3: Plots of $< O >$ verses p showing (a) first order and a (b) second order phase transitions.

considered are the ones that are gauge invariant under the gauge group G:

$$U_{x,\hat{\mu}} \rightarrow g_x U_{x,\hat{\mu}} g_{x+\hat{\mu}}. \tag{3.83}$$

These observables are called *order parameters* and they are monitored to distinguish hetween the different phases in a symmetry breaking phase transition.

The simplest such order parameter in a pure lattice gauge theory is the average action per plaquette. Consider the partition function

$$Z = \sum_{x,\mu} e^{-\beta S[U]}, \tag{3.84}$$

where $\beta = \frac{1}{g^2}$ is the analogue of the inverse temperature. In analogy with statistical mechanics, the *free energy* of the system is defined as

$$F = \frac{1}{N} \ln Z, \tag{3.85}$$

where N is the number of sites on the lattice. If F is differentiated with respect to β, then a phase transition is expected as a singularity in the infinite volume limit of F. Thus in d dimensions,

$$\begin{aligned} E &= -\frac{2}{d(d-1)} \frac{\partial}{\partial \beta} F \\ &= -\frac{2}{d(d-1)} \frac{\partial}{\partial \beta} \ln Z \\ &= < 1 - \Re e Tr U_{\Box} >, \end{aligned} \tag{3.86}$$

where the factor $\frac{2}{d(d-1)}$ is the ratio of sites to the number of plaquettes in a d-dimensional lattice. Eq. (3.86) gives the average action per plaquette or the internal energy which can serve as an order parameter. It will be discontinuous in β at a first order phase transition.

A generalization of the average action per plaquette is the trace of the product of links around a closed loop. Wilson considered this order parameter in order to answer

the question of quark confinement. This order parameter is known as the *Wilson loop* and is given by,

$$W(C) = < Tr \prod_{x,\mu} U_{x,\hat{\mu}} > . \tag{3.87}$$

Here C denotes a closed loop on the lattice and the product of the link fields are ordered along C. $W(C)$ is related to the quark-antiquark potential $V(R)$. The value of $W(C)$ will be unity if the link fields $U_{x,\hat{\mu}}$ on the loop are equal to the identity of the gauge group under investigation. It is expected that the value of $W(C)$ will decrease rapidly as the correlation between the link fields of the loop decreases. So, if the size of the loop becomes infinitely large, more link fields will be enclosed by the loop and the less correlated they will be. This will then result in the value of $W(C)$ to tend to zero. If C is considered as a rectangular loop of dimensions $T \times R$ (see Fig. 3.4) then for large T,

$$W(C) \sim e^{-V(R)T}, \tag{3.88}$$

where $V(R)$ is the ground state gauge field energy between the static quark and antiquark seperated by a distance R. The potential $V(R)$ is said to be confining if $V(R) \rightarrow \sigma R$ and

$$W(C) \sim e^{-\sigma RT}. \tag{3.89}$$

It will be shown later that in the strong coupling limit the Wilson loop obeys an area law such that for a large loop

$$W(C) \sim e^{-\sigma A(C)}, \tag{3.90}$$

where σ is a constant known as the *string tension* and $A(C)$ is the area enclosed by the path C. The string tension is defined as,

$$\sigma \rightarrow \frac{-\ln W(C)}{A(C)}, \tag{3.91}$$

for large C. For confinement, $\sigma \neq 0$ and for non-confinement, $\sigma = 0$. The string tension therefore is another important order parameter since it has a major implication in the criteria of quark confinement and allows the differentiation between confining

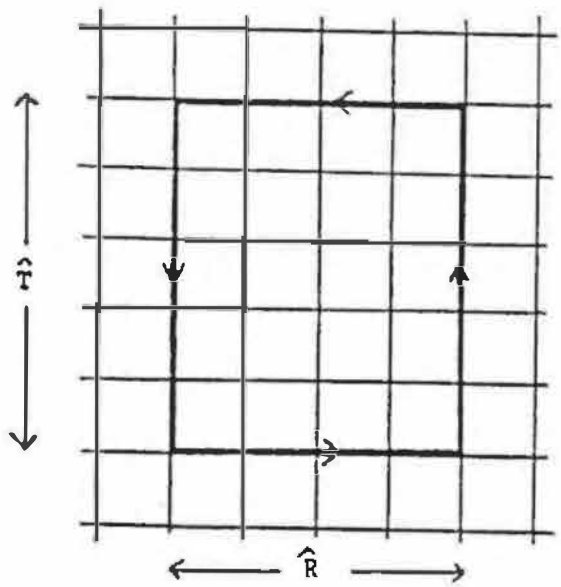

Figure 3.4: A rectangular Wilson loop with dimensions $T \times R$.

and non-confining phases. If the energy $V(R)$ does not go to infinity with the seperation then this will lead to a theory that does not confine the quarks. In such a theory, $W(C)$ becomes characteristic of a perimeter behaviour given by,

$$W(C) \sim e^{-\mu P(C)}, \tag{3.92}$$

where $P(C)$ is the perimeter of the loop C and μ is the self energy of the gauge fields.

Another useful order parameter, developed independently by Kuti *et al*[53] and McLerran *et al*[59], is the product of the link fields taken along a path in a specific direction on the lattice from one end to the other. Due to the periodic boundary condition imposed on the lattice, this path is closed and as such, the product is gauge invariant. This order parameter is known as the *Wilson line* or the *Polyakov loop* and is given by,

$$L(U) = < \prod_{x=1}^{N_s} TrU_{x,\mu} >, \tag{3.93}$$

where the product is over N_s, the number of sites along the path traversed in a constant spatial direction. If the free energy of the static external quarklike source is given by,

$$F = \frac{1}{N_t} \ln Z, \tag{3.94}$$

where N_t is the number of lattice sites in the temporal direction, then it can be shown that for infinitesmal variations in F,

$$L(U) = e^{-\beta \Delta F N_t}. \tag{3.95}$$

It is clear that if the quarks are confined then the free energy of the static external source will be infinite and $L(U)$ will be zero. On the other hand, if deconfinement exists then the free energy of the external source will be finite and $L(U)$ will be non-zero. The Polyakov loop is a useful order parameter when field theories are considered at finite temperatures.

3.6 Strong Coupling

One of the advantages of lattice gauge theory is that it is possible to carry out strong coupling expansions analogous to high temperature expansions in statistical and solid state physics[76]. In contrast to the standard perturbation treatment of the continuum theory, strong coupling expansions on the lattice is much simpler and reveals structures of the theory that are undetected by perturbation methods.

To construct a general strong coupling expansion on the lattice, the trace of the plaquette, which has been considered thus far, is replaced by a more generalised feature of group theory, the character χ of some irreducible representation of the group. The choice of χ is such that the trace of the irreducible representation of the group is real. With this the exponentiated action in the partition function is written

as,

$$exp\{\beta S\} = exp[\beta \sum_{\Box} \chi(U_{\Box})]. \tag{3.96}$$

Strong coupling expansion on the lattice entails expanding the Boltzman factor in the strong coupling approximation, $\beta = \frac{1}{g^2} \ll 1$, in powers of β,

$$exp\{\beta S\} = \prod_{\Box} [1 + \beta\chi(U_{\Box}) + \frac{\beta^2}{2}\chi^2(U_{\Box}) + \ldots]. \tag{3.97}$$

This series is then evaluated by integrating each term in the series over the corresponding lattice variables. In this way each order in β is associated with plaquettes randomly distributed on the lattice. This may result in a plaquette corresponding to a particular power of β appearing more that once on the lattice. In order to eliminate double counting, character expansions are performed which limits the number of contribution to each power of β[23]. The method described above leads to the derivation of specific rules for calculating directly the expansion coefficients for many physical quantities such as the string tension and correlation lengths, to only name a few. In the following, one such quantity, the Wilson loop, is discussed in detail using the strong coupling expansion on the lattice.

Consider the Wilson loop defined on a $T \times R$ rectangular lattice,

$$W(C) = Z^{-1} \int \prod_{x,\mu} dU_{x,\hat{\mu}} Tr U_{\Box} e^{-S_{\Box}}, \tag{3.98}$$

where $U_{x,\hat{\mu}} \in SU(N)$ and the action is given by

$$S_{\Box} = -\sum_{\Box} \frac{\beta}{2N}(TrU_{\Box} + TrU_{\Box}^{\dagger}). \tag{3.99}$$

Expansion of the Boltzman factor per plaquette in Eq. (3.98) gives.

$$\begin{aligned} W(C) = \quad & Z^{-1} \int dU_{x,\hat{\mu}} Tr U_{\Box} [1 - \beta \textstyle\sum_{\Box} Tr U_{\Box} + c.c \\ & + \tfrac{1}{2!}\beta^2 \textstyle\sum_{\Box} \sum_{\Box'} Tr U_{\Box} Tr U_{\Box'} + c.c + \ldots]. \end{aligned} \tag{3.100}$$

The integration over the link variables $U_{x,\hat{\mu}}$ is performed by means of the following orthogonality properties:

$$\int \quad dU_{x,\hat{\mu}} (U_{x,\hat{\mu}})_{ij} = 0, \tag{3.101}$$

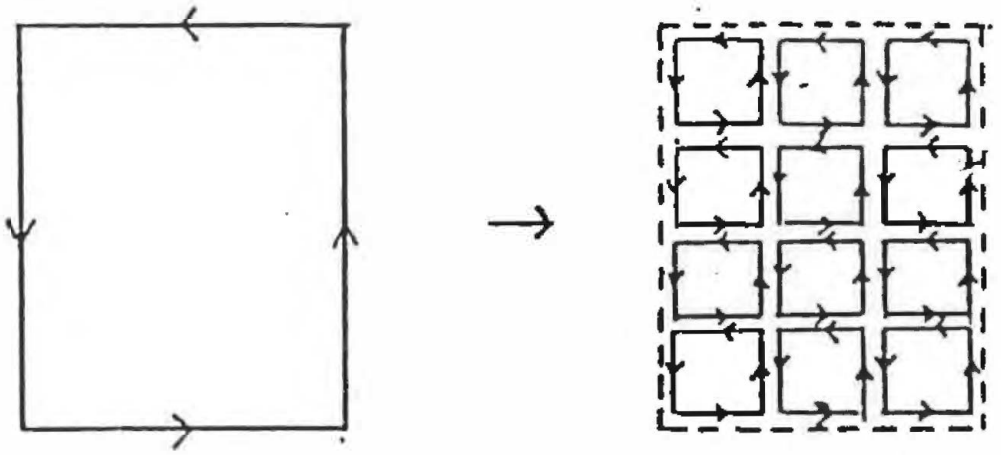

Figure 3.5: The tiling of the Wilson loop with elementary plaquettes

$$\int dU_{x,\hat{\mu}}(U_{x,\hat{\mu}})_{ij}(U^{\dagger}_{x,\hat{\mu}})_{kl} = \frac{1}{N}\delta_{il}\delta_{jk}, \tag{3.102}$$

$$\int dU_{x,\hat{\mu}}(U_{x,\hat{\mu}})_{ij}(U_{x,\hat{\mu}})_{kl} = 0. \tag{3.103}$$

It can be deduced form Eq. (3.101) that all Wilson loops will vanish as β goes to zero. In order to counteract these vanishing loops it is postulated that each link in $U_{\Box}$ must merge with at least one coresponding link from the exponential expansion in Eq. (3.100). Also each link defined in the action must be associated with another link, either from the action itself or from an adjacent plaquette. The first non-trivial contribution in the strong coupling series comes from the merging of at most two plaquettes in one link. This corresponds to tiling the loop with plaquettes as shown in Fig. 3.5. This contribution is evaluated from Eq. (3.102). Eq. (3.102) implies that two links oriented in opposing directions will eliminate each other, but, two links from adjacent plaquettes oriented in the same direction will merge to form a larger rectangular loop. By this it can be seen that only two-dimensional surfaces are permitted if the discussion is restricted to only the second term of the expansion. Also, each link carries a weight $\frac{1}{N}$ and each site on the surface a weight N. So for the

lowest order non-trivial contribution $W(C)$ has the form

$$W(C) \sim (\frac{\beta}{2N^2})^{TR}, \tag{3.104}$$

where TR gives the least number of plaquettes needed to cover the area enclosed by the loop C. This result only holds for $N > 2$. For the $SU(2)$ case $W(C)$ is given by $(\frac{\beta}{4})^{TR}$ due to the non-orientation of the plaquettes[12,23]. In any case it can be seen that if the area of the loop is given by

$$A(C) = a^2 TR. \tag{3.105}$$

then the strong coupling limit leads to an area law.

$$\begin{aligned} W(C) \sim (\frac{\beta}{2N^2})^{\frac{A(C)}{a^2}} &= e^{-\frac{TR}{a^2}\ln(\frac{2N^2}{\beta})} \\ &= e^{-KA(C)}. \end{aligned} \tag{3.106}$$

where the string tension K is given by

$$K = \frac{1}{a^2}\ln(\frac{2N^2}{\beta}). \tag{3.107}$$

It is possible to continue the above argument and incorporate higher orders of β but this becomes more tedious with increasing orders of β. In fact, Munster[68] has calculated the string tension up to the 12^{th} order in β for $SU(N)$. It however suffices to show that the first non-trivial contribution from the expansion does indeed lead to an area law which exhibits the properties of confinement.

In order to see if confinement holds for all values of β, it is necessary to consider the other extreme; the weak coupling limit when $\beta \to \infty$. This limit is of great importance since when the lattice spacing goes to zero, the weak coupling limit coincides with the continuum perturbation theory. Weak coupling or low temperature expansions on the lattice are performed in the same way as the standard perturbation expansions in the continuum theory. Besides being applied to a fundamentally non-perturbative theory, perturbation theory further complicates the analysis in that it results in the loss of

Lorentz covariance when applied to the discrete space-time of the lattice. Detailed studies of the weak coupling limit in relation to the continuum theory have been carried out by Hasenfratz and Hasenfratz[41] and Dashen and Gross[21]. This type of analysis is beyond the scope of this work.

Chapter 4

Monte Carlo Methods

4.1 Introduction

In the lattice formlation of quantum field theory it was shown that the problem with the ill defined Feynman path integral could be resolved by reducing the path integral to ordinary multiple integrals. This resorts to calculating observables of the form

$$< O >= Z^{-1} \int dU\, O[U] e^{-S[U]}, \tag{4.1}$$

where the integration is over the product of the link variables. Now suppose Eq. (4.1) is to be evaluated on a modest hypercubical lattice with 10 sites in each of the four space-time directions. This corresponds to a system with 10^4 space-time positions and 4×10^4 link variables. In the particular case of the group $SU(3)$, each of the link variables is parametrized by eight real parameters. Therefore Eq. (4.1) will be a 320000-fold integral. Such integrals are usually approximated by finite sums. In this case one cannot use, say, Simpson's rule since on a mesh of 10 points per integration, it will lead to a sum of 10^{320000} terms. If, say the rate of calculation is 10^8 terms per second, then it would take 10^{319992} seconds to evaluate the sum. This is certainly unimaginable when compared to the age of the universe which is only $\sim 10^{18}$ seconds.

Deterministic numerical methods for evaluation of such integrals are thus out of the question.

New techniques are therefore required which will lead to accurate estimates of $< \bullet >$ with realistic computing time. One way of achieving this is by using some stochastic sampling procedure which will generate a select sequence of lattice configurations with a certain probability distribution. The *Monte Carlo* methods of important sampling provides various and generally very successful applications. Monte Carlo techniques incorporate many statisical methods which need to be discussed. A preface to this discussion is a statistical background to solving integrals of the type defined in Eq. (4.1).

4.2 Statistical Background

To illustrate the underlying principle of the Monte Carlo method, consider the n-dimensional integral (the expectation value of the function $f(\boldsymbol{x})$)

$$< f >= \int f(\boldsymbol{x}) P(\boldsymbol{x})\, d^n x, \tag{4.2}$$

where $P(\boldsymbol{x})$ is a probability density:

$$\int P(\boldsymbol{x})\, d^n x = 1, \tag{4.3}$$

$$P(\boldsymbol{x}) \geq 0. \tag{4.4}$$

To evaluate Eq. (4.2), the probability density $P(\boldsymbol{x})$ is sampled over N random points $\boldsymbol{x}_1, \boldsymbol{x}_2, \ldots, \boldsymbol{x}_n$ giving a quadrature formula for the average value of $f(\boldsymbol{x})$:

$$\bar{f} = \frac{1}{N} \sum_{i=1}^{N} f(\boldsymbol{x}_i). \tag{4.5}$$

Using the central limit theorem for large N [69] the square of the variance σ^2 gives the error in the estimate

$$\sigma = \frac{1}{\sqrt{N}} [\frac{1}{N} \sum_{i=1}^{N} f^2(\boldsymbol{x}_i) - (\frac{1}{N} \sum_{i=1}^{N} f(\boldsymbol{x}_i))^2]^{\frac{1}{2}} \tag{4.6}$$

which shows that the uncertainty in the estimate decreases with $\frac{1}{\sqrt{N}}$. Therefore the error can be made as small as possible if the probability distribution is sampled over a large number of points. Also, the viability of the above argument being a reasonable estimate of Eq. (4.2) relies on $f(\boldsymbol{x})$ being a smooth function. It is evident that if $\mid f(\boldsymbol{x}) \mid$ varies over many orders of magnitude within a uniform sample of limited range, then many sample points will correspond to $f(\boldsymbol{x}) \approx 0$. Therefore a process is needed which allows the selection of sample points $\boldsymbol{x}_i$ which are distributed in a preffered interval where $f(\boldsymbol{x})$ is large. This process of selecting only important sample points is known as *important sampling.*

4.2.1 Important Sampling

For the sake of convenience consider a one dimensional integral:

$$I = \int_a^b f(x)\, dx. \tag{4.7}$$

Now multiply and divide the integral by a positive function $P(x)$ normalised such that

$$\int_a^b P(x)\, dx = 1. \tag{4.8}$$

This gives,

$$\begin{aligned} I &= \int_a^b \frac{f(x)}{P(x)} P(x)\, dx \\ &= < \frac{f(x)}{P(x)} > . \end{aligned} \tag{4.9}$$

From Eq. (4.6) the error in the estimate of Eq. (4.9) is,

$$\sigma = \frac{1}{\sqrt{N}} [< (\frac{f(x)}{P(x)})^2 > - < \frac{f(x)}{P(x)} >^2]. \tag{4.10}$$

To show how this error can be reduced a change of variables from x to

$$y(x) = \int_a^x P(z)\, dz \tag{4.11}$$

is made such that

$$\frac{dy}{dx} = P(x) \tag{4.12}$$

and

$$\begin{aligned} y(a) &= 0, \\ y(b) &= 1. \end{aligned} \tag{4.13}$$

By this change of variables the integral can then be written as

$$I = \int_a^b \frac{f(x(y))}{P(x(y))}\, dy. \tag{4.14}$$

The corresponding quadrature formula is therefore given as

$$I \approx \frac{1}{N} \sum_{i=1} N \frac{f(x(y_i))}{P(x(y_i))}, \tag{4.15}$$

where y_i are uniform random numbers in the interval $(0, 1)$. It can be seen that if the probability distribution is chosen such that a random sampling of $P(x)$ will concerntrate points in those regions where $\mid f(x) \mid$ is large, then $\frac{f(x(y_i))}{P(x(y_i))}$ can be made into a smooth function. This will then result in the error of the approximation of the integral to be small, provided $P(x)$ and $x(y)$ can be calculated appropriatly. The best choice of $P(x)$ is a function which copies the behaviour of $\mid f(x) \mid$.

In most cases however, the best choice of the probability distribution $P(x)$ is quite complicated and thus makes the importance sampling as difficult as the original problem. What is therefore needed is a process which allows some form of consistency between the choice of random points. One such process is the *Markov process* which is now discussed in detail.

4.2.2 Markov Processes

Let $c_1, c_2, \ldots, c_n$ be a set of points (configurations) in the space of field configurations. The *Markov process* is fully determined by the starting(the initial configuration c_1)

and the one-step probability $P(c, c')$. If the proccess has reached, after n steps, a configuration c_n, then the next step could be a particular configuration c_{n+1} with probability $P(c_n, c_{n+1})$. A sequence of configurations generated by this process is called a *Markov chain*.

The probability density $P(c, c')$ has the usual properties

$$\begin{aligned} \int P(c, c')\, dc' &= 1, \\ P(c, c') &\geq 0, \end{aligned} \tag{4.16}$$

for all c_i in configuration space. For a finite number of configurations n,

$$\begin{aligned} P^{(n)}(c, c') &= \int P(c, c_1) P(c_1, c_2) \ldots P(c_{n-1}, c') dc_1 dc_2 \ldots dc_{n-1} \\ &= \int P^{(n-1)}(c, c_\alpha) P(c_\alpha, c')\, dc_\alpha. \end{aligned} \tag{4.17}$$

This means that for a finite number of Markov steps a random walk in configuration space can lead from c to c'. It can be shown [13,39] that $P^{(n)}(c, c')$ has a definite limit that is unique when the number of configurations becomes infinite:

$$\lim_{n \to \infty} P^{(n)}(c, c') = P^*(c') \tag{4.18}$$

where according to Eq. (4.16), $P^*(c')$ satisfies

$$\begin{aligned} \int P^*(c')\, dc' &= 1 \\ P^*(c') &\geq 0. \end{aligned} \tag{4.19}$$

An important consequence of Eq. (4.18) is that the limit $n \to \infty$ of $P^{(n)}(c, c')$ is independent of the initial or starting configuration. Also, from Eq. (4.19) it can be seen that $P^*(c')$ is a probability distribution. If $P^*(c')$ is taken to be the appropriate or desired probability distribution then $P^{(n)}(c, c')$ can be used to sample $P^*(c')$. It can be shown [55] that a necessary condition for this is that the probability $P(c, c')$ must be in equilibrium with the desired probability distribution,

$$P^*(c') = \int P^*(c) P(c, c')\, dc, \tag{4.20}$$

such that it is left unchanged even if it is changed by a single step. This equilibrium condition is given by a condition of *detailed balance* or *microreversibility*:

$$P^*(c)P(c,c') = P^*(c')P(c',c). \tag{4.21}$$

This states that the probability of going from the configuration c to c' is the same as going from c' to c. It follows from Eq. (4.21) that

$$\begin{aligned} \int P^*(c)P(c,c')\,dc &= \int P^*(c')P(c',c)\,dc \\ &= P^*(c')\int P(c',c)\,dc \\ &= P^*(c'). \end{aligned}$$

Therefore detailed balance can be considered as a sufficient condition to reproduce Eq. (4.20). To specify the notion of equilibrium it is convenient to denote the probability of finding the configuration c in equilibrium by $P_{eq}(c)$. Eq. (4.20) can therefore be written as

$$P_{eq}(c') = \int P_{eq}(c)P(c,c')\,dc. \tag{4.22}$$

It now stands to be seen whether the desired probability distribution converges to $P_{eq}(c)$. Let the probability distribution at the n^{th} step of the Markov process be $P(c)$. The measure of the deviation from $P_{eq}(c)$ is given by

$$\Delta_n = \int \mid P(c) - P_{eq}(c) \mid dc. \tag{4.23}$$

The probability distribution at the next step, the $(n+1)^{th}$ step, is given by

$$P(c') = \int P(c)P(c,c')\,dc \tag{4.24}$$

and its deviation from $P_{eq}(c')$ is

$$\begin{aligned} \Delta &= \int \mid P(c') - P_{eq}(c') \mid dc' \\ &= \int \mid \int P(c)P(c,c')\,dc - P_{eq}(c') \mid dc'. \end{aligned} \tag{4.25}$$

Now using the normalization property in Eq. (4.16),

$$\begin{aligned}\Delta_{n+1} &= \int \mid \int [P(c) - P_{eq}(c)] P(c, c')\, dc \mid \, dc' \\ &\leq \int [\int \mid P(c) - P_{eq}(c) \mid P(c, c')\, dc]\, dc' \\ &= \int \mid P(c) - P_{eq}(c) \mid \, dc. \end{aligned} \tag{4.26}$$

So from Eq. (4.26) and Eq. (4.23),

$$\Delta_{n+1} \leq \Delta_n, \tag{4.27}$$

which means that the deviation decreases with each Markov step. Since $P(c, c') \neq 0$, the inequality in Eq. (4.27) is strict unless the system is in equilibrium, that is, $P(c) = P_{eq}(c)$ for all c. Therefore it can be concluded that the probability distribution converges to the equilibrium solution $P_{eq}(c)$.

The condition of detailed balance does not however specify $P(c, c')$ uniquely. Therefore, what is required is a Monte Carlo algorithm that will allow $P(c, c')$ to be specified fully. Such an algorithm is the *Metropolis algorithm.*

4.3 The Metropolis Algorithm

The Metropolis algorithm was originally developed by Metropolis *et. al.* [61] in 1953. It defines a possible one-step probability which satisfies the condition of detailed balance. Due to its calculational simplicity the Metropolis algorithm has been successfully used in many branches of physics.

Consider a probability distribution $P(C)$ which is used to generate a set of configurations $C^{(0)}, C^{(1)}, \ldots$ during a random walk through the space of configurations. The longer the walk, the closer the configurations will be to the desired distribution. Now, suppose the walk reaches a configuration $C^{(k)}$. To generate the next configuration $C^{(k+1)}$ a *trial step* to say $C^{(t)}$ is made. Here $C^{(t)}$ is a arbitrary configuration

somewhere about the immediate vicinity of $C^{(k)}$. The acceptance or rejection of $C^{(t)}$ as the next configuration is based on the value of the ratio

$$r = \frac{P(C^{(t)})}{P(C^{(k)})}. \tag{4.28}$$

If $r > 1$ then $C^{(k)}$ is accepted and $C^{(t)} = C^{(k+1)}$. If $r < 1$ then a random number ρ is generated uniformly in the interval (1,0). If $r > \rho$ then $C^{(t)}$ is accepted. In the cases where $C^{(t)}$ is rejected, $C^{(t)}$ is taken as $C^{(k+1)}$ and the updating preceeds as above.

It is now shown that the desired distribution does indeed converge to the equilibrium solution $P_{eq}(C)$. The following proof is based on the discussion by Jongeward *et.al.* [46]. Consider a set of configurations generated by the Metropolis algorithm. Let $P^{(N)}(C)$ be the probability of encountering the configuration C after N steps. The probability of encountering the same configuration after $N+1$ steps is given by,

$$\begin{aligned} P^{(N+1)} &= \int P^{(N)}(C')P(C',C)\,dC' + P^{(N)}(C) - \int P^{(N)}(C)P(C,C')\,dC' \\ &= P^{(N)} + \int [P^{(N)}(C')P(C',C) - P^{(N)}P(C,C')]\,dC'. \end{aligned} \tag{4.29}$$

It can be clearly seen that if $P^{(N)}$ satisfies the detailed balance condition, then $P^{(N+1)} = P^{(N)}$. Now if

$$\frac{P^{(N)}(C)}{P^{(N)}(C')} < \frac{P(C',C)}{P(C,C')}, \tag{4.30}$$

then after a single application (*iteration*) of the Metropolis algorithm, $P^{(N+1)} < P^{(N)}$. This implies that each successive iteration of the algorithm brings the desired distribution closer to being a solution of the detailed balance condition. Therefore it can be concluded that $P^{(N)}(C)$ converges to the equilibrium solution $P_{eq}(C)$.

In other words, if $P(C',C)$ is a one-step probability which satisfies the microreversibility condition

$$P(C,C') = P(C',C), \tag{4.31}$$

then the probability in going from C to C' is given by

$$P(C,C') = \begin{cases} 1 & \text{if } P(C') > P(C) \\ \frac{P(C')}{P(C)} & \text{if } P(C') < P(C) \end{cases} \tag{4.32}$$

It now remains to be shown that this satisfies the condition of detailed balance. In the case of $P(C',C) > P(C,C')$, $P(C,C') = 1$ and $P(C',C) = \frac{P(C)}{P(C')}$. Therefore

$$\frac{P(C,C')}{P(C,C)} = \frac{1}{\frac{P(C)}{P(C')}} \tag{4.33}$$

which gives the detailed balance condition in Eq. (4.21). In the other case when $P(C') > P(C)$ then $P(C',C) = 1$ and $P(C,C') = \frac{P(C')}{P(C)}$. Therefore

$$\frac{P(C,C')}{P(C',C)} = \frac{\frac{P(C')}{P(C)}}{1} \tag{4.34}$$

which implies Eq. (4.21) again.

4.3.1 The Modified Metropolis Algorithm

The problem with implementing the Metropolis algorithm is that the configurations generated by the random walk are not independent of each other. This is due to the choice of a configuration being taken in the neighbourhood of the preceeding configuration. As a result the configurations are not statistically independent of each other which makes the evaluation of the integral in Eq. (4.1) biased.

A way out of this predicament is to consider a large number of random walks simultaneously generating a sequence of configurations. Then after a series of steps the initial configuration will be forgotten and the sequence will converge to the desired distribution, $P(C)$. This results in a sequence of configurations which are independent since they are generated by different independent random walks. This however will lead to computational difficulties due to the coexistence of many random walks.

A more feasible alternative is to consider just a single random walk which begins at a particular configuration. It is expected that after a sufficient number of steps the walk will *thermalise*, that is, converge to the desired distribution. The time taken for the process from start to thermalisation is called the *relaxation time*. This relaxation

time can be greatly reduced if the initial configuration is sufficiently close to a member of the target sample. If the thermalisation takes place after say, N_{therm} steps, then the walk can be terminated and the configuration that it reaches at this point can be used as the starting configuration of the next random walk. This procedure is practical since there are no restrictions on the choice of the initial configurations and the relaxation time is greatly reduced for the second walk. Repeating this procedure N times leads to a set of N configurations $C^{(1)}, C^{(2)}, \ldots, C^{(N)}$. This procedure although efficient in reducing the computational time does however also results in the individual configurations being dependent or correlated with each other.

In order to reduce the correlation between successive sampled configurations it is necessary to increase the length of the random walks that give rise to each of the configurations $C^{(i)}$. This is done by increasing the steps from one to several steps, say N_{skip}. After thermalisation of the first walk, a number of steps which are equivalent to N_{skip} are skipped. Then only is the configuration taken to be the next one. It is evident that the larger N_{skip} is, the less correlated will he the configurations. Large N_{skip} values are however not practical since they will increase the computational time immensely.

4.4 Applications of the Metropolis Algorithm in Lattice Gauge Theories

Using the techniques described above, the Monte Carlo method is now used to simulate lattice gauge theories.

In the lattice model, the configurations C are field configurations $\{\Phi\}$ which contain the valnes of all the lattice elements that constitute the model. That is, $\{\Phi\}$ contains both the link fields $U_{x,\mu}$ and site fields ϕ_x, together with all the other parameters (masses,interaction strengths, etc.). The basic idea is to set up a Makovian process to

generate a set of configurations in equilibrium for a given value of $\frac{1}{\beta}$. The probability of encountering a configuration $\{\Phi\}$ at equlibrium must be proportional to the Boltzman factor:

$$P_{eq} \propto exp\{-\beta S[\{\Phi\}]\} \tag{4.35}$$

So by Eq. (4.21), the condition of detailed balance has the form,

$$e^{-\beta S[\{\Phi\}]} P(\{\Phi\}, \{\Phi\}') = e^{-\beta S[\{\Phi\}]} P(\{\Phi\}', \{\Phi\}), \tag{4.36}$$

where $P(\{\Phi\}, \{\Phi\}')$ is the probability distribution in going from the configuration $\{\Phi\}$ to $\{\Phi\}'$. $P(\{\Phi\}, \{\Phi\}')$ is specified by the Metropolis algorithm where Eq. (4.28) can be properly defined as

$$\begin{aligned} r &= \frac{e^{-\beta S[\{\Phi\}]}}{e^{-\beta S[\{\Phi\}']}} \\ &= e^{-\beta \Delta S}, \end{aligned} \tag{4.37}$$

where ΔS is the change in the action in going from $\{\Phi\} \rightarrow \{\Phi\}'$. So the configuration $\{\Phi\}'$ is accepted if $\Delta S \leq 0$, that is, if the action is lowered by the transition from $\{\Phi\} \rightarrow \{\Phi\}'$. If $\Delta S > 0$ then a random number ρ is selected in the interval $(0, 1)$. If $\rho \leq e^{-\beta \Delta S}$ then $\{\Phi\}'$ is excepted otherwise it is rejected and $\{\Phi\}' = \{\Phi\}$. To summarise, the conditional probability of accepting $\{\Phi\}'$ is often written as,

$$P(\{\Phi\}, \{\Phi\}') = min\{1, e^{-\beta \Delta S}\}. \tag{4.38}$$

Before any Monte Carlo simulations can be performed, there are a few very important preliminary considerations that have to be made regarding the underlying theory that govern the simulations. Firstly, the lattice size needs to be defined appropriety in accordance with the information needed to be extracted. It must be neither too small so that it induces finite size effects [42] nor too large so that it requires exorbitant computing time. Reasonably larger lattices are however preffered since it gives greater statistical accuracies provided effecient algorithms and fast computers are available. Further, boundary conditions must be imposed to eliminate the difference

between lattice points from the interior and from the boundary. Periodic boundary conditions are normally imposed on the lattice. Secondly, all parameters of the lattice gauge theory such as the mass and the self-interactions need to be defined. These parameters have direct implications on the observables that have to be measured.

The final consideration to take into account is the choice of the initial configuration. Since the aim of the Monte Carlo method is to generate configurations that are obtained after thermalisation is reached, a particular choice of an initial configuration is therefore irrelevant since it will ultimately give rise to statistical equilibrium. However, the choice of a particular configuration does affect the time taken to reach equilibrium. Different initial configurations are usually used as a measure of equilibrium. That is, to see if different starts will lead to the same equilibrium state. There are three types of starting configurations that are almost always used in the simulation of lattice models. These are:

1. The *cold* or *ordered* start. Here all the initial field variables are set equal to the identity of the gauge group under consideration. This corresponds to zero temperature or infinite β whence the action is minimal.

2. The *hot* or *disordered* start. In this case, the initial field variables are taken randomly from the the gauge group. This corresponds to a finite temperature or zero β.

3. The *mixed* start. This alternative consists of making part of the initial configuration ordered and the remainder part disordered. This is usually done by making the field variables with time coordinates less than say half the total time dimension of the lattice ordered and the remainder fields disordered.

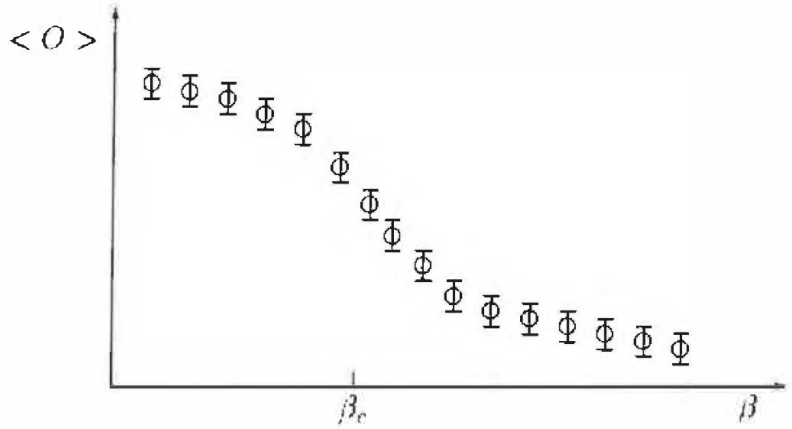

Figure 4.1: The dependence of $< O >$ on β with a possible inconsistency at β_c.

4.4.1 Interpretation of Numerical Results

The investigation of the dependence of the order parameters on various external parameters is of particular importance since they allow the study of the phase structure of the lattice model. These external parameters are usually the inverse temperature β, the mass m and other coupling constants including the self-interaction of the matter fields. Consider a series of Monte Carlo simulations that result in a plot of the order parameter $< O >$ as a function of β. Each sweep through the lattice evaluates $< O >$ for a value of β with appropriate errors (see Fig. 4.1). Assume that a phase transition occurs at the critical point β_c. To say what kind of phase transition it is, is as good as any guess due to the errors in the estimate of $< O >$. β_c could signal a first order phase transition (Fig. 4.2(a)), a second order phase transition (Fig. 4.2(b)) or even a rapid change in the value of β. So, how is it possible to determine what really happens to the model at the point $\beta = \beta_c$? The techniques of differentiating between these phases is now discussed below. It should be noted that at a phase transition two or more phases coexist in equilibrium. In lattice gauge theory this corresponds to the ground state of the system being degenerate at a first order phase transition. That is, for a minimum value of the action, two or more states may exist simultaneously.

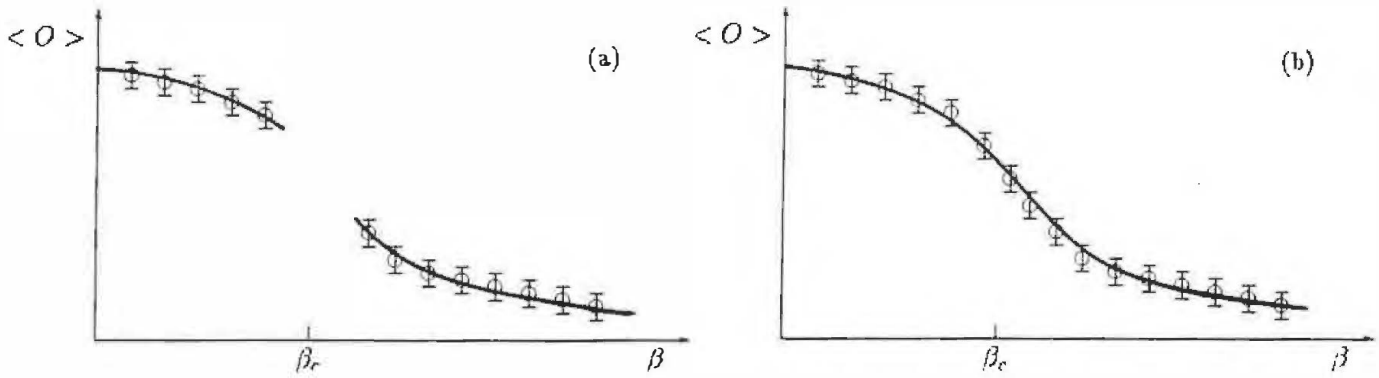

Figure 4.2: Two interpretations of Fig. 4.1, a first order (a) and a second order(b) phase transition.

However, these states may coexist with different values of $< O >$. Using this fact and fixing the model at β_c(assuming that it is a first order critical point) simulations can be carried out first using the cold start and then using the hot start. These different starts, as shown in Fig. 4.3, will produce different values of $< O >$ at equilibrium. After thermalisation, one of two situations could arise (see Fig. 4.4):

1. The two simulations will coincide and give the same value for the average value of the order parameter, that is, $< O >^{cold} = < O >_{hot}$.

2. The two simulations will produce different values for the average, that is, $< O >^{cold} \neq < O >_{hot}$.

The second situation where two distinct stable phases are produced will correspond to a first order phase transition. This is true only if the condition $< O >^{cold} \neq < O >_{hot}$ persists for a large number of iterations. In fact the number of iterations needs to be large enough so that the situation in (2) is not reproduced even if β is moved slightly away from β_c.

Another useful fact is that near a phase transition point, the relaxation time tends to increase. This can be used as a signal for the existence of a phase transition point.

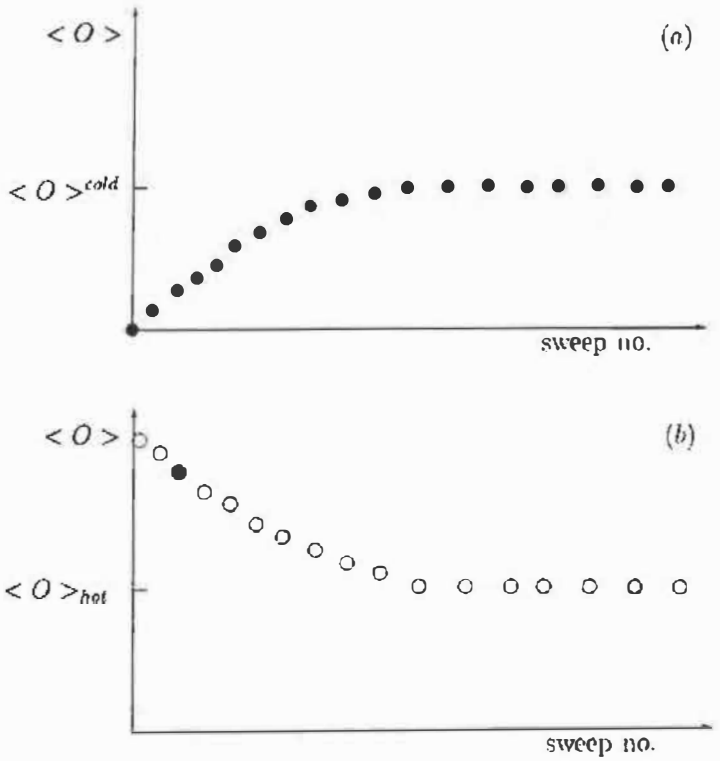

Figure 4.3: Monte Carlo simulations for different starts, (a) cold start and (b) hot start.

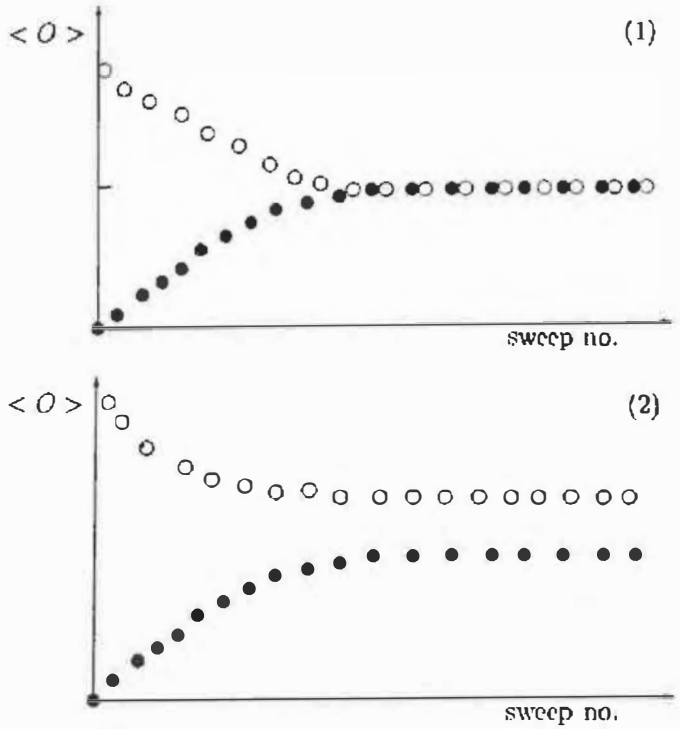

Figure 4.4: The two possible situations that could arise after thermalization.

Consider a first order phase transition that occurs at $\beta = \beta_c$. To study the dependence of the relaxation time both on the type of start and on β, different start simulations are performed for a set of β-values near β_c: $\beta_1^- < \beta_2^- < \beta_3^- < \beta_4^- < \beta_c < \beta_1^+ < \beta_2^+ < \beta_3^+ < \beta_4^+$. These simulations for different values of β should very likely correspond to the sequence of graphs ($< O >$ plotted against the iteration number) shown in Fig. 4.5. It can be seen from these graphs that the relaxation time is different for different type of starts and different vaules of β. For the hot start and β close to β_c but less than β_c the relaxation time is very large and approaches infinity for $\beta = \beta_c$. This corresponds to the existence of two different states with the same value of the action equal to the absolute minimum of the action (degenerate vacuum). It is also evident that for $\beta > \beta_c$, the realaxation time for the cold start simulation is larger. The fact that the relaxation time increases near the vicinity of the phase transition, allows one to perform *thermal cycles* in order to locate the position and possibly the type of the phase transition. In order to perform thermal cycles, all parameters of the model must be fixed except one, say β. Now suppose that a phase transition is expected in the interval (β_1, β_2). Using the value of β_1 a sweep can be performed until thermalization. Next, β_1 is incremented by a small step $\Delta\beta$ (typically $\Delta\beta = \frac{\beta_2 - \beta_1}{50}$). A new simulation is then performed for the new value $\beta_1 + \Delta\beta$. This simulation is performed over small number of iterations. That is, allow for a 'micro-thermalization' of say $N1$ iterations, then perform a 'micro-simulation' of say $N2$ iterations and then calculate $< O >$ only on these $N2$ configurations. This value of $< O >$ for the corresponding value of β can therefore be plotted on a $< O >$ verses β plot. Next the previous value of β is incremented once again by $\Delta\beta$ and the same procedure is repeated. This process continues until $\beta = \beta_2$ at the other end of the interval. At this point half a cycle of the thermal cycle is completed. This whole procedure is repeated in the opposite direction by changing the sign of the step. When the cycle is completed by reaching β_1 again, a graph of $< O >$ verses β is obtained. Fig. 4.6 shows a typical thermal cycle with a characteristic hysteresis loop. If a hysteresis

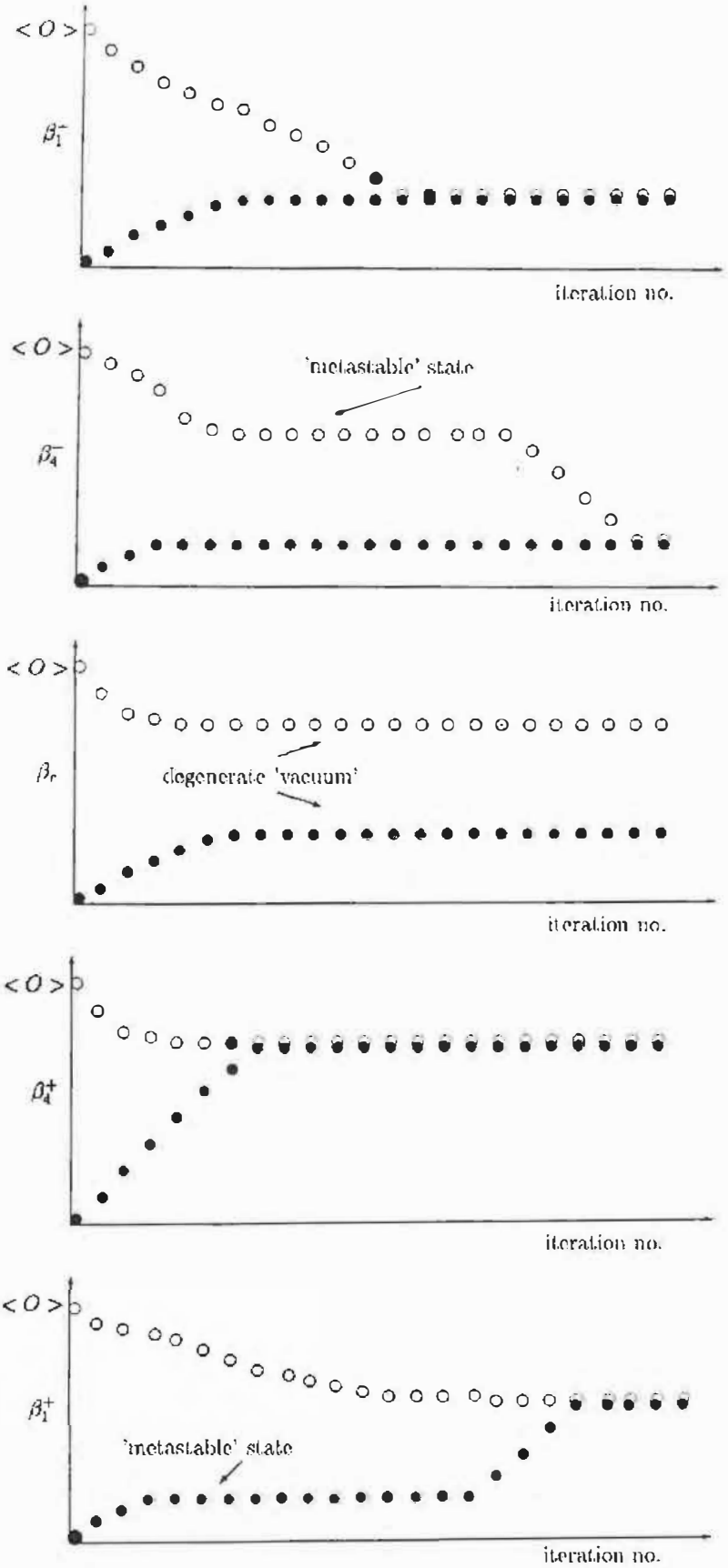

Figure 4.5: Sequence of graphs showing different start simulations in the vicinity of β_c.

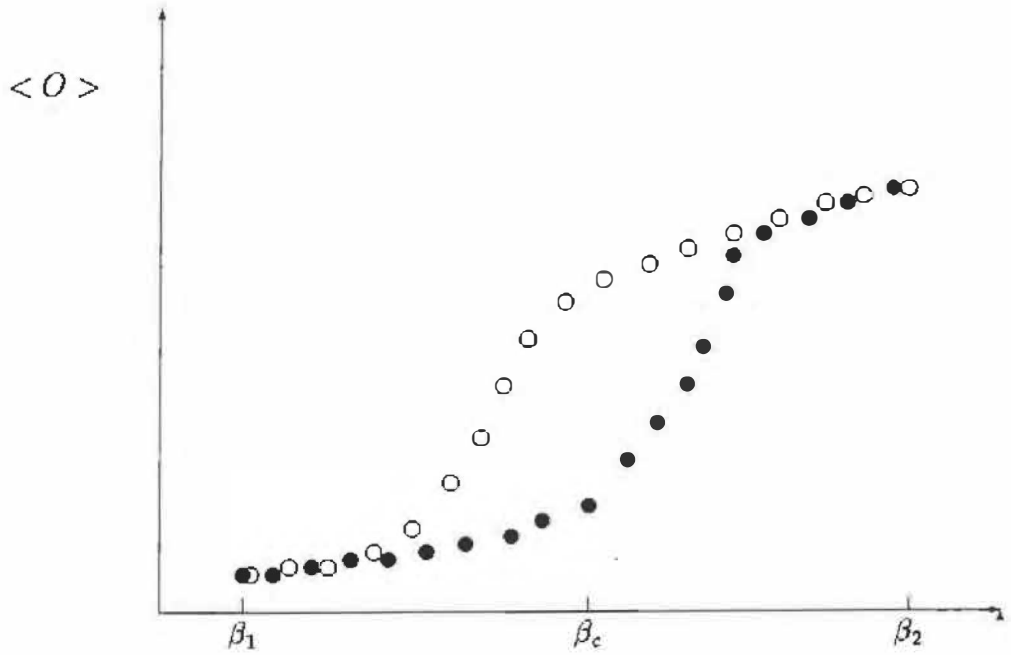

Figure 4.6: A typical thermal cycle

is present, then there is an abnormal increase of the relaxation time near β_c which causes the system to 'lag behind', not being able to thermalize quickly. This however does not specify the type of phase transition present. In order to tell what type of phase transition it is, two tests can be performed. The first test consists of seeing how the hysteresis loop is affected by changing the parameters of the cycle ($\Delta\beta, N1, N2$). If the hystersis loop tends to close with increasing $N1$ and decreasing $\Delta\beta$, then the phase transition is most likely to be of second order. If the hysteresis loop is still present no matter how much $N1$ is increased and $\Delta\beta$ is decreased, then the phase transition will be one of first order. The second test entails performing simulations from different starts for vaules of β from the left and right of β_c for a large number of iterations. If there is a value of β for which the values of $< O >$ do not coincide then a first order phase transition exists else it is probably a second order phase transition.

Chapter 5

Numerical Studies of some Lattice Gauge Models

5.1 Pure Lattice Gauge Theory

It was shown previously that the action defining a pure gauge theory (link fields only) is given by

$$S[U] = \beta \sum_{x,\mu\nu} \Re e Tr(1 - U_{\Box}), \tag{5.1}$$

where the link fields are elements of the gauge group under consideration. The corresponding partition function for such a model is given by

$$Z = \prod_{x,\mu} \int dU_{x,\mu} e^{-\beta S[U]}, \tag{5.2}$$

where the integration is over the invariant measure (the Haar measure) of the gauge group

Wilson [76] has pointed out that a lattice gauge theory of this type will lead to confinement in the strong coupling limit. In the Abelian case this theory gives the lattice version of quantum electrodynamics. In order for the theory to have any physical meaning it must also be able to describe deconfinement. For QED (gauge group

$U(1)$), the confinement phase must be sperated from the phase of unconfined photons while in the case of QCD (gauge group $SU(3)$) the confinement and unconfined phases must coexist as required by asymptotic freedom and there should not be a phase transition seperating them. Therefore it is of prime importance to investigate the phase structure of a given lattice gauge model. The original part of this thesis will be dedicated mainly to this task.

5.1.1 Abelian Lattice Gauge Theory

For the Abelian case, both the discrete group Z_N and the continuous group $U(1)$ are considered. It will be shown that both these groups give rich phase structures to the theory and as the order of the group becomes large enough, the Z_N theory begins to closely resemble the $U(1)$ theory.

The simplest of all Abelian groups are the discrete groups Z_N. In Z_N lattice gauge theory, the link fields take on a set of N values:

$$Z_N = \{e^{\frac{2\pi i}{N}\sigma_{x,\hat{\mu}}} \mid \sigma_{x,\hat{\mu}}, \ldots N-1\} \tag{5.3}$$

and the action is written as

$$S[\sigma] = \sum_{x,\mu\nu} (1 - \cos(\frac{2\pi}{N}\sigma_{x,\mu\nu})), \tag{5.4}$$

where $\sigma_{x,\mu\nu} = \sigma_{x,\hat{\mu}} + \sigma_{x+\hat{\mu},\hat{\nu}} - \sigma_{x+\hat{\nu},\hat{\mu}} - \sigma_{x,\hat{\nu}}$.

Although the lattice Z_N theory does not have a continuum analogue, it is used as a 'toy'-model and as a bridge to the study of $U(1)$ gauge theories. In fact Balian *et. al.* [5] have shown that the study of discrete groups allow the investigation and understanding of the phase structure of lattice gauge theories. Its discreteness enables much simpler analysis of the underlying theory as compared to the continuous group $U(1)$. Another important justification for the study of Z_N lattice gauge theories is that the group Z_N is the Abelian centre of $SU(N)$ which has important connections

in the fundamental theories of particle physics. The role of the group center in the phase transition of gauge theory was revealed by Mack and Petkova [58].

For $N = 2$, the lattice model corresponds to a generalised gauge invariant Ising model. This was first shown by Wegner [74] who is also credited for the original idea of putting gauge fields on the lattice. This generalisation introduced the concept of *duality* into lattice gauge theory. Without going into detail, the concept of duality allows the construction of a *dual model*, with the same dimensionality but with a different action. from the original model. This allows for a natural correspondence between the variables on the original lattice with the variables on its dual counterpart: The links of the lattice are associated with the plaquettes and the sites are associated with cubes. Therefore, a pure gauge theory where the plaquettes define the action would have a spin theory, which is defined on the links, as its dual. With this, a connection between the original model at the strong (or weak) coupling limit can be established with the dual model at the weak (or strong) coupling limit. Therefore, if phase transitions are present in the dual model a related transition can be found in the original one. This is desirable since in most cases the dual model is easier to handle theoretically than the original model. In the specific case when the action of the dual model is the same as the action of the original model, the model is said to be *self dual*. At the point of self duality, phase transitions are present which corresponds to a phase transition in the original model. It has been shown using the duality argument that in the two dimensional case(d=2), no phase transitions are present in the pure gauge Z_2 model [5]. However, for $d \geq 3$ phase transitions are present. This idea has beeen extended to investigate various vaules of N using Monte Carlo simulations [15,16,6]. A review of these results is now presented.

In the computer simulations of these models, thermal cycles were performed in β for varing values of the internal energy, E. The results of these simulations for various values of N are shown in Fig. 5.1. In all the simulations. hystersis loops are apparent which signifies phase transitions. For $N \leq 4$ the phase transition is of first order

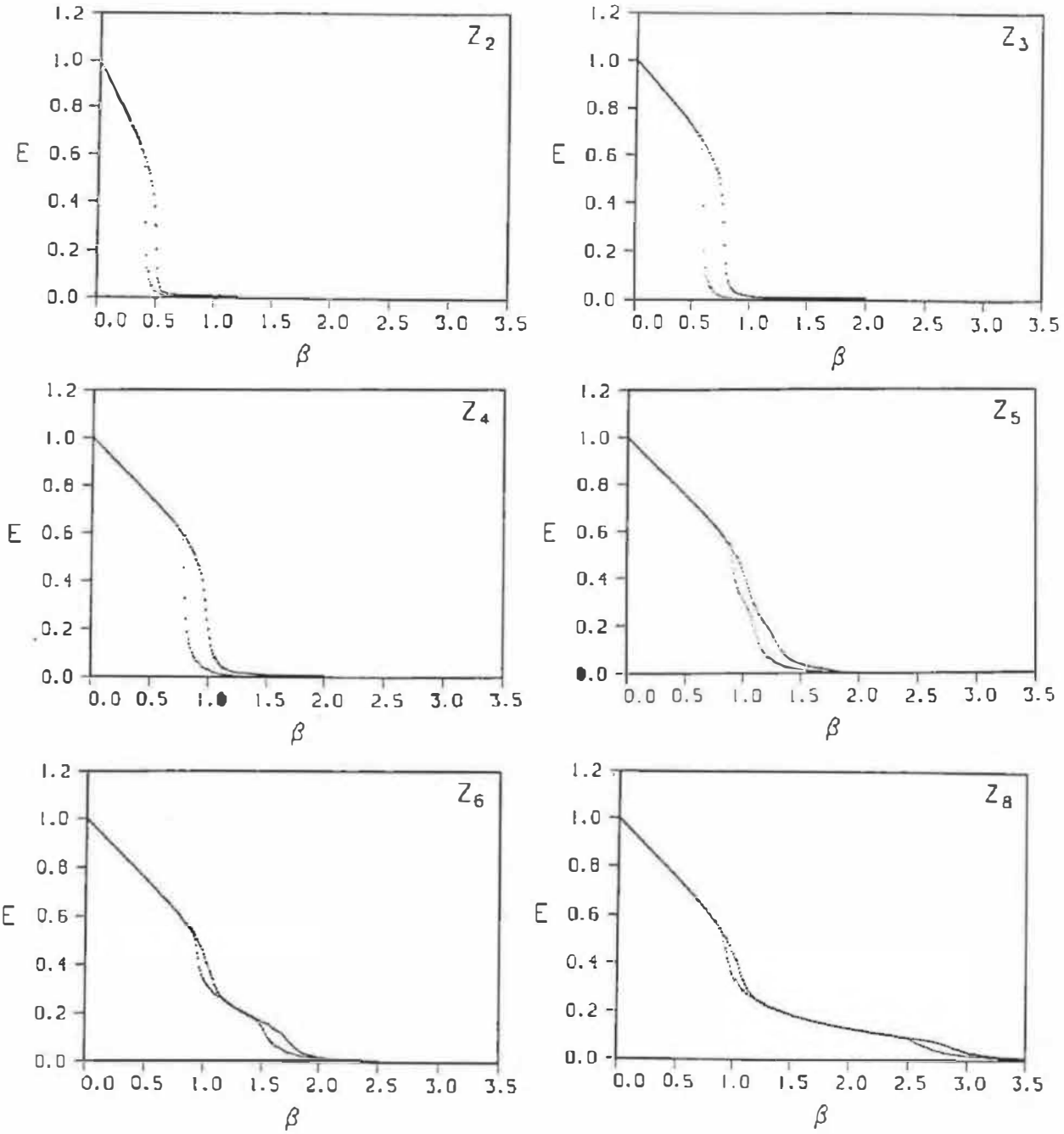

Figure 5.1: Thermal cycles for different values of N [16].

phase and seperates the confined (strong coupling) phase and the unconfined (weak coupling) phase. To see if this is really a first order phase transition, simulations from different starts as discussed before were performed. It can clearly be seen from Fig. 5.2. that for $N \leq 4$, two distinct ground states exist and there is no tunnelling between them. This agrees quite remarkably with the results obtained by Korthals-Altes [49,50] using the self duality argument. Using the duality argument, it was shown that the point of phase transition(β_c) was 0.44 for $N = 2$, 0.67 for $N = 3$ and 0.88 for $N = 4$. Employing the Monte Carlo technique for mixed starts the values for β_c are reproduced very accurately. This is shown in Fig. 5.3 where the simulations are done for values of β above and below β_c. For $N = 5$ the model begins to develope another phase transition seperating a third phase between the confined and unconfined phases. This becomes more distinct for $N = 6$ and higer values of N. Different start simulations for $N = 6$, as shown in Fig. 5.4(a), shows that the hot and cold starts converge to a unique value of E. This kind of behaviour is indicative of phase transitions of orders greater that one. Fig. 5.4(b) shows a simulation for Z_6 of the mixed start which converges to different values of E at thermalisation. This suggests the case of a continuous transition. It has been shown that the first phase transition point corresponds $\beta_c \approx 1$. The second point amongst a flurry of fluctuations appears around $\beta_c \approx 1.6$. For larger values of N, the first phase transition point becomes independent of N and remains at $\beta_c \approx 1$ but the second transition point shifts to infinity with the order of the group. Fig. 5.5 shows a plot of β_c against the order of the group as obtained from thermocycles for the corresponding groups. The phase structure of these models as obtained by Monte Carlo techniques agree very well with the theoretical results obtained by Guth [38] and Elitzur *et. al.* [26]. The primary investigation of the Abelian group is geared towards the study of $U(1)$ lattice gauge theory which describes quantum electrodynamics on the lattice. For the $U(1)$ case, the link fields are elements of the group $U(1)$ parameterized by a phase angle

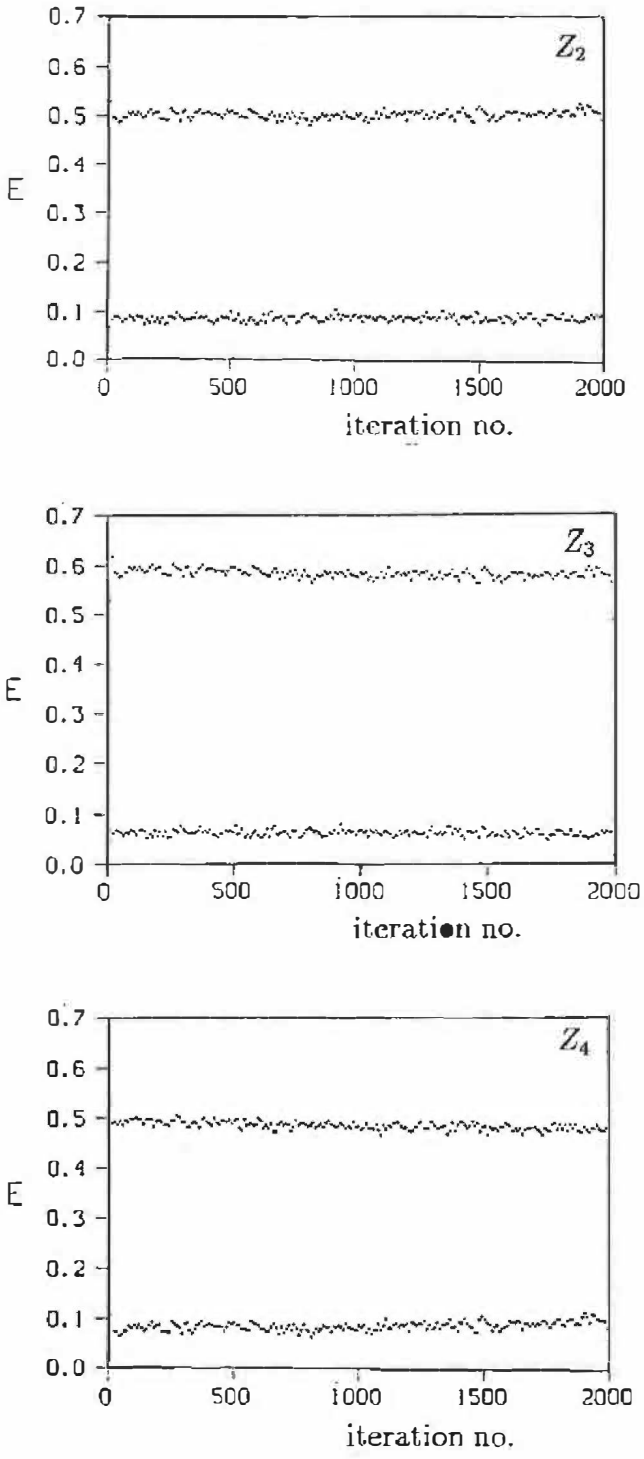

Figure 5.2: Monte Carlo simulations at β_c for the hot and cold starts [16].

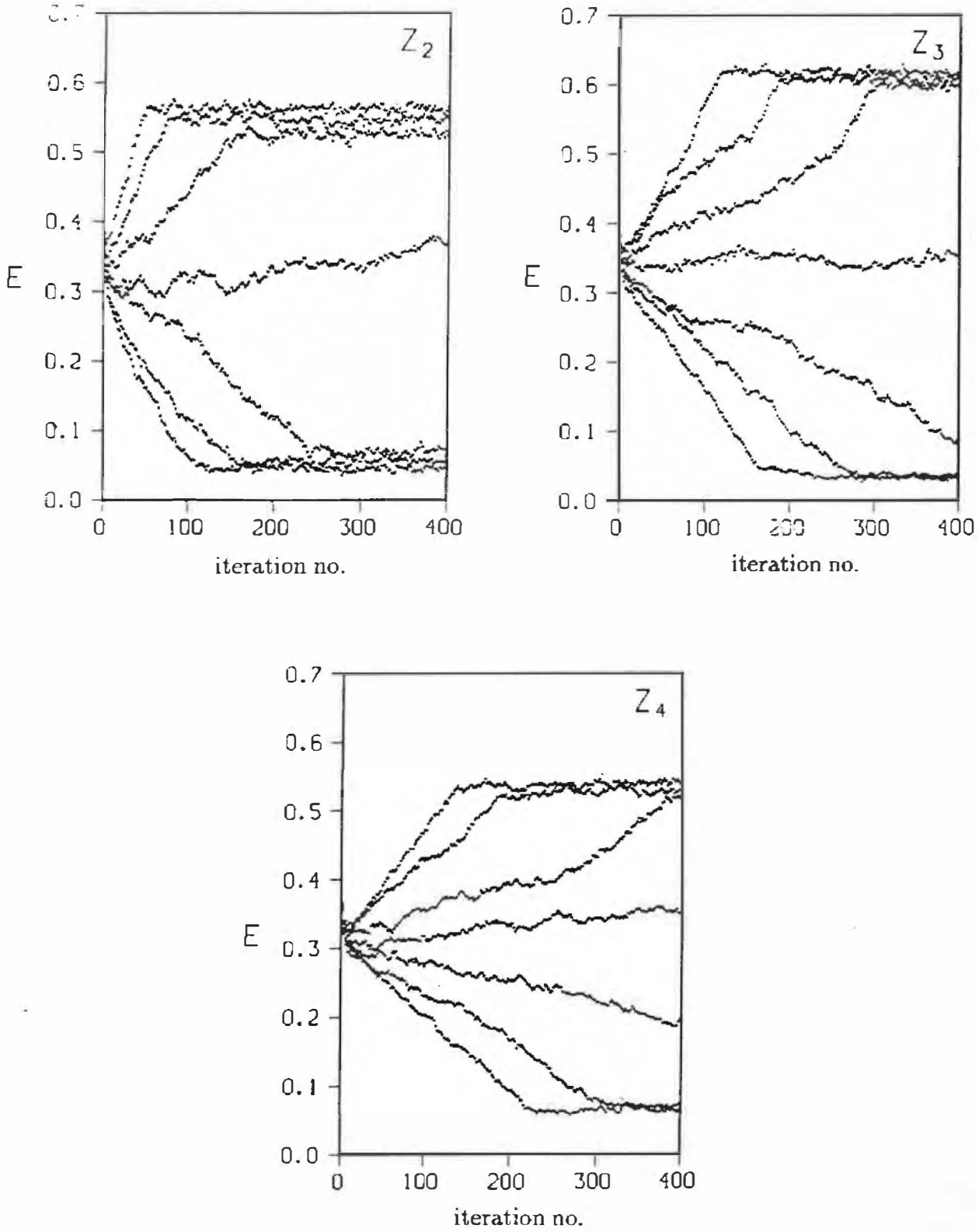

Figure 5.3: Mixed start simulations for β near β_c [16].

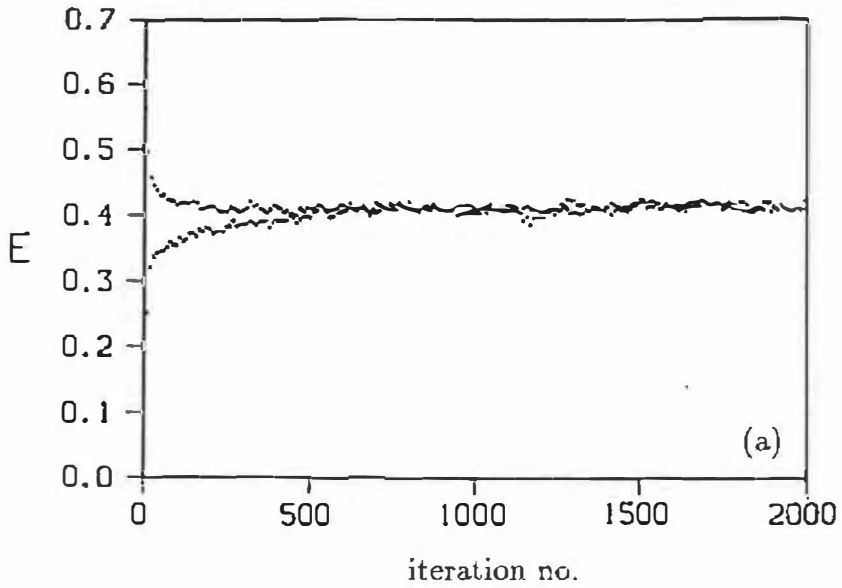

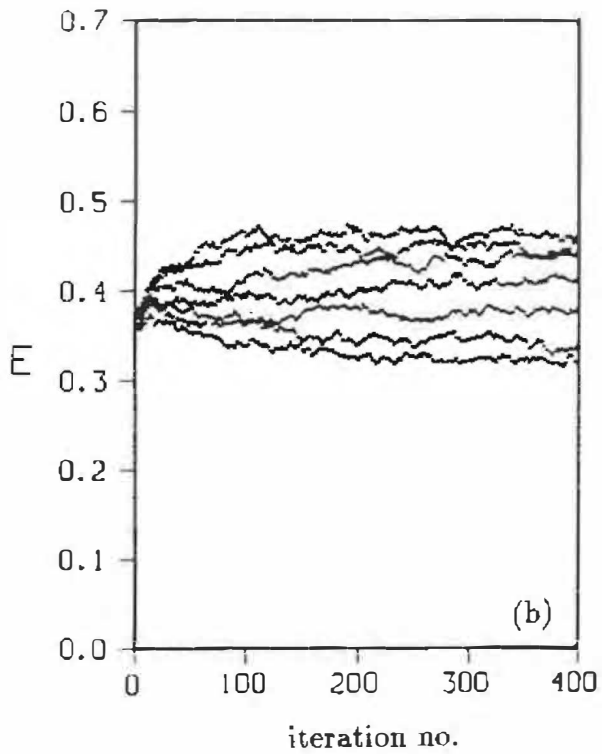

Figure 5.4: For Z_6: (a) Hot and cold starts convergence at thermalisation. (b) Mixed start simulation. [16]

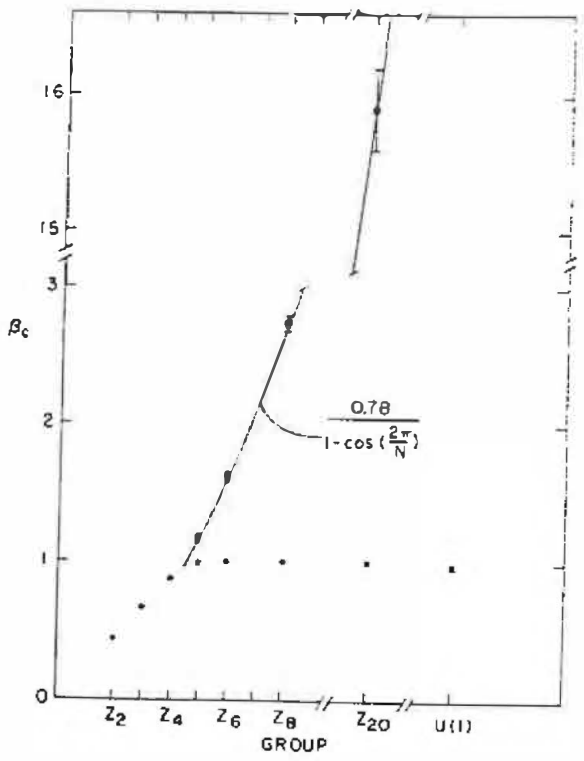

Figure 5.5: β_c plotted for Z_N and $U(1)$ [16].

$\theta_{x,\mu}$:

$$U_{x,\mu} = e^{i\theta_{x,\mu}} \tag{5.5}$$

for $-\pi < \theta_{x,\mu} \leq \pi$. The measure of integration for the partition function is the invariant $U(1)$ group measure:

$$\int d[e^{i\theta_{x,\mu}}] = \prod_x \int_{-\pi}^{\pi} \frac{d\theta_{x,\mu}}{2\pi}. \tag{5.6}$$

The partition function is a sum over all lattice configurations:

$$Z = \sum_\theta e^{-\beta S[\theta]}, \tag{5.7}$$

where the action has the form,

$$S[\theta] = \sum_{x,\mu\nu} (1 - \cos\theta_{x,\mu\nu}), \tag{5.8}$$

and $\theta_{x,\mu\nu} = \theta_{x,\hat{\mu}} + \theta_{x+\hat{\mu},\hat{\nu}} - \theta_{x+\hat{\nu},\hat{\mu}} - \theta_{x,\hat{\nu}}$. Monte Carlo simulations of this model reveal a single phase transition in four dimensions [16]. This is confirmed by by Fig. 5.6

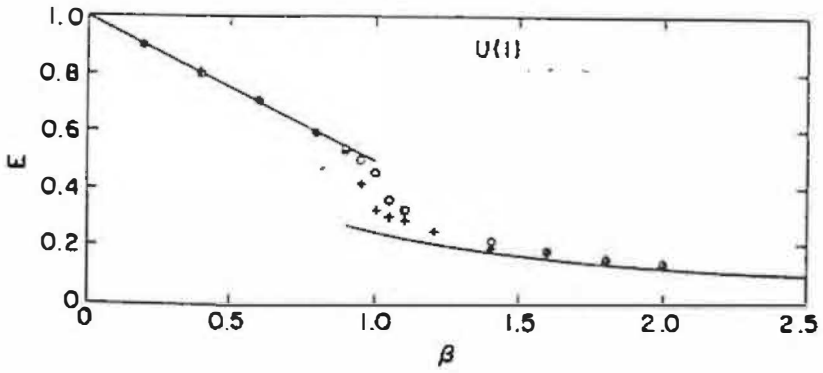

Figure 5.6: Thermal cycle for the group $U(1)$ [6].

which shows a thermal cycle in β. The critical value of β can be seen to be around 1.0 which corresponds to the values obtained for the Z_N model at $N \geq 4$. This phase transition seperates the confined phase from the unconfined phase which contains a massless photon. It has beeen shown using finite size scaling analysis [57] that this phase transition is of second order in four dimensions. Unlike the Z_N model, a second phase transition is not observed in four dimensions. For $d = 3$, no phase transitions are present, that is, the theory is present only in the confining phase for all values of the coupling. The behaviours of the $d = 3$ and $d = 4$ models are believed to be the result of certain topological excitations in the theory [22]. It has beeen shown that for $d = 3$, these topological excitations correspond to pointlike magnetic monpoles whereas in $d = 4$ they coresspond to strings of monopole current. For $d = 5$ evidence is given to support a first order phase transition [6].

5.1.2 Non-Abelian Lattice Gauge Theory

The study of non-Abelian gauge groups on the lattice is of great interest since quantum chromodynamics and the electroweak theory are based on such groups. In fact, Wilson's original motivation for developing the concept of lattice theories was to study the theory of strong interactions. Although the relevent group for strong interactions

is $SU(3)$, a study of the group $SU(2)$ is now presented. The reason for this is twofold. Firstly, $SU(2)$ has a much simpler structure than $SU(3)$ and secondly, if confinement is observed in $SU2)$ then it should also be observed in $SU(3)$.

For $U_{x,\hat{\mu}}$ an element of $SU(2)$, the link fields are parameterised as

$$U_{x,\hat{\mu}} = a_0 I + i\boldsymbol{a}\cdot\boldsymbol{\sigma}, \tag{5.9}$$

where σ_i, $i = 1,2,3$, are the Pauli matrices and I is the 2×2 identity matrix. a_μ is a real Euclidean four-vector of unit length:

$$a^2 \equiv a_0 + \boldsymbol{a}^2 = 1. \tag{5.10}$$

The invariant group measure (Haar measure) is given by[19]:

$$dU = \frac{1}{2\pi^2}\delta(a^2 - 1)d^4a. \tag{5.11}$$

The action for this model is a sum over all the plaquettes:

$$S = \sum_{\square} \Re e Tr(1 - \frac{1}{2}U_{\square}) \tag{5.12}$$

normalised such that the average plaquette gives a value in the interval $(0,1)$. It has been shown [18,19,56] that $d = 4$ is the critical dimension for $SU(2)$ lattice gauge theory and the confinement phase exists for all values of the coupling (see Fig. 5.7(a)). This means that no deconfining phase is present and at the continuum limit asymptotic freedom is observed. This observation has been confirmed analytically by Hasenfratz and Hasenfratz [41]. In Fig. 5.7(b) a clear hystersis effect for $d = 5$ is observered. This phase transition corresponds to a critical point of the coupling at $\beta_c \sim 1.642$. Further analysis using the different start simulations show that the hot and cold starts thermalize at different values of the average energy per plaquette. This is indicative of a first order phase transition.

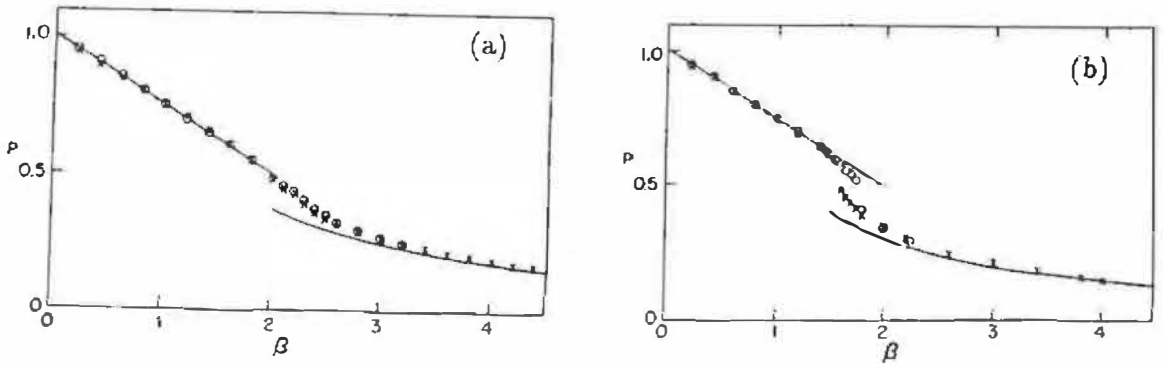

Figure 5.7: Thermocycle in $SU(2)$ for (a)four-dimensions and (b)five-dimensions. The solid lines represent the values obtained by the strong and weak coupling expansions. [19]

5.2 Lattice Gauge-Higgs Models

Thus far only lattice models with pure gauge fields have been considered. Realistic models however must contain dynamical matter fields that interact with the gauge fields. One such model is the interaction of the scalar fields with the gauge fields. This model as discussed previously for the continuum theory, gives rise to the Higgs mechanism where the interactions result in the gauge fields becoming massive. No massless Goldstone particles are present in this case. The study of lattice gauge-Higgs models allows for a better understanding of the mechanism of spontaneous symmetry breaking.

The action is of a lattice gauge-Higgs system is given by,

$$S = \beta \sum_{x,\mu\nu} S_G[U_{x,\mu}] + \sum_{x,\mu} S_H[\Phi_x, U_{x,\mu}], \tag{5.13}$$

where S_G is the usual pure gauge action and S_H the Higgs action. S_H is defined as

$$S_H = \Phi_x^* \Phi_x - \Phi_x^* U_{x,\mu} \Phi_{x+\mu} + V(\Phi_x), \tag{5.14}$$

where

$$V(\Phi_x) = \frac{1}{4}[\frac{m^2}{2}\Phi_x^*\Phi_x + \lambda(\Phi_x^*\Phi_x)^2]. \tag{5.15}$$

The Higgs fields on the lattice [70] are introduced as scalar fields Φ_x parameterized by a set of 'polar' variables (R_x, ϕ_x) such that $\Phi_x = R_x\phi_x$. R_x are called the *radial modes* or *radial degrees of freedom* which give the 'size' or 'length' of the scalar field. They take values in the interval $(0, \infty)$. The ϕ_x are usually taken from the fundamental representation of the group which means that they are unitary matrices. With this definition S_H takes on the form,

$$S_H = \sum_{x,\mu} [R_x^2 - R_x R_{x+\mu} \Re e Tr(\phi_x^* U_{x,\mu} \phi_{x+\mu}) + V(R)], \tag{5.16}$$

where

$$V(R) = \frac{1}{4}[\frac{m^2}{2} R_x^2 + \lambda R_x^4]. \tag{5.17}$$

The partition function for a lattice gauge-Higgs model can therefore be written as

$$Z = \int \prod_x d_\mu(R) d\phi_x \prod_{x,\mu} dU_{x,\mu} e^{-S[R,\phi,U]} \tag{5.18}$$

where the integration measures $d\phi_x$ and $dU_{x,\mu}$ are the corresponding group measures for the scalar fields and the link fields respectively. The definition of the measure $d_\mu(R_x)$ is not as restrictive or as well defined as the latter measures. In the early work on lattice gauge-Higgs models, the Higgs fields were constrained such that the modulus $\mid \Phi \mid$ was taken to be constant. This corresponds to the radial mode of the scalar field being *frozen*. The choice of freezing the length of the Higgs field is justified by the belief that at the continuum limit which is obtained at a critical point where the correlation length tends to infinity, the size of the scalar field should become irrelevent. Although this argument is, in principle, sound, varing the radial degrees of freedom does have a definite effect on the phase structure of this type of models. In §5.2.1 the frozen radial mode model is first discussed for both the Abelian and non-Abelian groups. In §5.2.2 the same models are studied for active or varing radial modes.

5.2.1 Frozen Radial Modes

Consider $V(R)$ in Eq.(5.17). By completing the square it can be shown that

$$\lambda R_x^4 + \frac{m^2}{2} R_x^2 = \lambda (R_x^2 + \frac{m^2}{4\lambda})^2 - \frac{m^4}{16\lambda}. \tag{5.19}$$

For large values of λ, the Higgs fields are radially frozen at a value $R_0 = -\frac{m^2}{4\lambda}$ for $m^2 < 0$ and at zero for $m^2 \geq 0$. The measure for the radial mode in the path integral can therefore be written as

$$d_\mu R \sim \delta(R_x - R_0) dR_x. \tag{5.20}$$

When the radial mode of the Higgs field is frozen the Higgs self-interaction $V(R)$ is constant and thus irrelevant for the action.

5.2.1.1 The Abelian Case

In the Abelian gauge-Higgs model with frozen radial modes the action has the general form

$$S = \beta \sum_{x,\mu\nu} \Re e Tr(1 - U_\Box) + \beta_H \sum_{x,\mu} \Re e Tr(1 - \phi_x U^l_{x,\mu} \phi_{x+\mu}). \tag{5.21}$$

where the Higgs coupling $\beta_H = R_x^2$ corresponds to the nearest neighbour Higgs field interaction. If the gauge and Higgs fields belong to the group Z_N then this action corresponds to a spin-gauge [20] system. In such a theory the Higgs fields are elements of Z_M such that $\phi_x = exp\{\frac{2\pi i m}{M}\}$ for $m = 1, \ldots, M$ and the gauge fields are elements of Z_N such that $U_{x,\mu} = exp\{\frac{2\pi i n}{N}\}$ for $n = 1, \ldots, N$. l gives the power of the coupled gauge field and is defined such that $l = \frac{N}{M}$ is an integer in order to ensure that Z_M is a subgroup of Z_N. The integer l is interpreted as the *charge* of the scalar field. The order parameters which are of interest in this model are the average link energy and the average plaguette energy defined respectively as,

$$L = -\frac{1}{4N_s} \frac{\partial}{\partial \beta_H} \ln Z(\beta, \beta_H) \tag{5.22}$$

and

$$E = -\frac{1}{6N_s}\frac{\partial}{\partial\beta}\ln Z(\beta,\beta_H), \tag{5.23}$$

where N_s is the number of lattice sites. The action in Eq. (5.21) is invariant under the local gauge transformation of the group Z_N and if $\phi_x = g_x^l$ where $g_x \in Z_N$ then the Higgs fields are unity. This corresponds to the unitary gauge as discussed in §2.2.2.

In the limiting regions of the couplings many interesting observations have been made [28,20,46]. For $\beta_H \to 0$, the Higgs fields randomize and the model reduces identically to the pure gauge Z_N theory. In the other extreme, that is, for $\beta_H \to \infty$ both L and E become zero if the Higgs fields are in the fundamental representation ($l = 1$) of the gauge group Z_N. For higher order representations ($l > 1$) however the theory reduces to a pure Z_l gauge theory. For the limit $\beta \to 0$ the model trivializes in the unitary gauge. Due to the absence of the gauge interactions, the gauge fields decouple and the corresponding order parameters become:

$$L(\beta = 0,\beta_H) = -\frac{\partial}{\partial\beta_H}\ln[\sum_{U\in Z_N} exp\{-\beta_H(1 - \Re eTr(U^l))\}] \tag{5.24}$$

and

$$E(\beta = 0,\beta_H) = 1 - (1 - L)^4\delta_{l1}. \tag{5.25}$$

For $\beta \to \infty$, all the plaquettes take on the identity of the group in order to maximize the action. The model then reduces to a pure Z_M gauge spin system with action $\beta_H \sum \phi_x\phi_{x+\mu}$.

These limiting regions of the coupling constants result in a fairly complicated phase diagram for the model. For both the limiting regions of β_H, lines of phase transitions are expected to enter the phase diagram as a result of the pure gauge characteristics of the model at these limits. These transitions correspond to confinement (area law in the Wilson loop) at the strong coupling regime($\beta < \beta_c$) and non-confinement (perimeter law in the Wilson loop) at the weak coupling regime($\beta > \beta_c$). The model for $\beta_H = 0$ has been studied extensively in §5.1. Also for $\beta_H \to \infty$ where the model

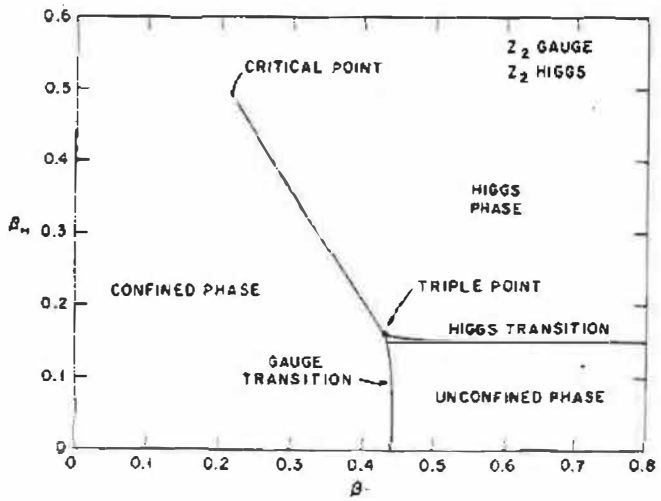

Figure 5.8: Phase diagram for the Z_2 lattice gauge-Higgs model [20].

reduces to a pure spin system phase transitions are expected as a result of the ordering of the Higgs fields. For β_H greater than some critical point, the global symmetry of Z_N is spontaneously broken and the Higgs fields develope nonzero expectation values. For β_H less than the critical point, the symmetry is restored and the expectation values of the Higgs fields are zero. These transition lines are called the *Higgs line* and correspond to the *Higgs phase* of the model.

Fig. 5.8 shows a summary of the phase diagram in four-dimensions for both the Higgs and gauge fields belonging to the gauge group Z_2 in the (β_H, β) plane for constant L and E as obtained by Creutz [20]. The gauge transition line enters into the phase diagram as a first order phase transition line seperating the confined and the unconfined phases. The Higgs transition line appears at large β as a second order phase transition line bordering the unconfined phase and the Higgs phase. At a triple point $(0.16 \pm 0.02, 0.43 \pm 0.02)$ this behaviour vanishes and for β decreasing a first order transition line is evident. This transition line seperates the Higgs phase from the confined phase and terminates at a critical point estimated at $(0.48 \pm 0.03, 0.22 \pm 0.03)$. In three dimensions Jongeward *et. al.* [46] showed that the Higgs phase and the confined phase are continuously connected, that is, connected by a region free of

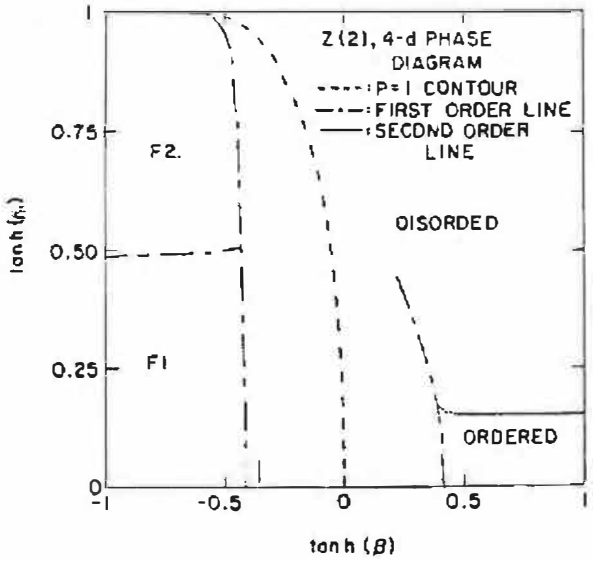

Figure 5.9: Z_2 phase diagram incorporating negative values of β [7].

phase transitions. They also show that for $d = 3$, a second order phase transition line is obtained between the confined and unconfined phases.

The Z_2 model has also been studied for negative values of the coupling constants [7]. Fig. 5.9 shows the phase diagram in four dimensions for a spin-gauge system incorporating negative values of β. For the limit $\beta \to -\infty$, β_H, the lattice is made up of random spins and ordered gauge fields where the latter is ordered according to certain gauge transformations. The phase corresponding to this region is represented by $F1$ in Fig. 5.9 This region is characterised by the constant values of the order parameters $L = 1$ and $E = 2$. In the second case where $\beta \to -\infty$ and β_H is allowed to increase in the positive direction, the theory tends to a critical point and the spins take on values depending on the value of the link fields. In Fig. 5.9 this phase is given by the region $F2$ and is characterised by $E = 2$ and a lower bound for the average link at $L = 0.5$. The regions denoted by $F1$ and $F2$ are termed *frustrated* phases. In the last case where $\beta \to -\infty$ and $\beta_H \to \infty$, both E and L vanish, suggesting a transition line extending to these limits. It can be seen from Fig. 5.9 that the frustrated phases $F1$ and $F2$ are seperated by a line of first order transitions that

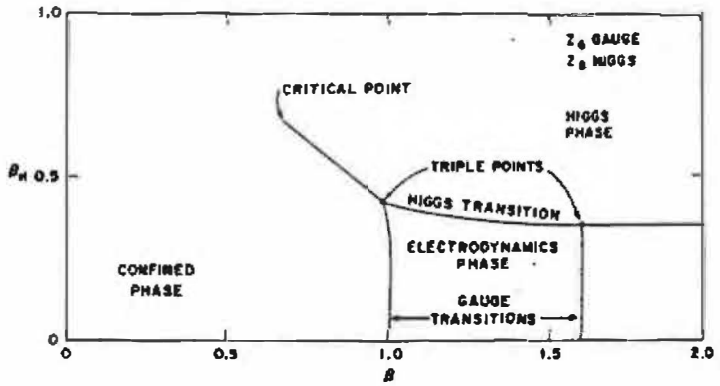

Figure 5.10: Phase diagram of the Z_6 gauge-Higgs model [20].

begin at $\beta = -\infty$ and terminate at a triple point $(0.56 \pm 0.01, -0.46 \pm 0.01)$. Both $F1$ and $F2$ are also seperated from the confined phase by a first order phase transion line. This line intersects the $P = 1$ line at $\beta_H = \infty$ and $\beta = -\infty$. In the case of $d = 3$, $F1$ and $F2$ are seperated by a second order transition line. A second order line is also evident in the seperation of $F1$ and the deconfined phase. For the gauge and Higgs fields belonging to the group Z_6 two distinct gauge transition lines of second order are observered containing the electrodynamic phase or Coulomb phase (see Fig. 5.10). As a result two triple points exist: a low-β triple point at $(0.42 \pm 0.03, 0.98 \pm 0.03)$ and a large-β triple point at $(0.35 \pm 0.02, 1.60 \pm 0.05)$. The critical point is given at $(0.67 \pm 0.05, 0.67 \pm 0.05)$. The Higgs transiion line of first order connects the two triple points and borders the Higgs and electrodynamic phases.

Thus far models where considered with both the Higgs and gauge fields belonging to the same group, that is, for $m = n$ or $l = 1$. Consider now the situation where the gauge fields belong to the group Z_6 and the Higgs fields to the Z_3. This model which has a phase structure (see Fig. 5.11) similar to the Z_6 case, possesses a residual Z_2 gauge theory at $\beta \to \infty$ which is apparent from $l = 2$. The Higgs transition line which is of first order smoothly joins the Z_2 gauge transition line which is also of first order. This shows that the Higgs and the confined phases are always seperated, even

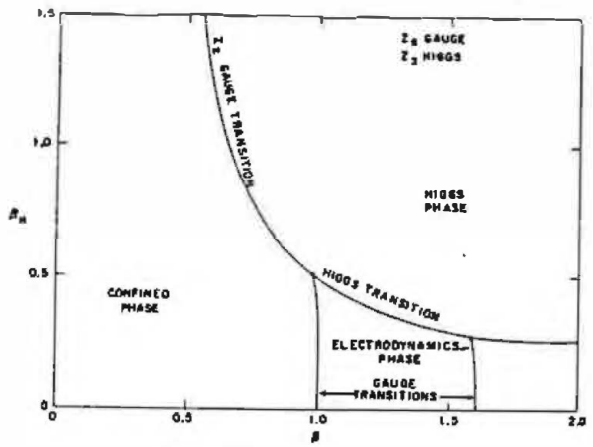

Figure 5.11: Phase diagram of Z_6 gauge fields and Z_3 Higgs fields [20].

at β_H and β going to infinity. This agrees with the theoretical results obtained by Fradkin and Shenker [28]. For all fields on the lattice belonging to the group $U(1)$, the gauge and Higgs fields are parameterized by the $U(1)$ elements $exp(i\theta_{x,\mu})$ and $exp(i\alpha_x)$ respectively. The standard action for such a model [28,9,8.71] is of the form

$$S = \beta \sum_{x,\mu\nu} (1 - \cos\theta_{x,\mu\nu}) + \beta_H \sum_{x,\mu} (1 - \cos(\Delta_\mu - q\theta_{x,\mu})), \tag{5.26}$$

where $\Delta_\mu \alpha_x = \alpha_x - \alpha_{x+\mu}$ and $\theta_{x,\mu\nu} = \Delta_\mu \theta_{x+\nu} - \Delta_\nu \theta_{x+\mu}$ for $-\pi < \alpha_x, \theta_{x+\mu} \leq \pi$. q is the charge of the Higgs field and in principle is an integer. It can be shown [8,9] that by expanding the cosine and setting $\beta = \frac{1}{e^2}$, $U_{x,\mu} = exp\{iaeA_\mu\}$ and $\sqrt{\beta_H}\phi_x = a\phi$, Eq. (5.26) gives the action for the scalar electrodynamics in the continuum limit:

$$S_{cont} = \int d^4x [\partial_\mu + iqeA_\mu]\phi + \frac{1}{4}F_{\mu\nu}^2]. \tag{5.27}$$

Eq. (5.27) corresponds to the usual electrodynamic Lagrangian in §2.1.1.

For $\beta_H = 0$, the Higgs fields decouple and the model reduces to a pure $U(1)$ gauge theory. As discussed in §5.1, a second order phase transition seperates the confined phase from the unconfined phase for the $d = 4$ case. In the limit $\beta_H \to \infty$ the Higgs part of the action in Eq. (5.26) vanishes and the gauge fields become unity. In the unitary gauge this corresponds to $\theta_{x,\mu} = \frac{2\pi p}{q}$ for $p = 0, \ldots, q$. This results in the gauge

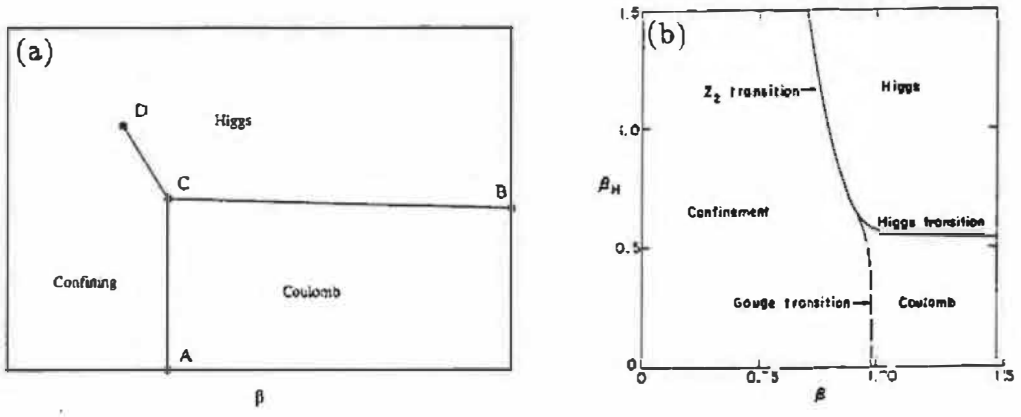

Figure 5.12: Phase diagrams for the $U(1)$ gauge-Higgs model with charge (a) $q = 1$ [1] and (b) $q = 2$ [9].

fields becoming elements of the gauge group Z_q. For $\beta = 0$, no phase transitions are present and in the unitary gauge the model reduces to a theory described by the action $\beta_H \sum [1 - \cos(q\theta_{x,\mu})]$. In the limit $\beta \to \infty$, the model is said to 'freeze' and the gauge part of the action in Eq. (5.26) vanishes. Also, the plaquettes take on the identity of the group and the action becomes $\beta_H \sum (1 - \cos[\alpha_{x+\mu} - \alpha_x)]$. This model pocesses a phase transition.

The phase structure of the $U(1)$ gauge-Higgs model is strongly influenced by the value of the charge q. Fig. 5.12 shows the phase diagram for the cases $q = 1$ and $q = 2$. For the case of $q = 1$, shown in Fig. 5.12(a), the phase diagram is analogous in structure to the Z_2 gauge-Higgs model. Early studies [9,8,71] based on this model did not give clear evidence of the order of the phase transitions observered. It was however shown that the model pocesses a triple point(C) at $(0.43 \pm 0.05, 0.92 \pm 0.05)$ and a critical point(D) at $(0.75 \pm 0.05, 0.6 \pm 0.1)$. Later work, done a few years ago, have shown that the point A represents a first order phase transition [27,3] and the point B represents a second order phase transition [45,4]. It was also shown that the Higgs transition line(BC) and the gauge transition line(AC) are second and first order lines respectively. Alonso *et. al.* [1] have shown that the Higgs phase and

the confined phases are seperated by a transition line of first order and the critical point(D) is a second order point.

The phase diagram for $q = 2$ as shown in Fig. 5.12(h) is similar in structure to the Z_6-gauge-Z_3-Higgs model except that it pocesses a single triple point. The results obtained by Callaway and Carson [9] show that the eletrodynamic phase is seperated from the confined phase by a second order phase transition line that joins the Z_2 and Higgs transition lines at a triple point, $(0.60 \pm 0.05, 0.92 \pm 0.05)$.

5.2.1.2 Non-Abelian Lattice Gauge-Higgs Models

For the gauge and Higgs fields belonging to the non-Abelian gauge group, consider the action in the form

$$S = \beta \sum_{x,\mu\nu} \Re eTr(1 - U_{\Box}) + \beta_H^{\chi} \sum_{x,\mu} \Re eTr(1 - \chi(\phi_x)\chi(U_{x,\mu})\chi(\phi_{x+\mu})), \qquad (5.28)$$

where χ is some irreducible representation of the non-Abelian group under consideration.

For the lattice fields belonging to the group $SU(2)$, two interesting cases arise. The first is where the Higgs fields transform under the fundamental or spin-$\frac{1}{2}$ representation of the group. This is similar to the $l = 1$ case for the Abelian gauge-Higgs model discussed in the previous section. The second case is where the Higgs fields transform under the adjoint or spin-1 representation of the $SU(2)$. In the Abelian case this is similar to $l = 2$. In the following section a review of these cases are discussed as first presented by Lang, Rebbi and Virasoro [54].

For the Higgs fields in the fundamental representation, the Higgs fields are elements of the three dimensional unit sphere S^3 in four dimensional Euclidean space. This allows the Higgs fields ϕ_x to be set in correspondence with a $SU(2)$ group element V_x

by the relation

$$V_x = \begin{pmatrix} \phi_x^1 & -\phi_x^{2*} \\ \phi_x^2 & \phi_x^{1*} \end{pmatrix}. \tag{5.29}$$

For computational speed-up the Higgs contribution to the action can be written as

$$S_H^{fund} = \beta_H^{fund} \sum_{x,\mu} \Re e Tr(1 - V_x U_{x,\mu} V_{x+\mu}^\dagger), \tag{5.30}$$

where V_x and $U_{x,\mu}$ belongs to the icosohedral subgroup $\tilde{Y}$ of $SU(2)$ which is the largest discrete non-Abelian subgroup of $SU(2)$.

In the adjoint representation the Higgs field belong to the quotient space $SU(2)/U(1) = S^2$. Here the Higgs fields are represented by Hermitian 2×2 matrices:

$$V_x = \cos\theta + i\boldsymbol{\sigma} \cdot \boldsymbol{\phi} \sin\theta, \tag{5.31}$$

where θ is a fixed angle that does not take on the values 0 or π. For the finite subgroup model, V_x are elements of the subgroup $\tilde{Y}/Z_{10}$ and the corresponding Higgs action can be written as

$$S_H^{adj} = (2\sin^2\frac{\pi}{2})^{-1} \beta_H^{adj} \sum_{x,\mu} \Re e Tr(1 - V_x U_{x,\mu} V_{x+\mu}^\dagger U_{x,\mu}^\dagger). \tag{5.32}$$

It must be noted, though, that the replacement of the continuous groups $SU(2)$ and $SU(3) = SU(2)/Z_2$ leads to numerical artifacts. Consider now the limiting values of the couplings for the fundamental representation. In the limit $\beta_H^{fund} \to \infty$ the gauge fields become frozen and both E and L go to zero. For $\beta_H^{fund} = 0$, the model reduces to a pure gauge system with the gauge fields belonging to the group $\tilde{Y}$. In the limit $\beta \to \infty$ the model reduces to a spin system invariant under the $SU(2)$ global gauge transformation. For $\beta = 0$, only the gauge fields affect the action. Fig. 5.13(a) shows the phase diagram in the (β_H^{fund}, β)-plane for this model. The transition line which originates at the point $(0, 6.05)$ is an artifact of the discrete approximation of the group $SU(2)$. The second line approximates the continuous group and it has been shown that this corresponds to a second order phase transition line. Unlike the

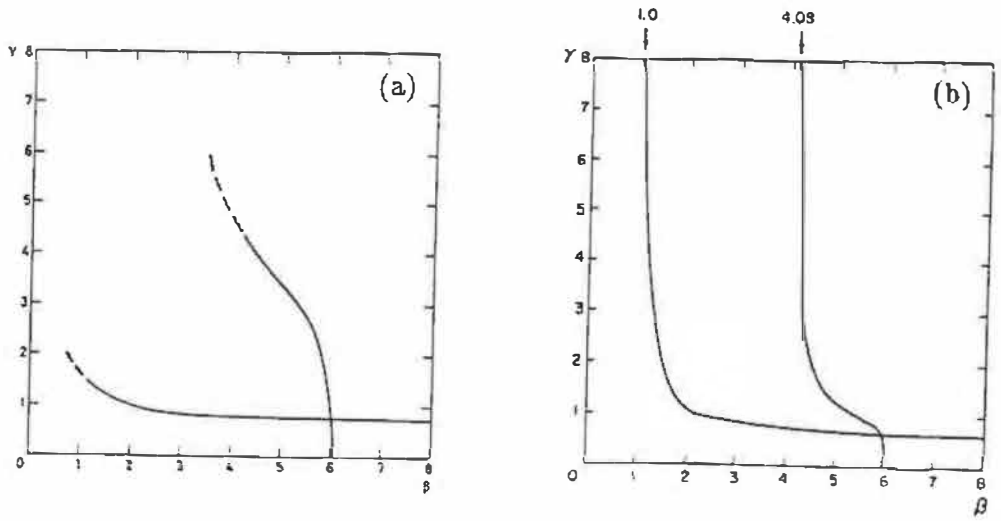

Figure 5.13: Phase diagrams for the $SU(2)$ model in the (a) fundamental and (b) adjoint representations [54].

Abelian case this line does not create an electrodynamic phase but terminates near the point $(1.5, 1.2)$ and possibly approaches $\beta_H^{fund} = 1.5$ asymptotically. This situation can be interpreted as the Higgs and the confined phases being analytically one and the same phase, which is exactly what Fradkin and Shenker [28] have predicted.

In the adjoint model, the transition line begining at $\beta = 6.05$ is also a consequence of the discretization of the gauge group. The most interesting case in this model is the limit $\beta_H^{adj} \to \infty$. In this limit the model reduces to a $Z_{1\bullet}$ theory, which as observered in the previous section for large orders of the group Z_N, should give two phase transitions of second order. Fig. 5.13(b) shows these two phase transitions at $\beta = 4.08$ and $\beta = 1$. The latter phase transition point, which corresponds to the transition line which approximates the continuous group, shows that the model leads to the $U(1)$ theory. As with the fundamental case there is no Coulomb phase. There is however a clearly seperated Higgs-confined phase which once again agrees quite remarkably with the analytical predictions of Fradkin and Shenker [28].

5.2.2 Active Gauge-Higgs Models with Radial Modes

Lifting the restriction on the Higgs fields ($\mid \Phi \mid = constant$) allows for the variation of the radial modes of freedom. Therefore the complete action including the scalar self-interactions can be considered. This introduces two new parameters, namely, the squared 'mass' m^2 and the 'self-interaction" λ. It should be noted that these are 'bare' (not yet renormalized) parameters and hence not directly related to observed masses and interaction strengths. The behaviour of the model is studied in the space of the parameters (β, m^2, λ). The model incorporates all models previously discussed as special cases for the limiting values of the parameters. In the limit $\lambda \rightarrow \infty$, the Higgs fields are radially frozen to the mean field value. This situation corresponds to the model discussed in §5.2.1. In the limit $m^2 \rightarrow \infty$, the radial modes vanish and the model reduces to a pure gauge theory as discussed in §5.1. The model not discussed thus far corresponds to the cases when $\beta \rightarrow \infty$ and $\beta \rightarrow 0$. In these two cases, S_G vanishes and the model becomes a theory of self-interacting Higgs fields.

In addition to the usual order parameters, this model allows for the study of phase transitions via the order parameter

$$\begin{aligned} < R^2 > &= Z^{-1} \int \prod_x d_\mu(R_x) d\phi_x \prod_{x,\mu} dU_{x,\mu} \Phi_x^* \Phi_x e^{-S} \\ &= -2 \frac{\partial}{\partial m^2} \ln Z(\beta, m^2) \end{aligned} \tag{5.33}$$

for fixed λ. In the Monte Carlo simulations of this model the lattice variables are updated in the usual way. For any given site on the lattice updating is first performed on R_x and then on α_x. The acceptance or rejection criteria for these variables are based on the Metropolis algorithm. The link fields are updated in the usual way.

To complement the numerical simulations, $< R >$ can be studied analytically by an effective potential method based on the Coleman-Weinberg procedure [11]. The idea behind this technique is to redefine the partition function so that the measure of integration is restricted to the radial modes alone. This results in an action that

is a function of only the R_x. One rewrites the partition function in the form

$$Z = \int \prod_x d_\mu(R_x)\tilde{Z}[R_x], \tag{5.34}$$

where $d_\mu(R_x)$ is some measure of integration over the radial modes. The significance of the choice of this measure will he discussed later. A radial partition function $\tilde{Z}$ is introduced defined such that

$$\begin{aligned}\tilde{Z}[R_x] &= e^{-\tilde{S}[R_x,\beta]} \\ &= \int \prod_x d\phi_x \prod_{x,\mu} dU_{x,\mu} e^{-S[R_x,\phi_x,U_{x,\mu}]}.\end{aligned} \tag{5.35}$$

The new action $\tilde{S}$ can be represented by a power series in β:

$$\tilde{S}[R_x,\beta] = \tilde{S}_0 + \beta\tilde{S}_1 + \beta^2\tilde{S}_2 + \ldots. \tag{5.36}$$

where the expansion coefficients are independent of β and are given by

$$\tilde{S}_0 = -\ln \tilde{Z} \mid_{\beta=0}, \tag{5.37}$$

$$\tilde{S}_1 = -\tilde{Z}^{-1}\frac{d}{d\beta}\tilde{Z} \mid_{\beta=0}, \tag{5.38}$$

$$\tilde{S}_2 = \frac{1}{2}(\tilde{S}_1^2 - \tilde{Z}^{-1}\frac{d^2}{d\beta^2}\tilde{Z}) \mid_{\beta=0}. \tag{5.39}$$

The expression in Eq.(5.36) can be considered as a new action which depends only on the radial modes R_x. Employing a mean field technique an effective potential can be derived from the new action. It should be pointed out at this stage that the term 'mean field' has various interpretations in physics and should not be confused with the method used here. In lattice gauge theory, the basic idea behind the mean field approximation is that the field at each point is affected by a mean field due to its neighbours. The techniques used for this approximation are fairly complicated and are based on variational and saddle point approximation [23]. In this case however a 'crude' version of the mean field is used where the radial fluctuations of the model are replaced by its average value $\bar{R}$; that is, $R_x = R_{x+\mu} = \bar{R}$. The effective potential to

lowest order as obtained in the same way as the Coleman-Weinberg effective potential can therefore be written as

$$V_{eff}(\bar{R}) = \frac{1}{N_t}\tilde{S}[R_x]\,|_{R_x=\bar{R}} = \sum_{k=0} \beta^{(k)} V_{eff}^{(k)}(\bar{R}), \tag{5.40}$$

where

$$V_{eff}^{(k)} = \tilde{S}_{(k)}[\bar{R}]. \tag{5.41}$$

In most cases, for values $k > 0$, the effective potentials vanish at $\bar{R} \rightarrow \infty$ and $V_{eff}^{(0)}$ becomes a good enough approximation.

5.2.2.1 The Abelian Case

Consider first the group Z_N. Here the Higgs fields are parameterized as $\Phi_x = R_x exp\{\frac{2\pi i}{N}\phi_x\}$ for $\phi_x = 0, 1, \ldots, N-1$ and the gauge fields as $U_{x,\mu} = exp\{\frac{2\pi i}{N}\sigma_{x,\mu}\}$ for $\sigma_{x,\mu} = 0, 1, \ldots, N-1$. The model is described by an action

$$\begin{aligned} S &= \beta \sum_{x,\mu} (1 - \cos[\frac{2\pi}{N}\sigma_{x,\mu\nu}] + \sum_{x,\mu} \{(1 + \frac{m^2}{8})R_x^2 + \frac{\lambda}{4}R_x^4 \\ &\quad - R_x R_{x+\mu} \cos[\frac{2\pi}{N}(\phi_x - \phi_{x+\mu} - \sigma_{x,x+\mu})]\} \end{aligned} \tag{5.42}$$

with partition function

$$Z = \int \prod_x dR_x \frac{1}{N} \sum_{\phi_x=0}^{N-1} \prod_{x,\mu} \frac{1}{N} \sum_{\sigma_{x,\mu}=0}^{N-1} e^{-S}. \tag{5.43}$$

The $N = 2$ model has been studied extensively by Munehisa and Munehisa [66,67]. This study was based on the (β, m^2) plane with fixed values of λ at 0.1 and 1.0. The Monte Carlo simulations of this model are based on thermocycles which measure the average plaquette energy and the average squared length of the Higgs fields. In the former case β is varied for fixed m^2 and in the latter, m^2 is varied for fixed β. A summary of these simulations are shown in Fig. 5.13. In the case of $\lambda = 1.0$ it has been shown that for $m^2 \rightarrow \infty$, $\beta = 0.44$, which is the critical point of the

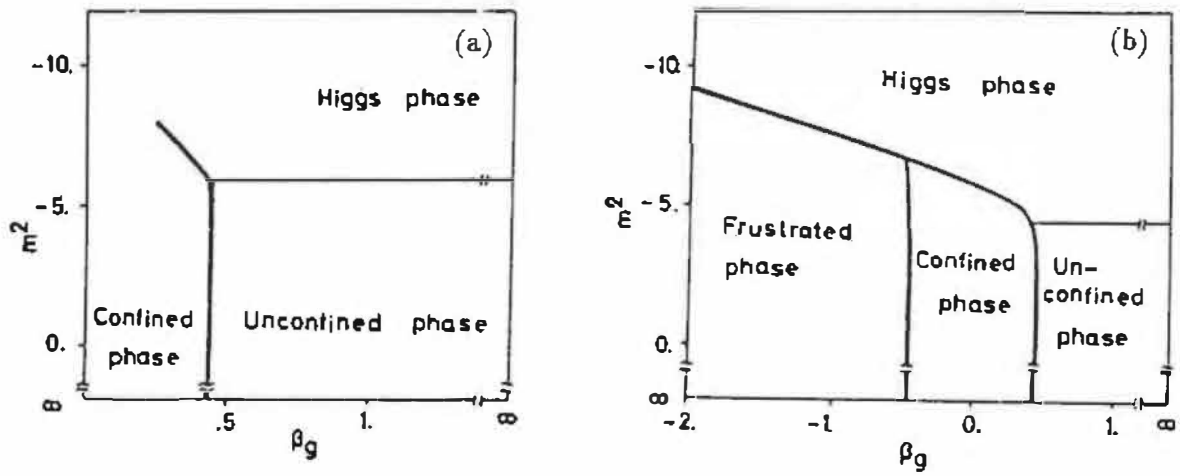

Figure 5.14: Phase structure in the (β, m^2)-plane for (a) $\lambda = 1.0$ and (b) $\lambda = 0.1$ [67].

pure Z_2 gauge theory. In fact there is a line of first order phase transition points which seperates the confined and unconfined phases and terminates at the triple point $(0.43 \pm 0.06, -6.0 \pm 0.4)$. The critical point that ends the seperation of the Higgs and confining phases is at $(0.25 \pm 0.05, -8.0 \pm 0.5)$. It can be seen from Fig. 5.14(a) that the phase diagram for $\lambda = 1.0$ closely resembles that of the Z_2 radially frozen model as discussed in § 5.2.1.1. Fig. 5.14(b) shows the phase diagram of the $\lambda = 0.1$ case incorporating negative values of β. Here two triple points are evident and the confining phase is enclosed by first order phase transition lines. A new region, the frustrated phase, which corresponds to the average plaquette energy equal to two is seperated from the Higgs phase by a first order phase transition line. Unlike the frozen model, only a single frustrated phase emerges. Further observations made on the dependence of λ on the phase transition at $\beta = 0$, show that for λ less that $\lambda_c = 0.35 \pm 0.05$, the model undergoes a first order phase transition. A more general study has been made by Gerdt, Ilchev and Mitrjushkin [29] where different orders of the group Z_N have been considered between $N = 2$ and $N = 300$. They have shown that for the extreme case of β at fixed λ, the dependence of the phase transition point m^2 on the order of the group ceases to exist at values greater than $N = 5$ for $\beta = 0$ and $N = 10$ for $\beta = \infty$. Mean field approximations [29,67] to lowest order performed

on these models compare fairly well with the Monte Carlo results.

For the gauge group $U(1)$, the Higgs fields are parameterized as $\phi_x = R_x exp(i\alpha_x)$ and the gauge fields as $U_{x,\mu} = exp(i\theta_{x,\mu})$ for $0 \leq \alpha_x, \theta_{x,\mu} < 2\pi$. The general radially active model for the Higgs fields in the fundamental representation is given by the action,

$$\begin{aligned} S &= \beta \sum_{x,\mu\nu} (1 - \cos\theta_{x,\mu\nu}) + \sum_{x,\mu} \{(1 + \frac{m^2}{8})R_x^2 + \frac{\lambda}{4}R_x^4 \\ &\quad - R_x R_{x+\mu} \cos(\Delta\alpha_x - \theta_{x,x+\mu})\}, \end{aligned} \tag{5.44}$$

where the integration in the partition function is over the Haar measures of the group given by $d\phi = \frac{d\alpha_x}{2\pi}$ and $dU_{x,\mu} = \frac{d\theta_{x,\mu}}{2\pi}$. The radial measure for the Higgs fields is taken to be $dR_x = R_x dR_x$.

For $m^2 \to \infty$ this model reduces to the pure $U(1)$ theory as discussed in §5.1.1 an undergoes a second order phase transition at $\beta \approx 1$. For $\lambda \to \infty$ this model corresponds to the radial modes being frozen which was discussed in §5.2.1.1. A comprehensive study of this model both numerically and using the effective potential method has been carried out by Gerdt *et. al.* [30,31]. A sumary of these observations together with the results obtained by Munehisa [65] is shown in Fig. 5.15 which gives the phase diagram in the (m^2, β)-plane for different values of λ. For relatively small values of λ a first order transition line exists seperating the confining phase from the Higgs phase for $\beta < 1$. Munehisa[8] has conjectured that this transition line is a consequence of the radial degrees of freedom. Fig. 5.15(a)-(b) shows that this transition line is also observered for negative values of β. As λ increases the phase transition line terminates at a second order phase transition end point which moves to the left and crosses the point $\beta = 0$. for increasing λ. This end point signifies the point where the Higgs and the confining phases become analytically connected [51]. Also, as β approaches from large values to a triple point the model possesses a Coulomb phase bounded by a Higgs-Coulomb transition line and the gauge transition line at $\beta \approx 1$. It has been shown [65] that the radial degrees of freedom bring first

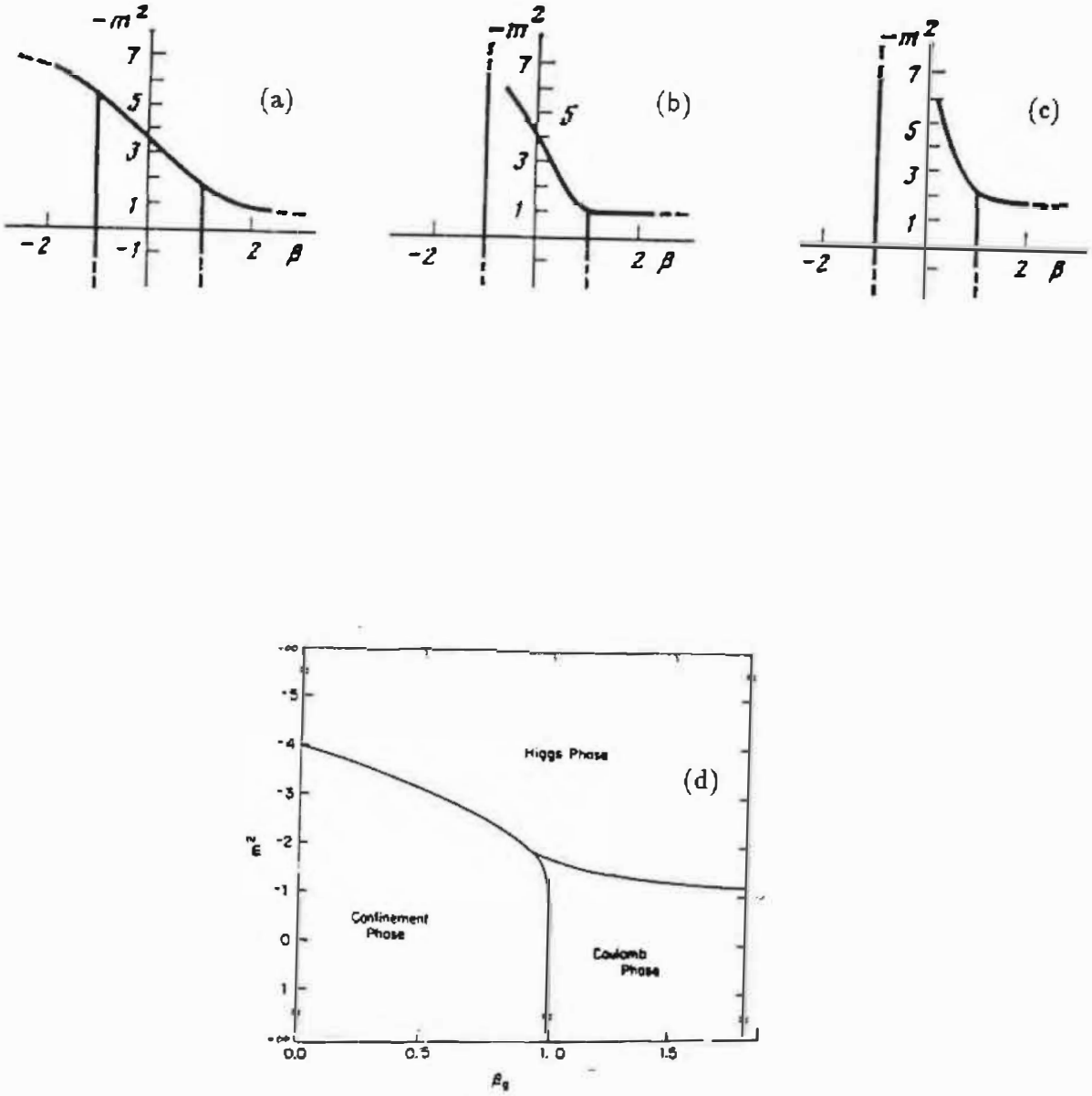

Figure 5.15: Phase diagrams for different λ: (a) $\lambda = 0.125$, (b) $\lambda = 0.25$, (c) $\lambda = 0.5$ [30] and (d) $\lambda = 0.8$ [65].

order Higgs-Coulomb transitions into the phase diagrams in addition to the higher order transitions observed in the radially fixed model. It has been suggested that this first order phase transition is a realization of the Coleman-Weinberg mechanism [11] on the lattice.

5.2.2.2 The Non-Abelian Case

The Higgs fields Φ_x in the fundamental representation of $SU(2)$ are parameterised as,

$$\Phi_x = \frac{1}{R_x}\begin{bmatrix} \phi_i^{(1)} & -\phi_i^{(2)*} \\ \phi_i^{(2)} & \phi_i^{(1)*} \end{bmatrix}, \tag{5.45}$$

with the action given by,

$$\begin{aligned} S &= \beta\sum_{x,\mu\nu} \Re eTr(1-\frac{1}{2}U_\Box) + \sum_x \{\frac{1}{4}(\frac{m^2}{2}R_x^2 + \lambda R_x^4) \\ &\quad + R_x^2 - R_x R_{x+\mu}\frac{1}{2}\Re eTr(\phi_x U_{x,\mu}\phi_{x+\mu}^\dagger)\}. \end{aligned} \tag{5.46}$$

In the corresponding partition function, the integration is over the Haar measures of the group and the radial measure is usually taken to be $R_x^3 dR_x$. The action in Eq. (5.46) has been studied is a different form by Kuhnelt *et. al.* [52]. Here they have considered the action in the form,

$$\begin{aligned} S &= \beta'\sum_{x,\mu\nu} \Re eTr(1-U_\Box) + \sum_{x,\mu} \{\frac{1}{2}(\lambda'(\rho_x^2-1)^2 + \rho_x^2) \\ &\quad - \kappa\rho_x\rho_{x+\mu}\Re eTr(\phi_x U_{x,\mu}\phi_x^\dagger)\}. \end{aligned} \tag{5.47}$$

Writing $R_x = \sqrt{2\kappa\rho_x}$ and defining $\beta = \beta'$, the relation between Eq. (5.46) and Eq. (5.47) is made:

$$\lambda = \frac{\lambda'}{2\kappa^2}, \qquad m^2 = \frac{(1-2\lambda'-8\kappa)}{k}. \tag{5.48}$$

This model has been studied extensively in references [32,33,34,35] using the action defined in Eq. (5.46). It was shown using the effective potential method and

Monte Carlo simulations that there is a strong dependence of the shape of the phase transition on λ, and for $m^2 \to \infty$ and $\lambda \to \infty$, the theory reduces to a pure $SU(2)$ gauge theory with a crossover point at $\beta = 2.2$. Results also revealed that for finite β and small enough λ, first order phase transitions were observed. It was shown that for fixed λ, lines of first order phase transitions exist in the (β, m^2)-plane which have end points corresponding to second order phase transitions. These results are however different from those obtained by Kuhnelt *et. al.* who have observed only second order phase transitions. It has heen stated that this discrepancy is only seeming, caused by a different choice of the model parameters. Using the relationships of the different parameters defined in Eq. (5.48), it was shown that the point $(\lambda', \beta', \kappa) = (0.5, 2.25, 0.27)$ corresponds to the point $(\lambda, \beta, m^2) = 91.715, 2.25, -8)$. The resaon for the second order phase transitions observed by Kuhnelt *et al* is justified in the model defined by Eq. (5.46) in that for $\lambda \leq 1$ hoth minima obtained by the effective potential method were so close to each other that they are indistinguishable in the Monte Carlo analysis.

Gerdt *et. al.* [34,35] have suggested that the existence of an end point on the first order phase transition line corresponds to the complementary principle proposed by Fradkin and Shenkar [28], where the end point is a critical point analogous to a phase diagram of the 'gas-liquid-ice' type.

Chapter 6

The Kazakov-Migdal Model

The Kazakov-Migdal (K-M) model [47] was proposed a few years ago and still attracts considerable interest. Kazakov and Migdal suggested a new lattice gauge model where the Yang-Mills interaction could be *induced* by minimal coupling to a massive scalar field which transforms in the adjoint representation of the gauge group. The mass of the scalar acts as an effective ultraviolet cutoff for the theory. The novelty in the K-M model is the absence of the plaquette term for the gauge fields. This means that the gauge fields cannot propagate (has no kinetic term) and is just a background field. In all the rest the K-M action is the same as for the standard lattice gauge-Higgs theory discussed in §5.2. Upon partially integrating over the scalar fields, the model was hoped to give a theory that in the continuum limit would lead to QCD which is the only renormalizable, asymptotically free and confining theory in four dimensions. This model has attracted much attention and, in fact, has inspired a series of papers that have investigated both analytical and numerical consequences of the underlying theory.

6.1 The K-M Model

The model is defined on a D-dimensional hypercubic lattice with partition function

$$Z = \int \prod_x d\Phi_x \prod_{x,\mu} dU_{x,\mu} e^{-S[\Phi,U]}, \tag{6.1}$$

where the action is defined as

$$S[\Phi,U] = \sum_x N\,Tr(V(\Phi_x)) - \sum_{x,\mu} \Phi_x U_{x,\mu} \Phi_{x+\mu} U^{\dagger}_{x,\mu}. \tag{6.2}$$

Here Φ_x are scalar fields which are traceless $N \times N$ matrices belonging to $SU(N)/Z(N)$ which is the adjoint representation of $SU(N)$. They are coupled to the gauge fields $U_{x,\mu}$ which are $N \times N$ unitary matrices belonging to the group $SU(N)$ satisfying the condition $U_{x,\mu} = U^{\dagger}_{x+\mu,-\mu}$. It should be noted that the lack of a kinetic term for the gauge fields in Eq. (6.2) results in their dynamics being determined solely through their interaction with the adjoint scalar fields. This is one of the main features of the model that differentiates it from the standard lattice gauge-Higgs models and can, as such, be said to be equivalent to the infinitely strong coupling limit($\beta \to \infty$) of the standard model.

By integrating over the scalar fields in the partition function of the model an effective action for the gauge fields can be obtained:

$$\int \prod_x d\Phi_x \prod_{x,\mu} dU_{x,\mu} e^{-S[\Phi,U]} \propto \int \prod_{x,\mu} dU_{x,\mu} e^{-S_{ind}[U]} \tag{6.3}$$

where,

$$e^{-S_{ind}[U]} = \int \prod_x d\Phi_x e^{-S[\Phi,U]}. \tag{6.4}$$

As a result of the gauge invariance of the model the induced action is given as an infinite sum over all possible Wilson loops on the lattice. These Wilson loops will also be in the adjoint representation which is an attribute inherited from the scalar fields. If the potential is considered to be in the quadratic form $V(\Phi) = \frac{1}{2} m_0^2 Tr\Phi^2$,

then the Φ integral is Gaussian and the induced action is given by the large mass expansion which can be represented as a sum over lattice loops C of a scalar field in an external gauge field:

$$S_{ind}[U] = -\sum_{C} \frac{2^{l(C)} \mid Tr\, W(C) \mid^2}{l[C] m_0^{2l(C)}}, \tag{6.5}$$

where $l(C)$ is the length of the path C and $W[C] = \prod_{x,\mu} U_{x,\mu}$ is the standard Wilson loop. In the weak smooth gauge field limit a critical point for the bare mass at $m_0^2 = 2d$, which seperates the strong coupling region, where d is the dimensionality of the Euclidean space-time, is expected. On averaging over the fluctuations of the gauge fields the critical point will shift to some different value m_c^2. It is suggested that near this value one could take the continuum limit for the smooth part of the gauge field. Kazakov and Migdal have argued that in the continuum limit this action gives rise to the Yang-Mills action,

$$S_{ind}[U] \sim \beta Tr F_{\mu\nu}^2 + \ldots, \tag{6.6}$$

where the coupling constant β depends on the renormalised scalar mass, $m^2 = m_0^2 - m_c^2$, and the lattice spacing:

$$\beta = \frac{N}{96\pi^2} \ln(\frac{1}{m^2 a^2}). \tag{6.7}$$

In the continuum limit this model is supposed to induce QCD and by observing Φ_x as a heavy constituent field, their mass m must act as an effective ultraviolet cutoff.

In a similar way, but by integrating over the gauge fields first an effective action for the scalar fields can be induced. This is achieved by taking the Itzykson-Zuber integral [40,44,60]:

$$I(\phi,\psi) = \int dU\, exp(NTr\phi U \psi U^\dagger) \propto \frac{\det_{ij} exp(N\phi_i\psi_j)}{\Delta(\phi)\Delta(\psi)}, \tag{6.8}$$

where φ_i are the eigenvalues of the matrix ϕ_x and

$$\Delta(\phi) = \prod_{i<j} (\phi_i - \phi_j) \tag{6.9}$$

is the Vandermonde determinant. This allows the derivation from Eq.(6.2) of the corresponding partition function in terms of only the eigenvalues ϕ_x of the scalar field at each site. The partition function is therefore given as follows

$$Z = \int \prod_{x,i} d\phi_x^i e^{-V(\phi_x^i)} \Delta^2(\phi_x) \prod_{x,\mu,i} \frac{\det_{ij} exp(N\phi_x^i \phi_{x+\mu}^j)}{\Delta(\phi_x)\Delta(\phi_{x+\mu})}. \tag{6.10}$$

The resulting theory is expressed in terms of the eigenvalues of the matrix Φ_x. Kazakov and Migdal hoped that Φ_x could be the *master field* for large-N QCD. It should be noted that the integration over the gauge fields is obtained explicitly only because the pure gauge term is not present in the action.

6.2 Gauge Symmetries in the K-M Model

An interesting attribute of the K-M model is that it possesses some unique lattice artifacts which make it different from the standard Wilson formulation of lattice QCD [48,62,63]. These artifacts are manifest in the rich gauge symmetries that the model exhibits.

The original action defined in Eq. (6.2) has two local gauge symmetries which play an important part in its understanding. The first is related to the usual $SU(N)$ gauge transformations:

$$\begin{aligned} U_{x,\mu} &\rightarrow V_x U_{x,\mu} V_{x+\mu}^\dagger, \\ \Phi_x &\rightarrow V_x \Phi_x V_{x+\mu}^\dagger, \end{aligned} \tag{6.11}$$

where $V_x \in SU(N)$. These transformations leave the action invariant. Gross [37] was the first to notice that the model is invariant under $(D-1) \times (N-1)$ extra local $U(1)$ gauge symmetries.

Further, the K-M model is also invariant under local Z_N transformations:

$$U_{x,\mu} \rightarrow Z_{x,\mu} U_{x,\mu}, \tag{6.12}$$

where $Z_{x,\mu} \in Z_N$ which is the center of the group $SU(N)$. Kogut *et. al.* [48] have emphasised that this symmetry exists because of the adjoint representation of the fields and will also appear for any induced QCD model where the scalar fields are invariant under the center of the group. This local symmetry has a negative effect on the model's apparent reformulation of QCD. It has been shown in §3.6 that in the strong coupling limit the Wilson loop gives rise to an area law, $W(C) = e^{-kA(C)}$, which implies confinement of the quarks. Under a local transformation,

$$W(C) \rightarrow W'(C) = e^{\frac{2\pi i}{N}n} W(C), \tag{6.13}$$

results in $W(C) = 0$. The vanishing of the Wilson loop implies in the context of the area law that the string tension, (k), is infinite. This means permenant local confinement.

6.3 Numerical Study of the $SU(2)$ K-M Model

The first numerical study of the K-M model was made by Gocksch and Shen [36] and further extended upon by Aoki *et. al.* [2]. They have studied the case of the $SU(2)$ K-M model which is the simplest nontrivial version of the K-M model. If this model is to induce QCD then there should be a continuum limit with an appropriate critical point corresponding to the usual $SU(2)$ gauge theory. By first integrating over the gauge fields, the resulting partition function can easily be studied using Monte Carlo simulations.

Consider the path intergral given in Eq. (6.1). In order to proceed and solve this equation, the $SU(2)$ parameterization for the fields and measures need to be defined. The scalar fields are defined as $\Phi_x = R_x \sigma_3$ where,

$$\sigma_3 = \begin{pmatrix} 1 & 0 \\ 0 & -1 \end{pmatrix}, \tag{6.14}$$

is one of the Pauli matrices. The gauge fields are parameterised as

$$U = \begin{pmatrix} \alpha & \beta \\ -\beta^* & \alpha^* \end{pmatrix}, \tag{6.15}$$

where α and β are given by the Euler angles:

$$\begin{aligned} \alpha &= \cos(\tfrac{\theta}{2}) e^{i(\frac{\varphi+\psi}{2})}, \\ \beta &= i \sin(\tfrac{\theta}{2}) e^{i(\frac{\varphi-\psi}{2})}. \end{aligned} \tag{6.16}$$

The normalised group measure for the gauge fields is given by

$$dU = \frac{1}{16\pi^2} d\theta d\varphi d\psi \sin\theta \tag{6.17}$$

and the radial measure is chosen in the form

$$d_\mu R = R^2 dR. \tag{6.18}$$

Consider first the integral over the gauge fields:

$$\int \prod_{x,\mu} dU_{x,\mu} e^{N \sum_x \sum_{x,\mu} Tr(\Phi_x U_{x,\mu} \Phi_{x+\mu} U^\dagger_{x,\mu})}. \tag{6.19}$$

Using the above parameterizations the solution to Eq. (6.19) proceeds as follows:

$$\prod_{x,\mu} \frac{1}{16\pi^2} \int_0^\phi e^{2 \sum_x \sum_{x,\mu} R_x R_{x+\mu} Tr(\sigma_3 U_{x,\mu} \sigma_3 U^\dagger_{x,\mu})} \sin\theta \, d\theta d\varphi d\psi \tag{6.20}$$

$$= -\frac{1}{2} \prod_{x,\mu} \frac{1}{4 R_x R_{x,\mu}} e^{4 R_x R_{x,\mu} \cos\theta_{x,\mu}} \Big|_0^\pi \tag{6.21}$$

$$= \prod_{x,\mu} \sum_x \sum_{x,\mu} \frac{\sinh 4 R_x R_{x+\mu}}{4 R_x R_{x+\mu}}, \tag{6.22}$$

where the cosine in Eq. (6.20) is obtained from $Tr(\sigma_3 U \sigma_3 U^\dagger) = 2(|\alpha|^2 - |\beta|^2) = 2\cos\theta$. The complete partition function can therefore be written as,

$$\begin{aligned} Z &= \int \prod_x R_x^2 dR_x e^{-2 \sum_x TrV(R_x)} [\prod_{x,\mu} \frac{\sinh(4 R_x R_{x,\mu})}{4 R_x R_{x+\mu}}] \\ &= \int \prod_x \prod_{x,\mu} dR_x exp\{\sum_x [\ln R_x^2 - 2 TrV(R_x) + \sum_{x,\mu} \ln\{\frac{\sinh(4 R_x R_{x+\mu})}{4 R_x R_{x+\mu}}\}]\}. \end{aligned} \tag{6.23}$$

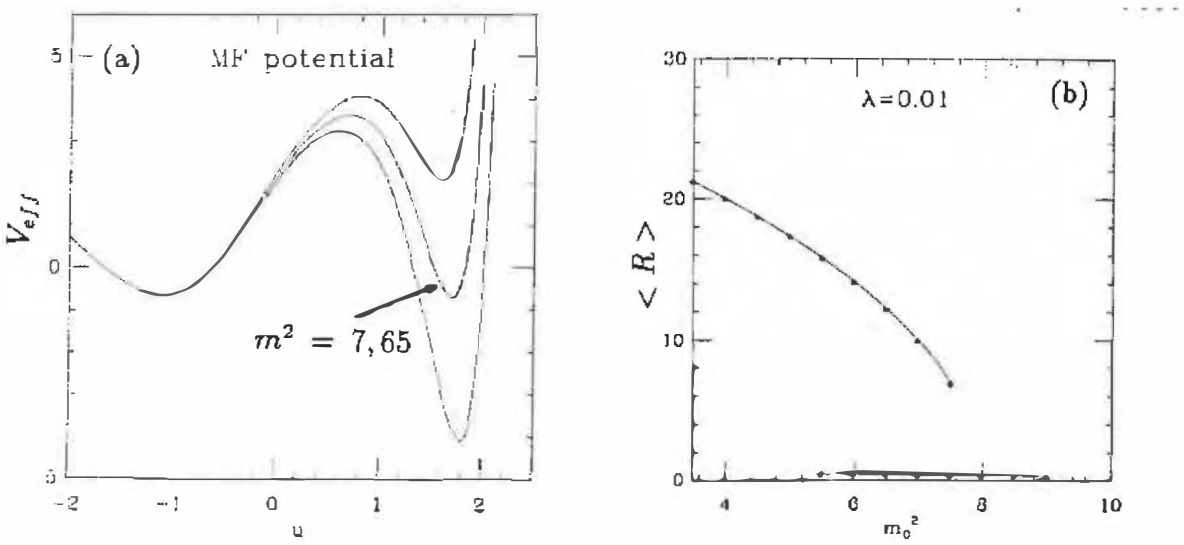

Figure 6.1: (a) The mean field approximation at $\lambda = 0.01$ (b) Thermal cycle for $< R >$ where the solid line gives the mean field approximation and $*$ gives the Monte Carlo results [36].

Choosing the scalar potential as $V(R_x) = \frac{m^2}{2}R_x^2 + \frac{\lambda}{4}R_x^4$, the phase diagram can be studied in the (λ, m^2)-plane. Also a simple mean field approximation can be carried out by setting $\bar{R} = e^{\mu}$. The results of the mean field approximation as shown in Fig. 6.1(a), shows for $\lambda = 0.01$ a degenerate state at $m^2 = 7,65$. Fig. 6.1(b) shows a thermal cycle in the $< R >$ for varing m^2. The phase transition of first order obtained here is conclusive of the results obtained by the mean field approximation. Fig 6.2(a) shows that at a critical point $(2.57, 4.515)$, obtained by the mean field approximation and confirmed by Monte Carlo simulations, the confined and unconfined phases are inseperable. The continuum limit $\lambda \rightarrow 0$ however does not exist in this model. This was also observered by Gross [37]. This model has also been extended to incorporate the gauge fields in the Monte Carlo simulations rather than to integrate them out [2]. This enables the average adjoint plaquette to be measured. Aoki *et. al.* [2] have shown that the value for the average plaquette at the weak coupling limit does not agree with the value obtained from QCD. Fig. 6.2(b) shows the adjoint plaquette at

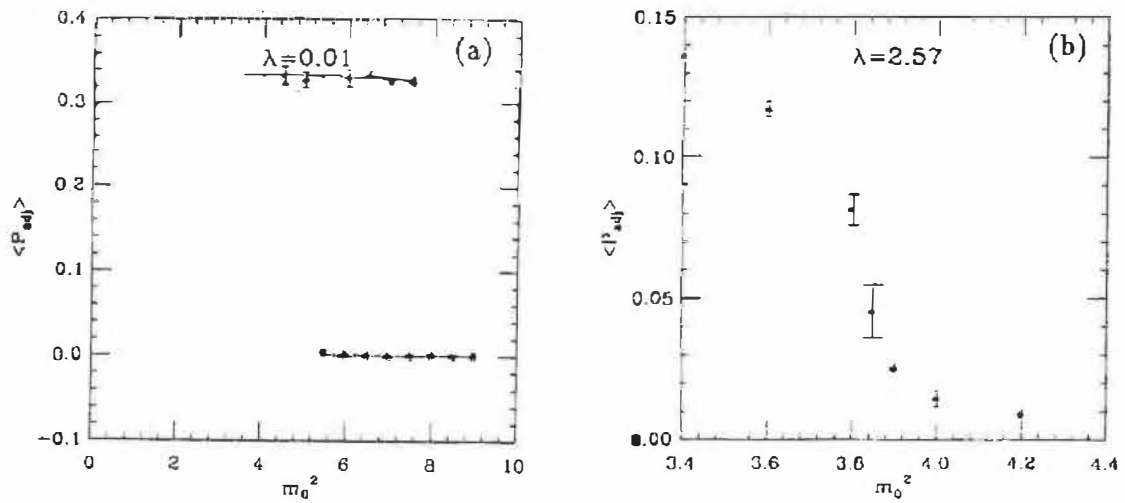

Figure 6.2: (a) Phase diagram showing the end point of the phase transitions in the (λ, m^2)-plane [36], (b) Monte Carlo results for the average adjoint plaquette at the critical value of $\lambda = 2.57$ [2].

the critical value of $\lambda = 2,57$. It can be seen that the value of the plaquette is rather small, even for small values of m^2 it is only ≈ 0.14 With these results Aoki *et. al.* have come to the conclusion that this model does not look anything like the usual $SU(2)$ gauge theory.

Chapter 7

The Mixed Fundamental-Adjoint Model

In the previous chapter the Kazakov-Migdal model which presented an interesting approach for inducing QCD was introduced. There are ample foundations for doubting whether this theory does indeed lead to QCD in the continuum limit. These doubts are at least partially attributed to the additional local Z_N symmetry that the induced model aquires. Several attempts at breaking this symmetry has been made. Migdal [64] was the first to consider adding new degrees of freedom for eliminating the local Z_N symmetry. He proposed considering a mixed model where besides the gauge fields and the adjoint scalars, there are also fermions in the fundamental representation of the group. Despite the usual difficulities associated with handling fermions on the lattice, there is a serious drawback to this model. Cline and Pahen [10] have pointed out that this model requires too many fermion flavours in order for it to remain solvable at the large N limit. In this chapter, a new approach to induced QCD is proposed [43]. It involves a modification of the original K-M model by adding to it scalar fields in the fundamental representation of the gauge group. These scalar fields are coupled to the gauge fields by the usual Higgs link term which breaks the unwanted local Z_N

symmetry.

7.1 The Mixed Fundamental-Adjoint Model of Induced QCD

The action for the mixed fundamental-adjoint model is defined in terms of the adjoint(A) scalars, Φ_x and the fundamental(F) scalars, Ψ_x:

$$S(\Phi,\Psi,U)=\sum_x\sum_{x,\mu}S_A(\Phi_x,U_{x,\mu})+\sum_x\sum_{x,\mu}S_F(\Psi_x,U_{x,\mu})+\sum_x S_{A-F}(\Phi_x,\Psi_x), \quad (7.1)$$

where S_A is the K-M model action given by,

$$S_A = N\,Tr\{V(\Phi_x)-\Phi_x U_{x,\mu}\Phi_{x+\mu}U^\dagger_{x,\mu}\} \quad (7.2)$$

and the other terms (new terms) are given by

$$S_F = N\,Tr\{V(\Psi_x)-\Psi_x U_{x,\mu}\Psi_{x+\mu}\}, \quad (7.3)$$

$$S_{A-F} = \gamma N\,Tr(\Phi_x\Phi_x\Psi_x\Psi^\dagger_x), \quad (7.4)$$

where γ is the bare fundamental-adjoint interference constant. This model is invariant under the local gauge transformations,

$$U_{x,\mu}\rightarrow\Omega_x U_{x,\mu}\Omega^\dagger_{x+\mu}, \quad \Phi_x\rightarrow\Omega_x\Phi_x, \quad \Psi_x\rightarrow\Omega_x\Psi_x\Omega^\dagger_x, \quad (7.5)$$

where $\Omega_x\Omega^\dagger_x=1$.

An attractive feature of this model is that it can be treated in a similar fashion as the K-M model. That is, one can employ the mechanism of inducing a theory out of the gauge background fields by partially integrating over the scalar degrees of freedom. The incorporation of the fundamental scalars with their corresponding link terms into the action explicitly breaks the Z_N symmetry of the K-M action. A consequence of this is that the Wilson loop will obtain nonzero expectation values,

thus producing finite values for the string tension. It is therefore expected that the gauge bosons in the induced theory will not be permanently confined. An extensive study of this model would be quite a formidable task in view of the large number of parameters involved. Even for the simple choice of the quadratic scalar potentials,

$$V(\Phi_x) = NTr\{\frac{1}{2}m_A^2(\Phi_x\Phi_x) + \frac{1}{4}\lambda_A(\Phi_x\Phi_x)^2\} \tag{7.6}$$

$$V(\Psi_x) = NTr\{\frac{1}{2}m_F^2(\Psi_x^\dagger\Psi_x) + \frac{1}{4}\lambda_F(\Psi_x^\dagger\Psi_x)^2\}, \tag{7.7}$$

there are five parameters compared with only two in the original K-M model. The fifth parameter is the strength of the fundamental-adjoint interference term.

7.2 Study of the $SU(2)$ Mixed Fundamental-Adjoint Model

For computational simplicity, the study of this model is restricted to the lattice fields belonging to the gauge group $SU(2)$. This does not affect the main features of the mechanism by which the effective gauge theory is induced.

The scalar fields Ψ_x in the fundamental representation of $SU(2)$ are given by the 'polar' cordinates $\Psi_x = R_x^F\psi_x$. The ψ_x are elements of $SU(2)$ and are parameterized as,

$$\psi_x = a_0 I + i\boldsymbol{a}\cdot\boldsymbol{\sigma}, \tag{7.8}$$

where $\boldsymbol{\sigma} = (\sigma_0, \sigma_i)$ and σ_i are the three Pauli matrices. The a_μ satisfy $a_0 + \boldsymbol{a}^2 = I$ for I the unitary matrix of the group. The adjoint scalars are given by $\Phi_x = R_x^A\phi_x$ where the ϕ_x are elements of $SU(2)/Z_N$ and are parameterized as,

$$\phi_x = \boldsymbol{v}\cdot\boldsymbol{\sigma}, \tag{7.9}$$

for $\boldsymbol{v}^2 = I$.

The simulations for this model were performed on a 4×8^3 hypercubic Euclidean lattice with periodic boundary conditions. All updatings of the degrees of freedom were done by employing the Metropolis algorithm. The observable of prime interest in the Monte Carlo simulations was the average plaquette,

$$< \Box >=< \frac{1}{2} Tr U_{\Box} > . \tag{7.10}$$

In a phase where this observable has a nonzero value the larger Wilson loops will also be nonzero and the string tension can have a finite value. Other observables that were measured were the average size of the adjoint scalars $< R^A >$ and the average size of the fundamental scalars $< R^F >$. Simulations were performed such that four of the five parameters m_A^2, m_F^2, λ_A, λ_F and γ were kept constant while thermal cycles were performed on the remaining parameter. Thermal cycles in m_A^2 were performed for several values of λ_F while the bare adjoint mass and the self interaction strength were kept fixed at m_A^2 and $\lambda_A = 1$ respectively. The bare fundamental-adjoint interference was kept fixed at $\gamma = 1$. The average plaquette as well as the average size of the fundamental and the adjoint scalars were monitored and their response to the thermal cycles for $\lambda_F = 1$ is shown in Fig. 7.1(a)-(c). It can be seen that there is a clear signal for a phase transition in the behaviour of all the observables. The average plaquette, which is also the elementary Wilson loop, changes from zero to nonzero values. This can be interpreted as local confinement. Further simulations from ordered and disordered starts at the critical value of m_F^2, show that this phase transition is of first order.

It should be noted, though, that the symmetry breaking term $-Tr(\Psi_x^\dagger U_{x,\mu} \Psi_{x+\mu})$ in Eq. (7.3) is of second order in R_F and thus will vanish for large values of the bare fundamental mass when the fundamental scalars decouple from the model. When this happens, the local Z_N symmetry is restored and the average Wilson loop vanishes in accordance with Elitzurs's theorem. This is clearly seen in Figs. 7.1(a)-(c) and 7.2.

The mechanism of inducing QCD or any similar theory requires the existence of

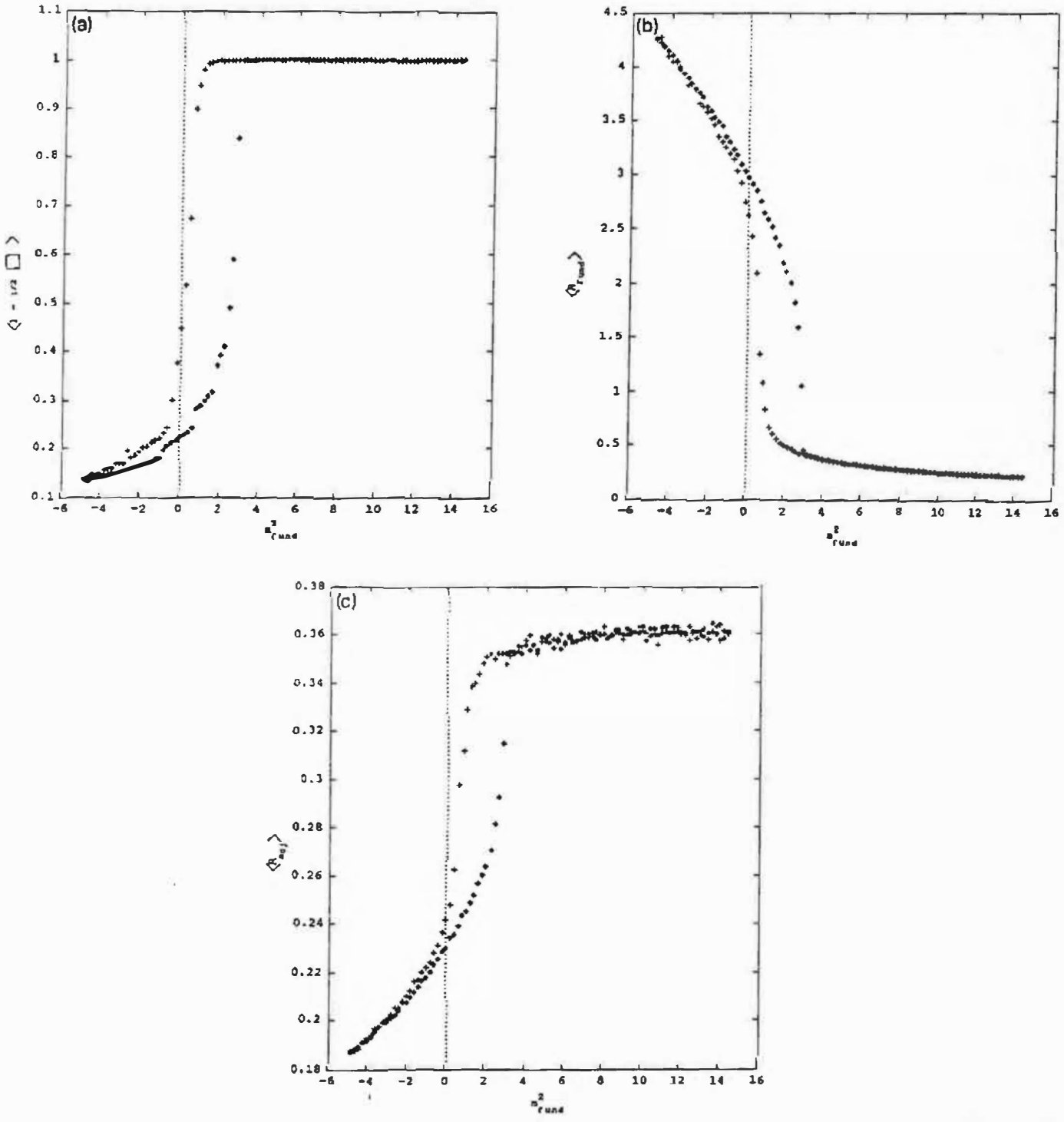

Figure 7.1: Thermal cycles in m_F^2 for $\lambda_F = 0.5$. The plots show the behaviour of (a) $< 1 - \frac{1}{2}\Box >$, (b) $< R_F >$ and (c) $< R_A >$. The values of the other parameters are $\lambda_A = 1$, $m_A^2 = 5$ and $\gamma = 1$

at least one critical point of the underlying theory. To prove the existence of such a point in this model, the line of first order phase transitions in the (m_F^2, λ_F)-plane was followed for the same fixed values of the other parameters. The results of the thermal cycles in m_F^2 for several values of λ_F are summarized in Fig. 7.2. The disappearance of the hystersis for $\lambda \geq 3$ points to an end point of the line of first order phase transitions and this end point is itself a second order phase transition point at which the correlation length of the model becomes infinite. This critical point is not a unique point for this model and there are indeed infinitely many similar critical points which form the boundary of the (hyper) surfaces of first order phase transitions in the space of the parameters of the model.

The results of these Monte Carlo simulations indicate that this proposed mixed model of induced QCD possesses a rich phase structure. The behaviour of the average plaquette shows that together with the phase of local confinement of the gauge fields there exists also a phase where the string tension has a finite value. These two phases are seperated by a surface of first order (local) confinement-deconfinement phase transitions. The existence of a boundary to the surface of phase transitions proves that this model possesses infinitely many critical points. The fact that this boundary is not at infinity means that the local confinement and the local deconfinement phases are connected in the sense of the complementary principle [28].

An unappealing feature of this proposed model is that it possesses a large number of parameters which makes an exhaustive study of its ground state time consuming. It is possible however to modify this model in a way such that its main features are preserved while reducing the number of parameters. One way to achieve this is to consider the limits in which one of the scalar fields has its radial modes frozen while the other is kept active. Such a study of this modified induced model is now presented.

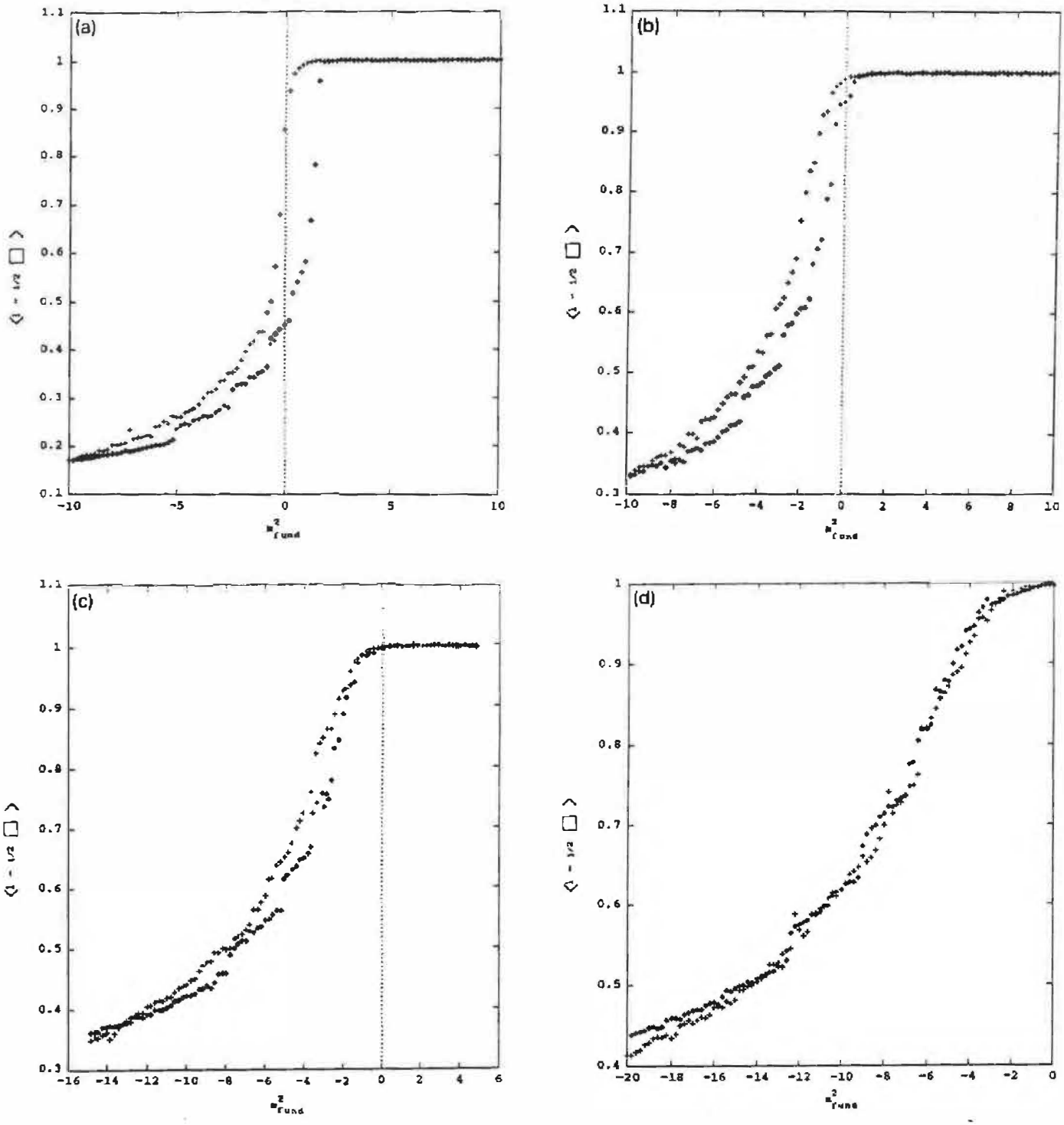

Figure 7.2: Thermal cycles in m_F^2. The plots show the behaviour of $< 1 - \frac{1}{2}\Box >$ for different values of λ_F; (a) $\lambda_F = 1.0$, (b) $\lambda_F = 2.0$, (c) $\lambda_F = 3.0$ and (c) $\lambda = 0.5$. The other parameters have the same values as in Fig. 7.1

7.3 The Role of the Choice of Integration Measure for the Radial Modes

In order to have self interaction the compact fundamental scalar fields must have a radial degree of freedom (otherwise the potential term in the action will be a constant). In induced models one needs to integrate over not only the gauge part but also over the radial part of the scalar fields. Another appealing feature of the mixed fundamenta-adjoint model is that it allows the treatment of Abelian groups while the original K-M model trivializes in the Abelian case. In what will follow, we shall outline the results of our study of a family of Abelian mixed fundamental-adjoint models. This study is primarily concerned with the extent to which the different choices of the radial measure of integration affects the phase structure of these models. Both Monte Carlo simulations and the mean field approximation method were used to study the discrete groups Z_N for various values of N as well as the continuous group $U(1)$.

In the Abelian theory, the adjoint scalars decouple from the gauge fields and the mixed fundamental-adjoint model reduces to a purely fundamental lattice gauge theory with action,

$$S(\Psi_x, U_{x,\mu}) = Tr \sum_x \{\frac{m^2}{2}(\Psi_x^\dagger \Psi_x) + \frac{\lambda}{4}(\Psi_x^\dagger \Psi_x)^2 - \sum_{x,\mu}(\Psi_x^\dagger U_{x,\mu} \Psi_{x+\mu})\}. \qquad (7.11)$$

Eq. (7.11) is analagous to models studied in §5.2.2.1 except that it does not possess the extra bilocal interaction term $2\Psi_x^\dagger \Psi_x$. So it can be seen that by adding the fundamental link to the induced model, one is able to treat the Abelian theories which is an important part of the Standard Model, namely, the QED. Now recalling the 'polar' parameterization, $\Psi_x = R_x \psi_x$, the partition function for this model is written as,

$$Z = \int \prod_x d_\mu(R_x) d\psi_x \prod_{x,\mu} dU_{x,\mu} e^{-S} \qquad (7.12)$$

where $d\psi_x$ and $dU_{x,\mu}$ are the Haar measures for the Abelian group under consideration

and $d_\mu(R_x)$ the radial measure of integration. It is the choice of the latter measure which is of prime importance in this study.

The requirement for gauge invariance of the theory imposes very stringent restrictions on the choice of the integration measure over the gauge fields as well as the phases of the scalar fields. In fact, there is practically no freedom in the choice of these measures of integration and they must be the corresponding invariant and normalized (Haar) measures for the gauge group in question. On the other hand, gauge invariance does not restrict the choice of the integration measure over the radial modes of the scalar fields present in the model because the gauge transformationa leave the radial modes unaffected. In realistic models like the $SU(2)$ and $SU(3)$ gauge-Higgs systems, the choice of the radial integration measure, $\prod_x d_\mu(R_x)$, is usually determined from the requirement that the lattice action would lead to the corresponding continuum action in the naive continuum limit (that is, in the leading order in the lattice spacing a). This leads to the following integration measures over the radial modes:

$$d_\mu(R_x) = R_x dR_x \tag{7.13}$$

for the $U(1)$ gauge-Higgs model and

$$d_\mu(R_x) = R_x^3 dR_x \tag{7.14}$$

for the $SU(2)$ gauge-Higgs model. Now in the case of an induced gauge model, where the role of the scalars are, technically, restricted to producing some effective theory from a gauge background field, there are no restrictions on the choice of radial measure of integration for the scalars no matter what representation of the gauge group the latter are in. The scalars in an induced model can be interpreted as corresponding to some internal structure of the gauge bosons. Since the dynamical features of such a structure are unknown, there could, in principle, be no other restrictions on the choice of the radial measure of integration. One may argue that this choice is not very important since at approaching the continuum limit, the correlation length will

increase to infinity and, because of universality, models with different chioces of the radial measure will lead to the same effective theory. On the other hand, everything could be changed should it turn out that the choice of the radial measure of integration could lead to significant changes in the phase structure of the lattice model. In order to investigate the role of the choice of the radial measure of integration, numerical simulations were performed of the Abelian induced model.

Here are some possible choices of radial measures of integration:

1. $d_\mu(R_x) \sim \delta(R_x - \overline{R})dR_x$. This corresponds to the radial mode being frozen and is the situation where the radial mode is restricted to an average value around $R_x = \overline{R}$,

2. $d_\mu(R_x) \sim dR_x$. In this case the radial fluctuations are taken to be uniform,

3. $d_\mu(R_x) \sim exp\{-\frac{(R_x-\overline{R})^2}{2\sigma^2}\}dR_x$. Here the radial modes fluctuate with normal distribution and when $\sigma \to 0$ the integration measure reduces to the case described in (1),

4. $d_\mu(R_x) \sim R_x^\alpha dR_x$ for $\alpha = 0, 1, \ldots, N$. This measure bears resemblance to the usual radial measure in polar corordinates: $\alpha = d - 1$ in a d-dimensional Euclidean space. For other values α this measure has no obvious analogue.

7.3.1 The Z_N Induced model.

Parameterizing the gauge and scalar fields in the usual way for Z_N,

$$U_{x,\mu} = e^{\frac{2\pi i}{N}\theta_{x,\mu}}, \qquad \Psi_x = R_x e^{\frac{2\pi i}{N}\psi_x} \tag{7.15}$$

for $\theta_{x,\mu}, \psi_x = 0, 1, \ldots, N-1$ the action can be written as,

$$S = Tr \sum_x \{\frac{m^2}{2}R_x^2 + \frac{\lambda}{4}R_x^4 - \sum_{x,\mu} R_x R_{x+\mu} \cos[\frac{2\pi}{N}(\psi_x - \psi_{x+\mu} - \theta_{x,x+\mu})]\} \tag{7.16}$$

with corresponding partition function

$$Z = \int \prod_x R_x^{\alpha} dR_x \frac{1}{N} \sum_{\psi_x} \prod_{x,\mu} \frac{1}{N} \sum_{\theta_{x,\mu}} e^{-S}. \tag{7.17}$$

An exhaustive study of this model for various orders of the group ($N = 2, 3, \ldots, 10$ and $N = 100$) has been done by employing different Monte Carlo techniques. Both the average plaquette and the average size of the scalar field were monitored for signals for phase transitions.

Thermal cycles were initially performed in order to locate the phase transitions of these models. Fig. 7.3 shows an example of the thermal cycles obtained (with the characteristic hysteresis loop), for the group Z_4 at $\lambda = 0.5$, for both the average scalar and the average plaquette. The phase transitions observed were of first order. This is shown in Fig. 7.4 for the different start simulations (of both the average scalar and average plaquette) for Z_4 at $\lambda = 0.5$ and $m^2 = 1$.

For a fixed value of λ it was observered that the dependence of the phase transition point m^2 on the order of the group ceases to exist. As shown in Fig. 7.5, for $\lambda = 0.5$, the dependence ceases at about $N = 7$. This agrees favourably with the observations made by Gerdt *et al*[]. It was also observered that for $\alpha = 0$ and for increasing λ, the phase transition point moves to smaller values of m^2 and at a critical value of λ, the hysteresis loop seems to close. Fig. 7.6 and Fig. 7.7 shows this effect for the case of the two extreme groups studied. For Z_2 the transition line seperating the confined and unconfined phases terminates at $\lambda = 10$ and for Z_{100} this occurs at $\lambda = 5$. By increasing α (therefore changing the radial measure of integration) for a fixed value of λ, it was noticed that the phase transition point moves to larger values of m^2. For large values of α the phase transition terminates. Fig. 7.8 shows this effect for the case of Z_{100} (which is practically equivalent to the induced $U(1)$ model) and $\lambda = 1$.

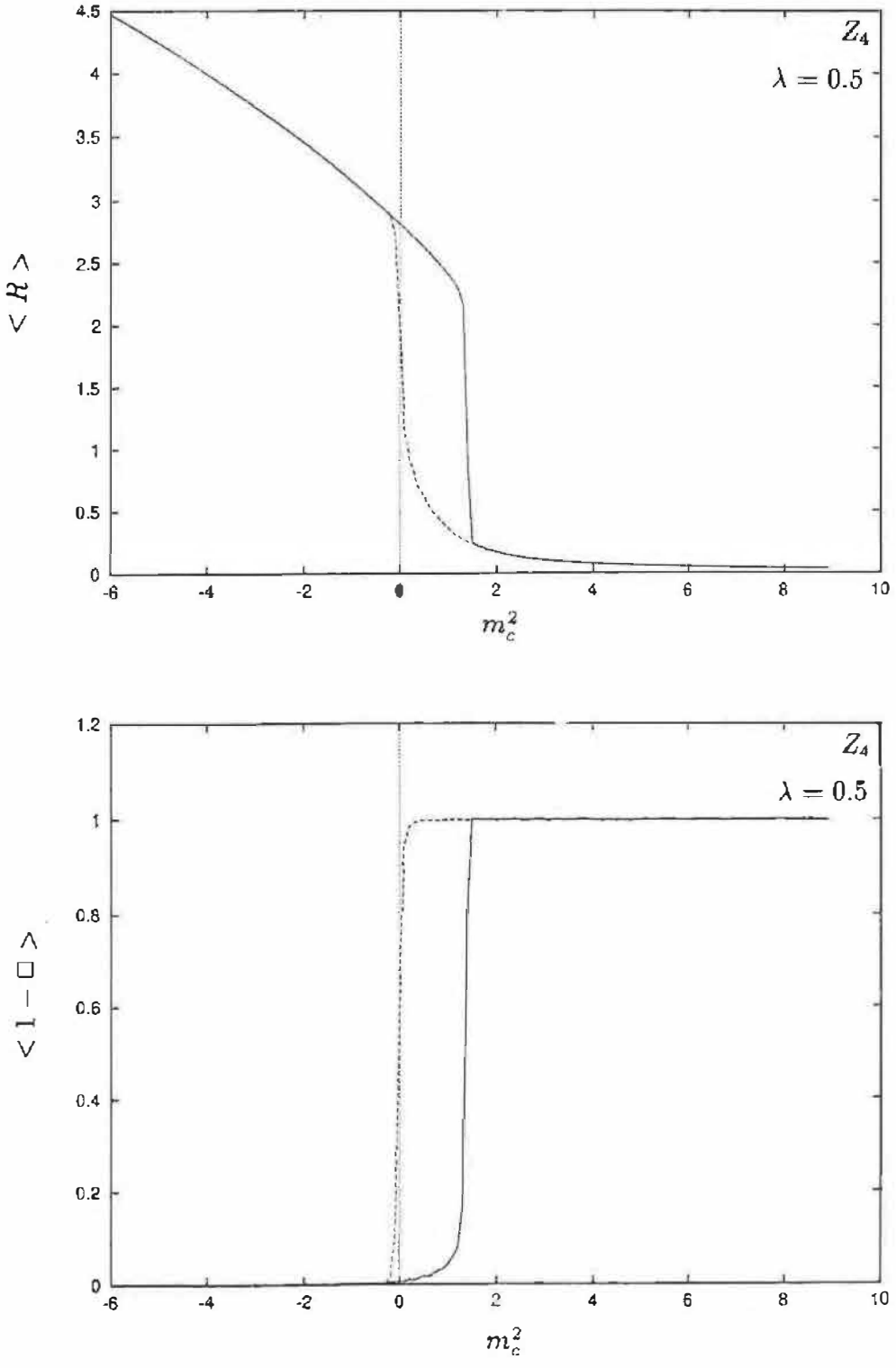

Figure 7.3: Thermal cycle for the average scalar and the average plaquette for the group Z_4 at $\lambda = 0.5$.

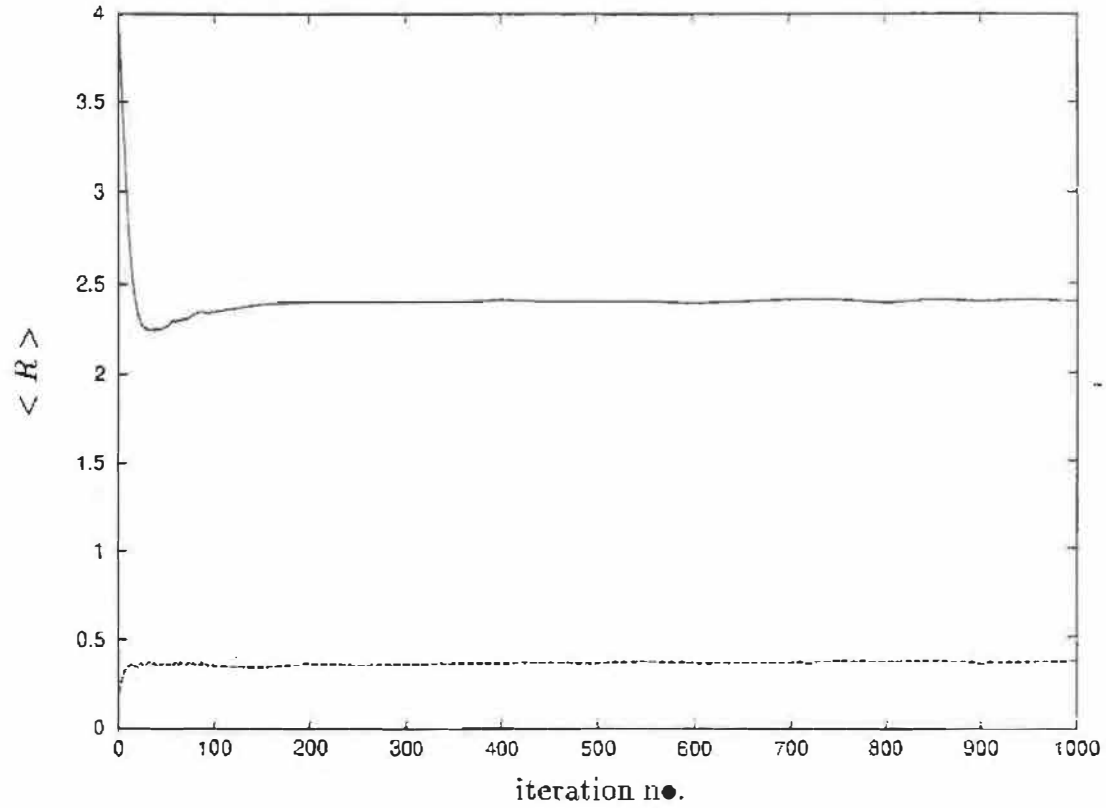

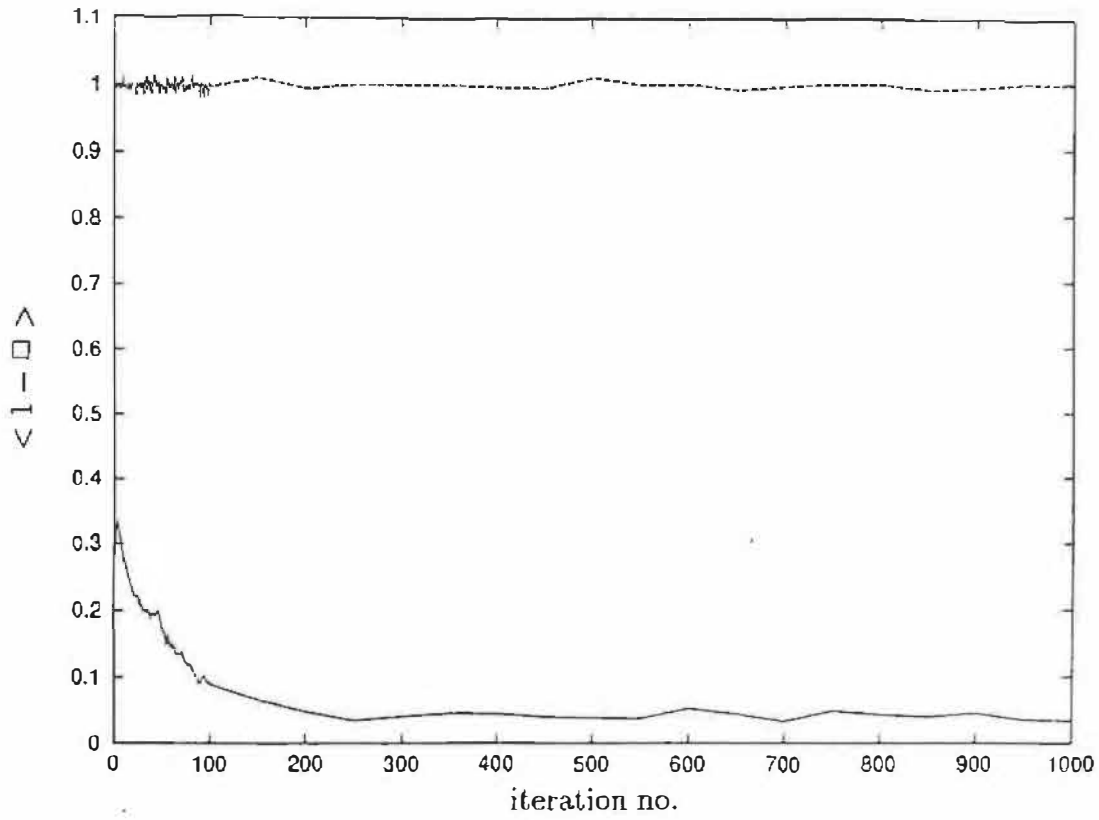

Figure 7.4: Different start simulation for Z_4 at $\lambda = 0.5$ and $m^2 = 1$.

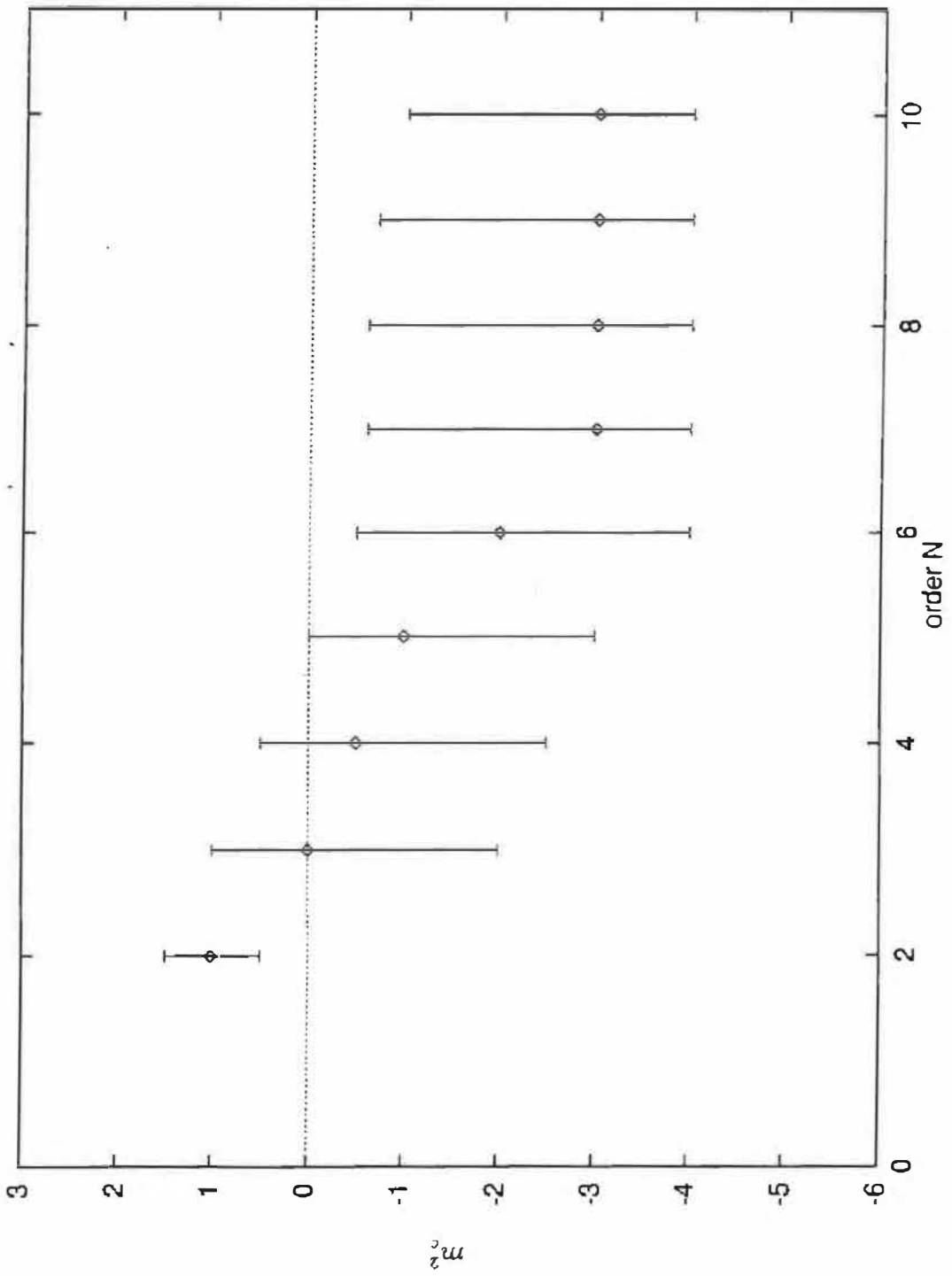

Figure 7.5: Plot of m_c^2 against various orders of the group Z_N for $\lambda = 1$.

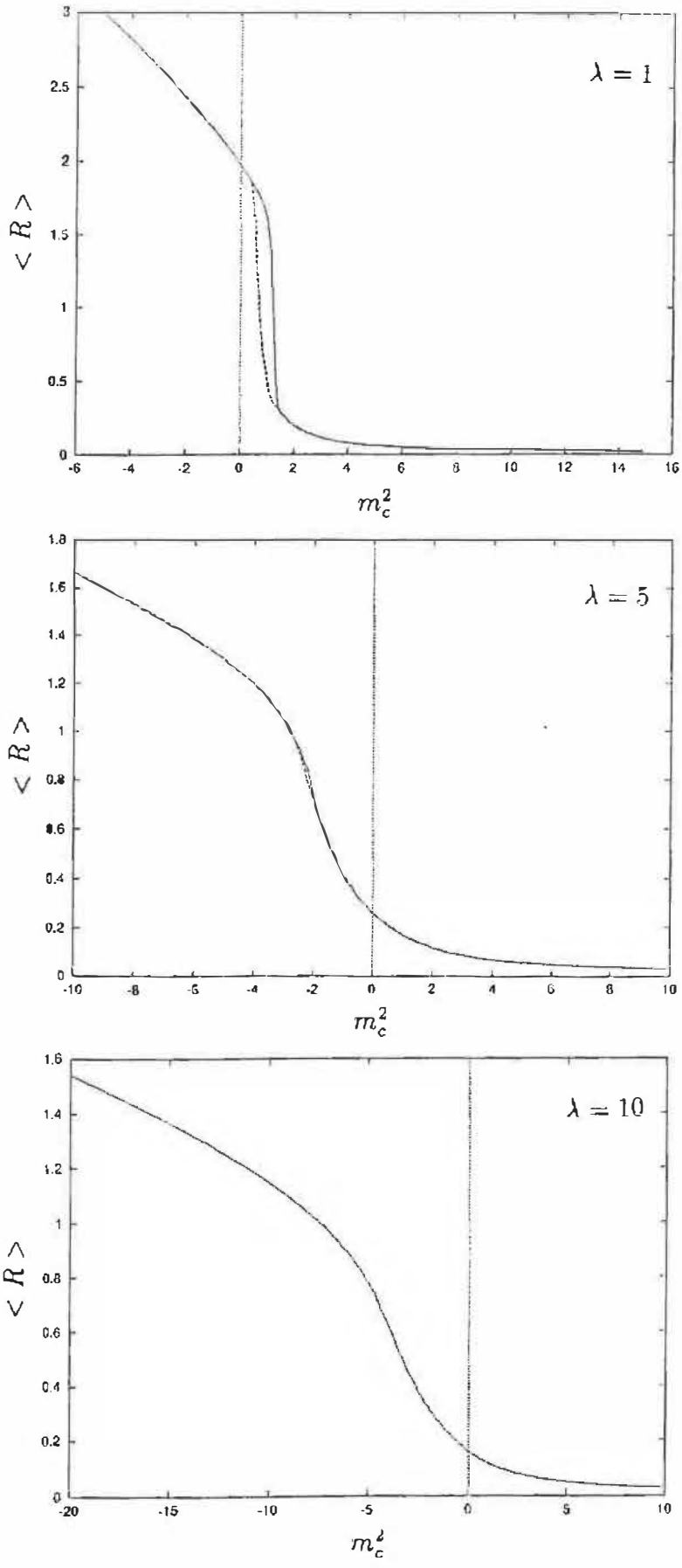

Figure 7.6: Thermal cycles for Z_2 for increasing values of λ at $\alpha = 0$.

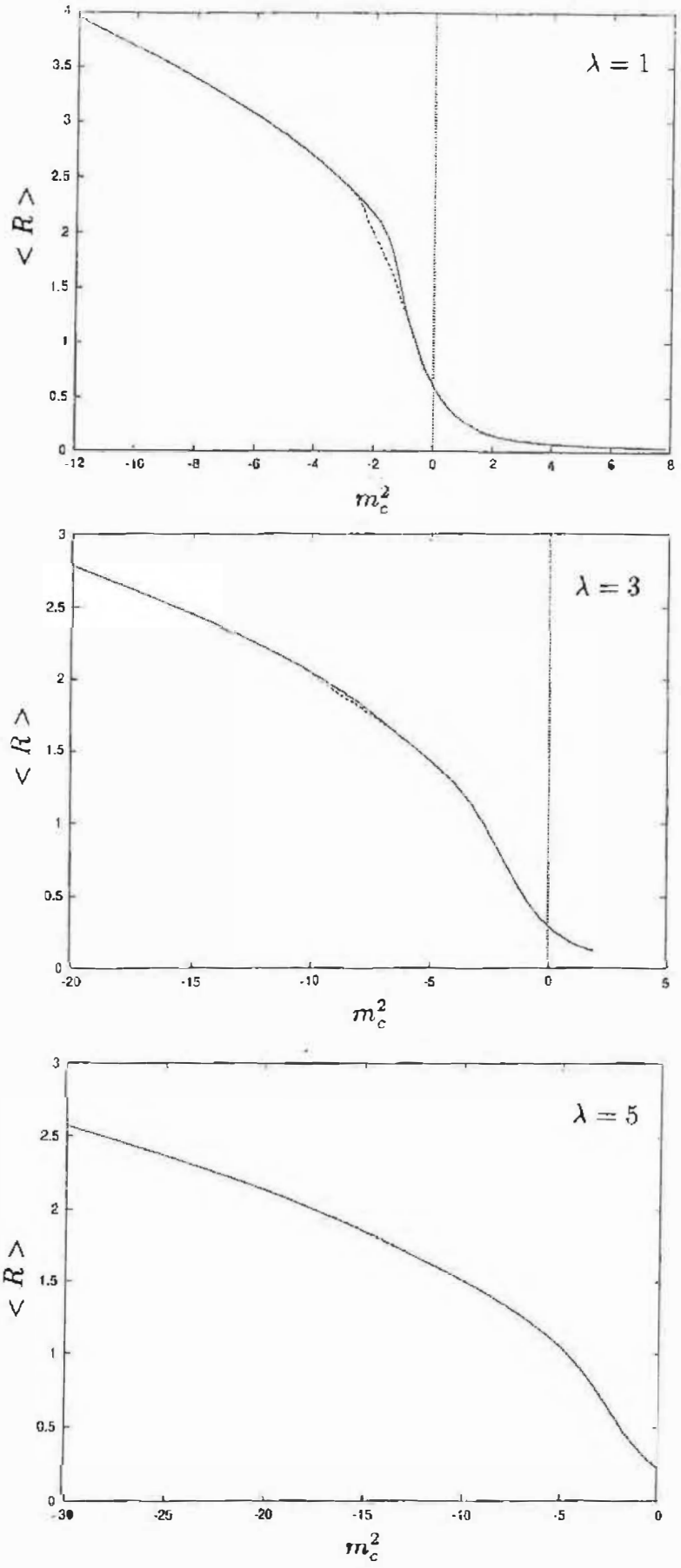

Figure 7.7: Thermal cycles for Z_{100} for increasing λ at $\alpha = 0$.

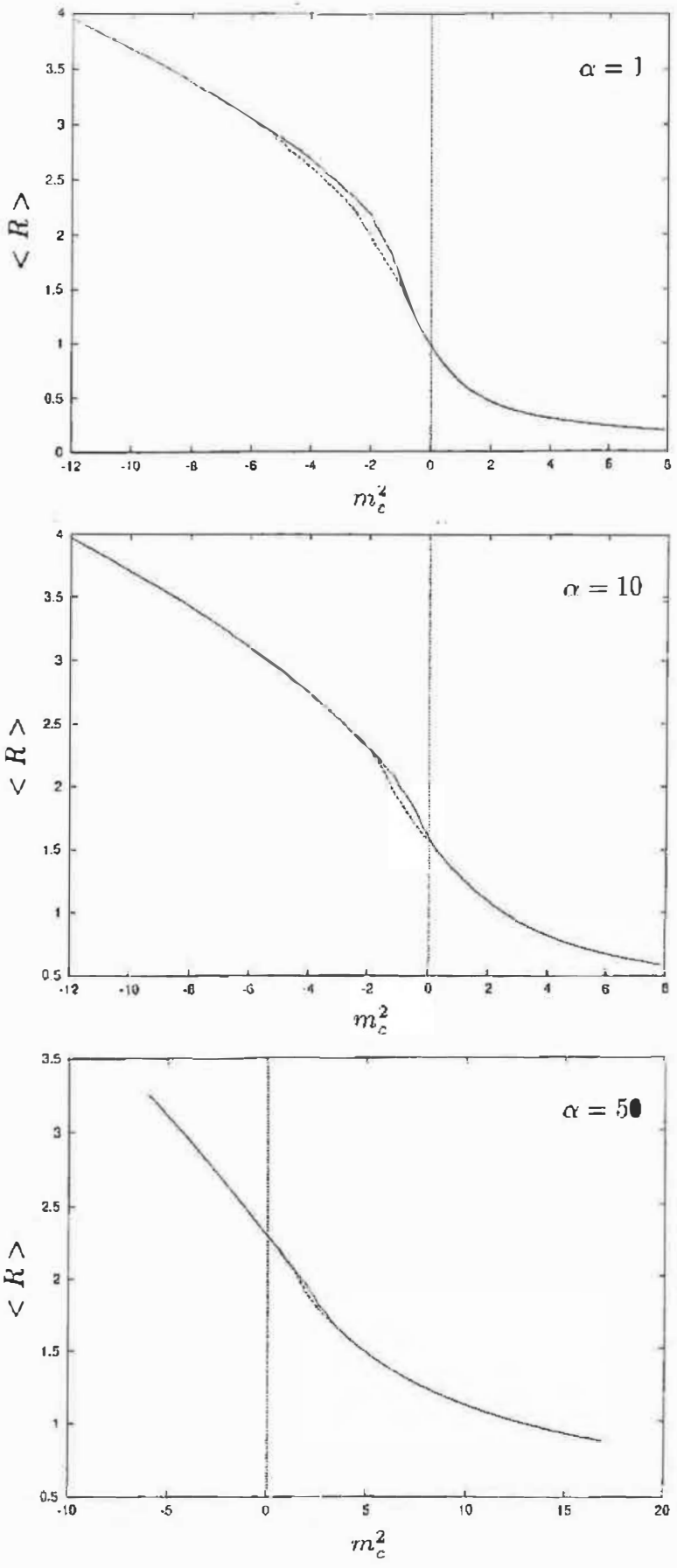

Figure 7.8: The evolution of the hysteresis loop for Z_{10} at $\lambda = 1$ for increasing values of α.

7.3.1.1 Mean Field Approximation

Following the technique described in §5.2.2, mean field approximations can be used to calculate the effective potential as a function of the mean radial mode for values around the m_c^2.

Consider the partition function in Eq.(7.17). This can be rewritten as,

$$Z = \int \sum_x dR_x \tilde{Z}(R_x), \tag{7.18}$$

where

$$\begin{aligned} \tilde{Z} &= e^{-\tilde{S}} \\ &= e^{-\frac{m^2}{2}R_x^2+\frac{\lambda}{4}R_x^4} R_x^\alpha \frac{1}{N}\sum_{j=0}^{N-1} e^{R_x R_{x+\mu}\cos\frac{2\pi}{N}j}. \end{aligned} \tag{7.19}$$

The new action which is a function of only the radial modes is therefore

$$\tilde{S} = \sum_{x,\mu}\{\frac{m^2}{2}R_x^2 + \frac{\lambda}{4}R_x^4 - \ln[\frac{1}{N}\sum_{j=0}^{N-1} e^{R_x R_{x+\mu}\cos\frac{2\pi}{N}j}] - \ln R_x^\alpha\}. \tag{7.20}$$

Following the Coleman-Weinberg procedure, the effective potential to first order is given by,

$$\begin{aligned} V_{eff}(\bar{R}) &= \frac{1}{N}\tilde{S}(R_x)_{R_x=\bar{R}} \\ &= \frac{m^2}{2}\bar{R}^2 + \frac{\lambda}{4}\bar{R}^4 - \ln[\frac{1}{N}\sum_{j=0}^{N-1} e^{\bar{R}^2\cos\frac{2\pi}{N}j}] - \ln\alpha\bar{R}. \end{aligned} \tag{7.21}$$

For the case of $N = 2$ it can be shown that Eq. (7.21) becomes

$$V_{eff} = \frac{m^2}{2}\bar{R}^2 + \frac{\lambda}{4}\bar{R}^4 - \ln\cosh(\bar{R}^2) - \alpha\ln\bar{R}. \tag{7.22}$$

From the plot (see Fig. 7.9(b)) of $V_{eff}(\bar{R})$ against the average scalar length, $\bar{R}$, for $\lambda = 0.1$ and varing values of m^2, it was found that the model has a double minima at $m_c^2 \approx 3.2$. This is clearly in aggreement with the Monte Carlo simulations in Fig.7.9(a) which shows that the point $m_c^2 \approx 3.2$ is well within the hysteresis loop.

Unfortunately the mean field approximation method only seems to give good results in agreement with the Monte Carlo simulations for the group Z_2. For values greater than $N = 2$ a marked exponential behaviour for V_{eff} was observered. In order to curtail this behaviour it is obvious that higher order correction terms need to be added to Eq.(7.21).

7.3.2 The $U(1)$-Symmetric Induced Model

For the $U(1)$ case, the fields are parameterized in the usual way:

$$U_{x,\mu} = e^{i\theta_{x,\mu}}, \qquad 0 < \theta_{x,\mu} < 2\pi, \tag{7.23}$$

and the scalar fields which transform in the fundamental representation of $U(1)$ is

$$\Phi_x = R_x e^{i\phi_x}, \qquad 0 < \phi_x < 2\pi. \tag{7.24}$$

The corresponding partition function is

$$Z = \int \prod_x R_x^\alpha \frac{d\phi_x}{2\pi} \prod_{x,\mu} \frac{d\theta_{x,\mu}}{2\pi} e^{-S} \tag{7.25}$$

where

$$S = NTr \sum_x \{\frac{m^2}{2} R_x^2 + \frac{\lambda}{4} R_x^4 - \sum_{x,\mu} R_x R_{x+\mu} \cos(\phi_{x+\mu} - \phi_x + \theta_{x,x+\mu})\}. \tag{7.26}$$

As seen in the case of Z_N above, for $\alpha = 0$ and for increasing λ, the phase transition point moves to the left and finally disappears at a critical value of λ. This is shown in Fig.7.10 where $\lambda_c \approx 5$. The critical value of λ for $U(1)$ is identically the critical value for Z_{100}-this once again confirms the fact that the Z_N theory approaches the $U(1)$ theory for large N. Fig.7.11 shows the effect on the phase structure by increasing α. It can be seen that for $\lambda = 0.5$, the characteristic hysteresis loop vanishes for $\alpha > 100$ and the confined and unconfined phases are no longer separated. It can therefore be seen that both the Z_N and the $U(1)$ models are affected in the same way by the

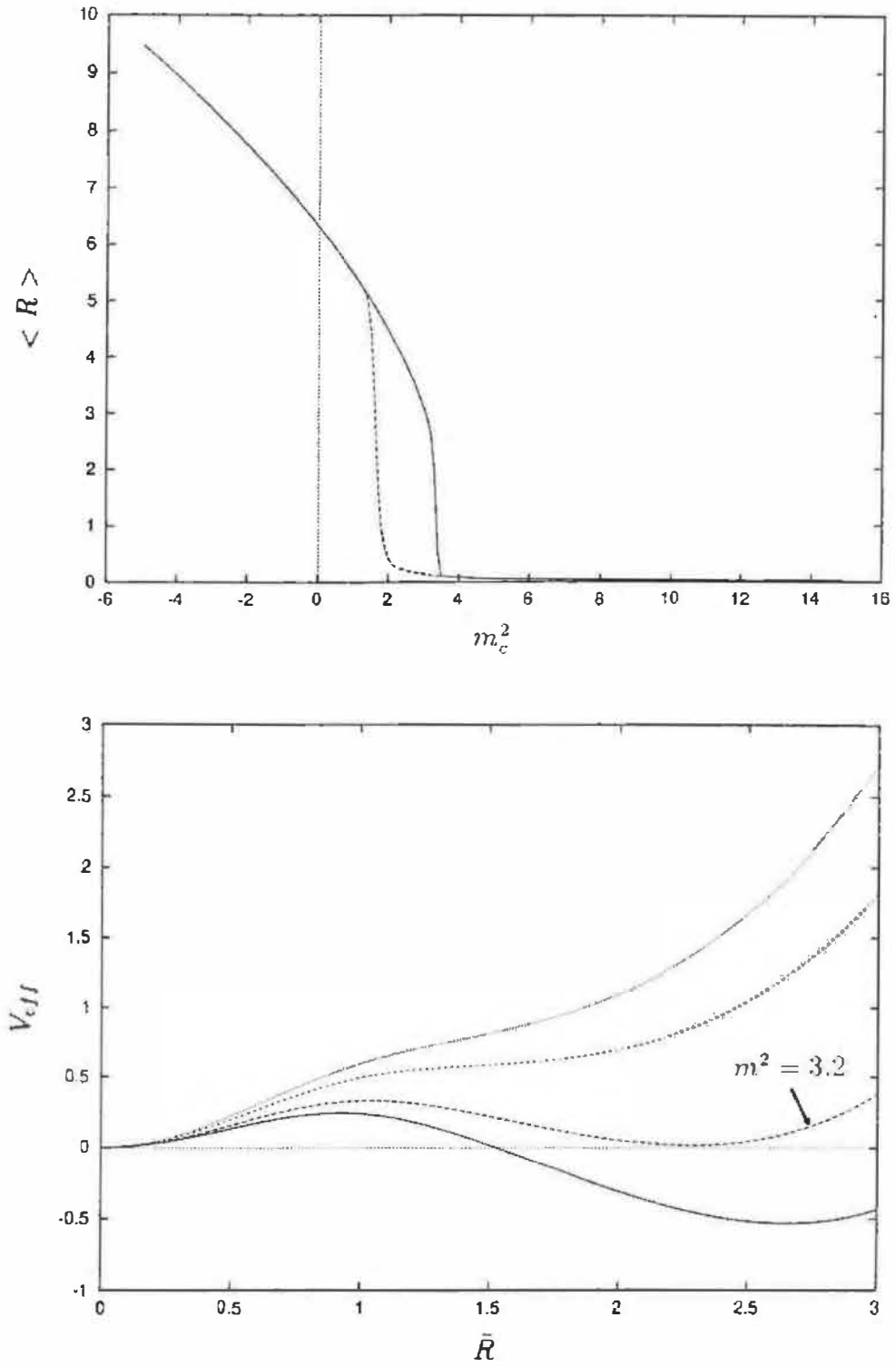

Figure 7.9: (a) Thermal cycle for Z_2 at $\lambda = 0.1$ showing phase transition point around $m_c \approx 3$. (b) Mean field approximation of Z_2 showing plot of V_{eff} against $\bar{R}$ near the phase transition point.

different choices of the radial measure. An interesting observation here is that by appropriatly tuning α and λ, any of these models can be made to exhibit analytical continuation between the confined and unconfined phases.

7.3.2.1 Mean Field Approximation

In the case of $U(1)$:

$$\begin{aligned} \tilde{Z} &= e^{-\tilde{S}} \\ &= [exp\{-(\frac{m^2}{2}R_x^2 + \frac{\lambda}{4}R_x^4)\}]R^\alpha I_0(R_x R_{x+\mu}) \end{aligned} \tag{7.27}$$

where I_0 is the modified Bessel function,

$$I_0 = \int_0^{2\pi} exp\{R_x R_{x+\mu}\cos(\theta_{x+\mu} - \theta_x - \theta_{x,\mu}\}\, d\theta_{x,\mu}. \tag{7.28}$$

The R_x dependent action is therefore given by,

$$\tilde{S} = \frac{m^2}{2}R_x^2 + \frac{\lambda}{4}R_x^4 - \ln I_0(R_x R_{x+\mu}) - \ln R_x^\alpha, \tag{7.29}$$

and by the Coleman-Weinberg procedure the effective potential to first order is

$$V_{eff}(\bar{R}) = \frac{m^2}{2}\bar{R}^2 + \frac{\lambda}{4}\bar{R}^4 - \ln I_0(\bar{R}^2) - \ln \bar{R}^\alpha. \tag{7.30}$$

Fig.7.12 shows the plot of V_{eff} against the mean scalar for values above and below the critical mass for $\lambda = 0.5$. The thermal cycle for this value of λ is shown in Fig.7.13(a) with the mean field approximation in the vicinity of m_c^2 shown in Fig.7.13(b). It can be seen that the mean field results which shows the phase transition point at $m_c^2 \approx 0.39$ is in very good aggreement with the results obtained by Monte Carlo simulations.

From these results one can draw the following conclusions:

1. The $U(1)$ induced model and even the simple Z_N induced model possesses a rich phase structure.

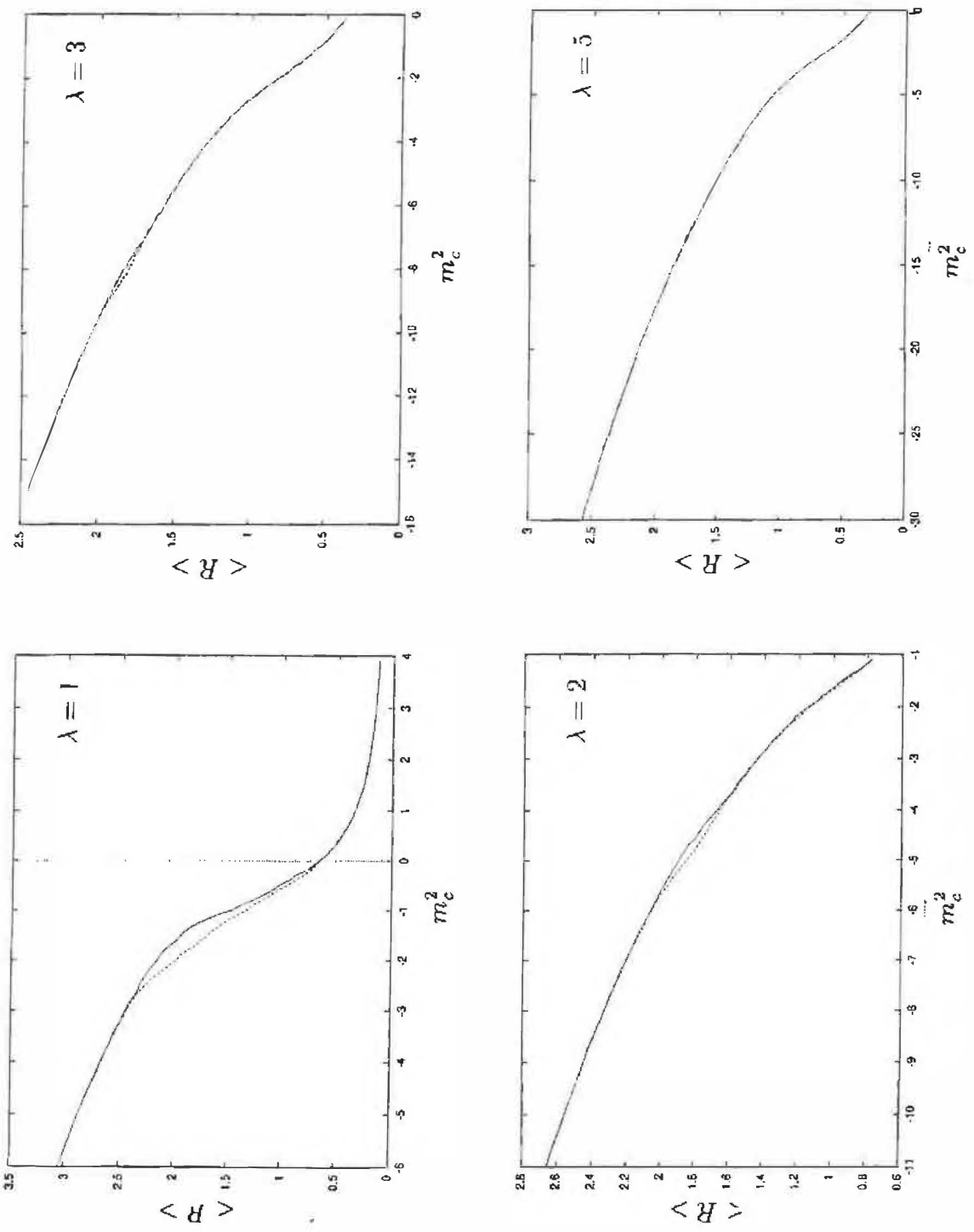

Figure 7.10: Thermal cycles in $U(1)$ for increasing values of λ. The hysteresis loop closes at $\lambda \approx 5$.

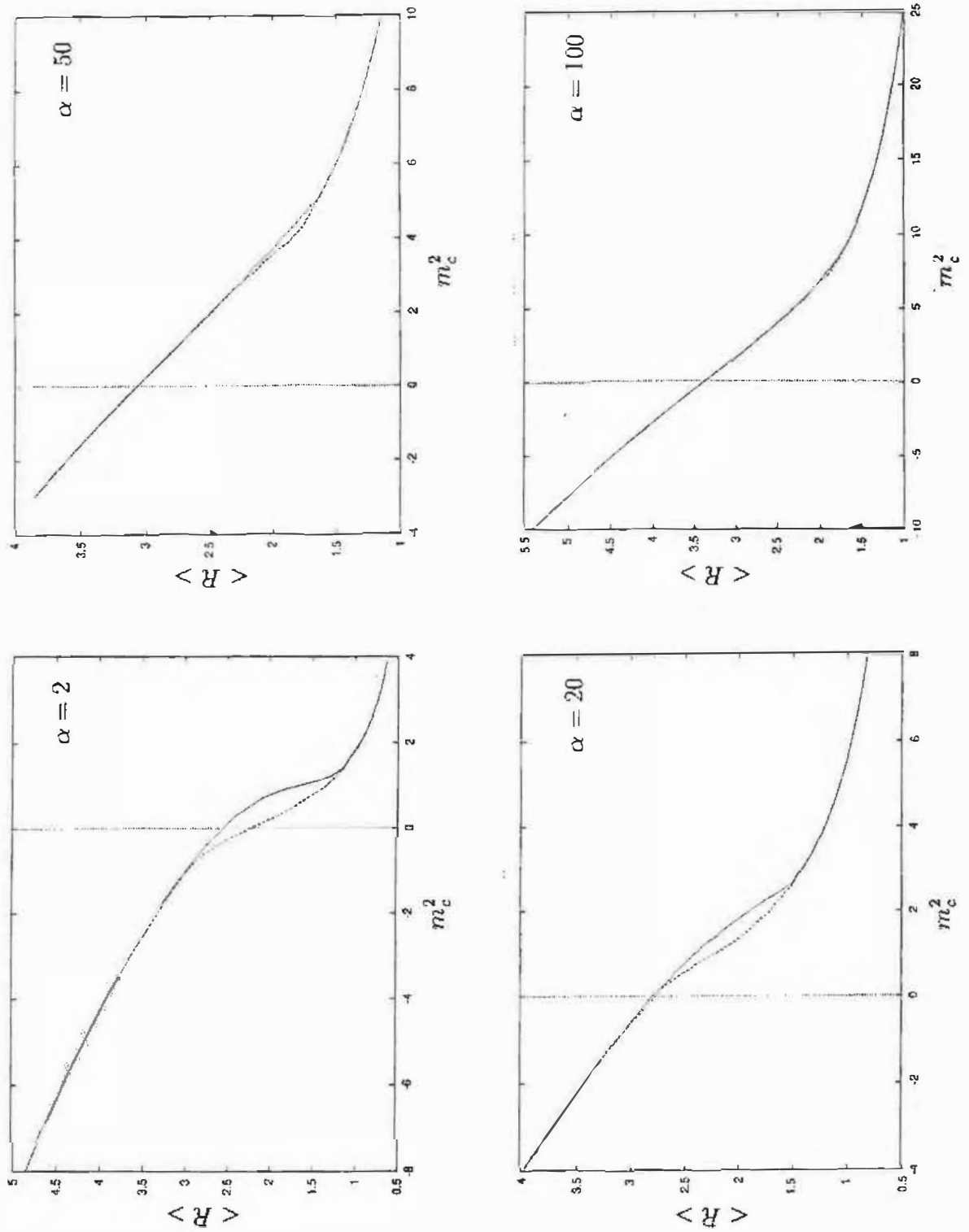

Figure 7.11: Thermal cycles in $U(1)$ for fixed λ and increasing α. The hysteresis loop closes at $\alpha \approx 100$.

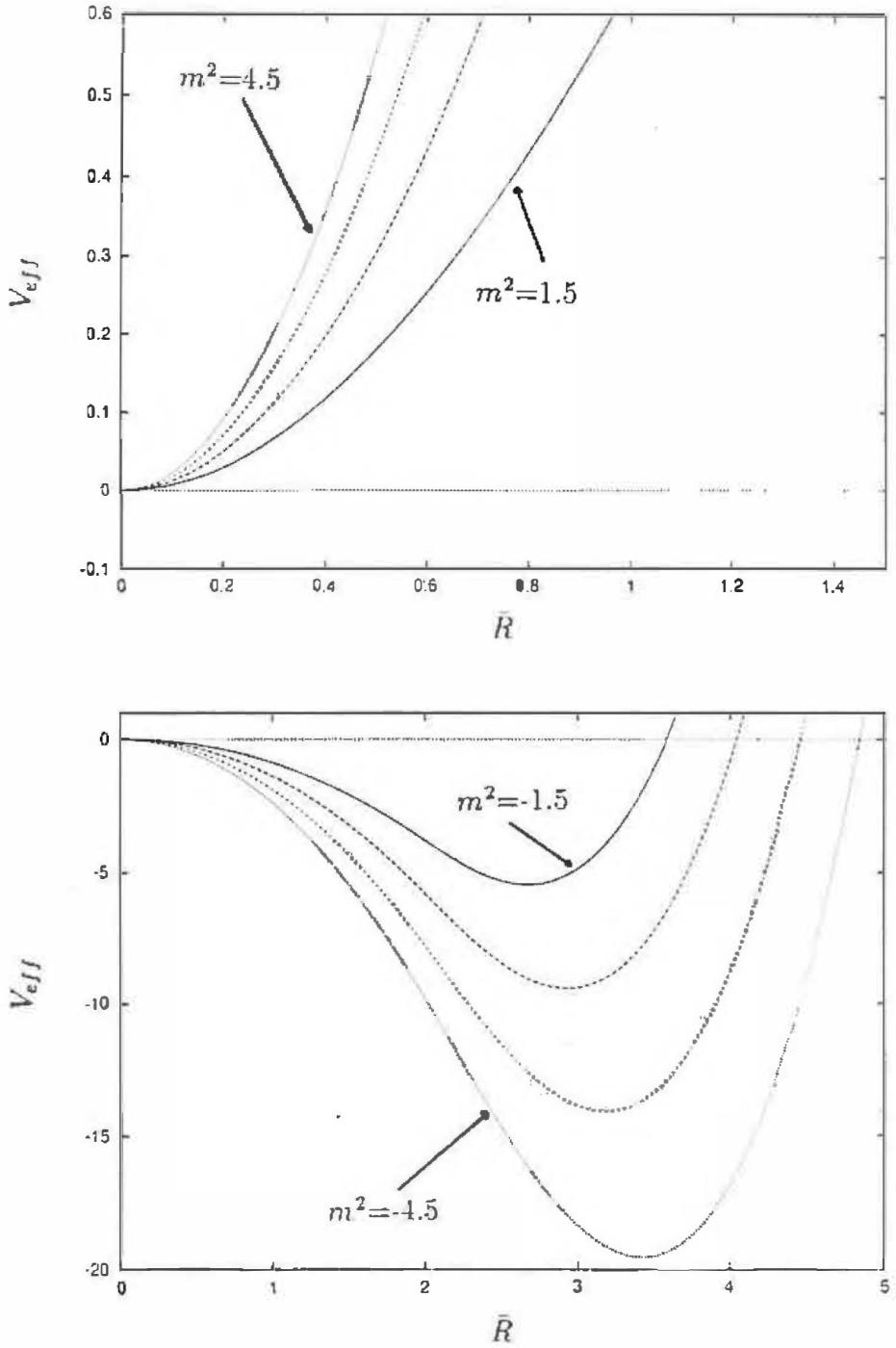

Figure 7.12: Mean field approximations for $U(1)$ at $\lambda = 0.5$: (a) below m_c^2 and (b) above m_c^2.

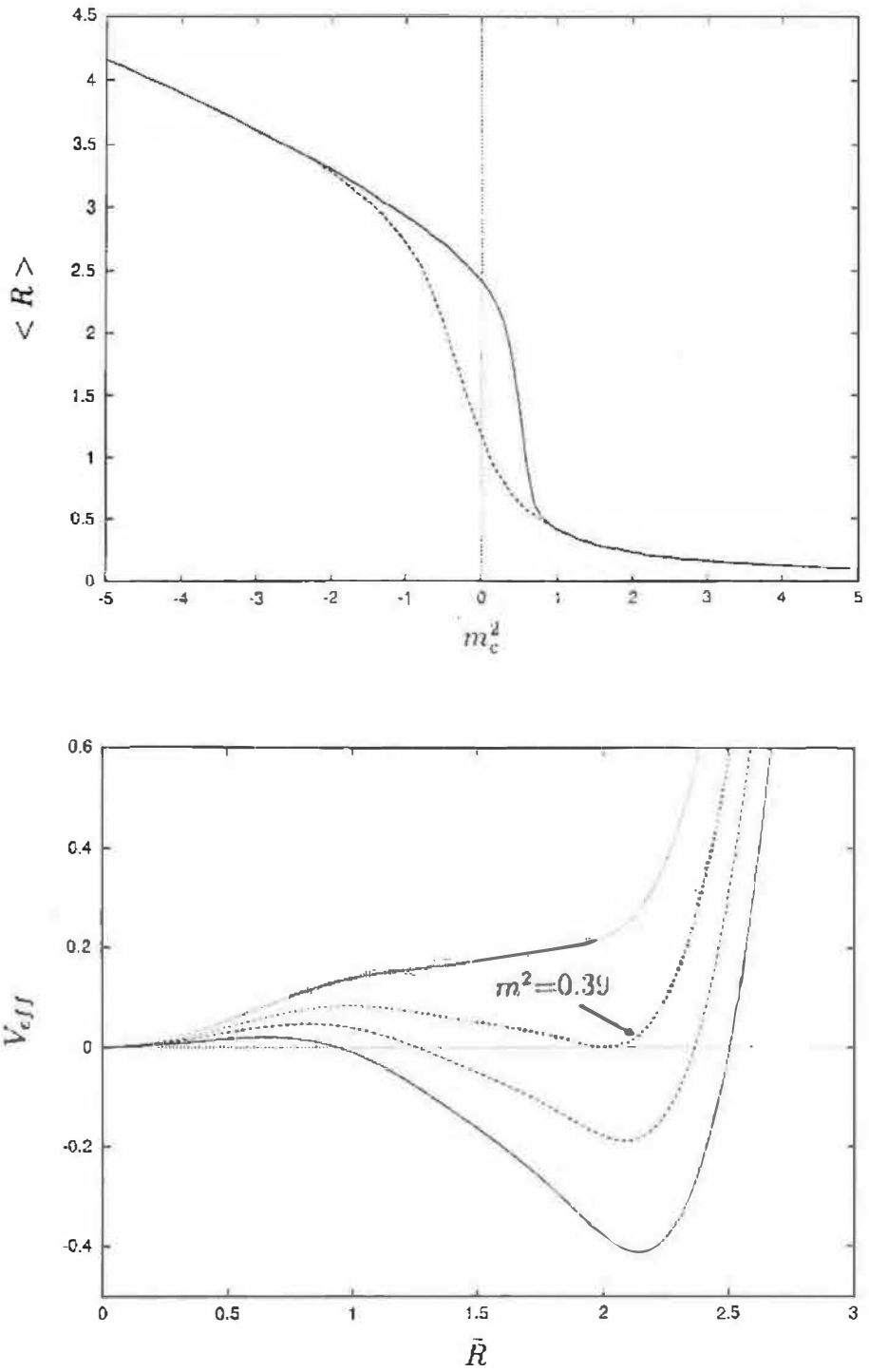

Figure 7.13: (a) Thermal cycle for $U(1)$ at $\lambda = 0.5$. (b) Mean field approximation showing critical point at m_c^2.

2. The phase transitions between local confinement ($< 1 - \Box >= 1$) and deconfinement ($< 1 - \Box >$) are of first order and the phase transition lines in the (λ, m^2) plane terminate at a critical point.

3. The phase transitions of the model are affected by the choice of radial integration measure. The parameter α from the radial integration measure, $d_\mu(R_x) = R_x^\alpha dR_x$, can be considered as yet another action-defining parameter of the model alongside λ and m^2. Moving along the α-axis, in the now three dimensional space, one encounters a critical (second order phase transition) point.

All these facts point to the significance of the choice of the radial integration measure in induced theories.

7.4 Summary and Conclusion

The induced lattice gauge models were inspired by the idea of Kazakov and Migdal, that selfinteracting scalars in the adjoint representation of $SU(N)$ could induce QCD of N-colours through their interaction with a background gauge field. It was hoped that this would lead to a soluble large-N limit of QCD but the subsequent research showed that the original Kazakov-Migdal model does not have the desired continuum limit. Nevertheless, the interest in the study of lattice systems of matter fields coupled to a gauge background has not died out. This research presented some results obtained by means of Monte Carlo simulations of Abelian induced models as well as some analytical results derived within the mean field approximation.

The models considered here differed from the Kazakov-Migdal model in the choice of the scalar fields which was taken in the fundamental representation of the gauge group. This allowed for the formulation and the study of the Abelian induced models which are inaccessible to the Kazakov-Migdal model. The simplicity of the Z_N symmetric

models and their limiting case - the $U(1)$ symmetric induced model, made it possible to also study the role of the choice of the integration measure over the radial modes of the scalar fields. It was found that the Abelian induced models, have a rich phase structure. They possess critical points at which the correlation length diverges and the positions of these critical points in the space of the model-defining (bare) parameters depend on the choice of integration measure over the radial modes of the scalars.

References

1. Alonzo, J.L., *et al*, Phys. Lett., **B296**, 154, 1992.
2. Aoki, S., Gocksch, A. and Shen, Y, Phys. Rev., **D47**, 1645, 1993.
3. Azcoiti, V.,Di Carlo, G.,Grillo, A., Phys. Lett., **B268**, 101, 1991.
4. Azcoiti, V.,Di Carlo, G.,Grillo, A., Phys. Lett., **B258**, 207, 1991.
5. Balian, R.,Drouffe, J.M.,Itzykson, C., Phys. Rev., **D10**, 3376, 1975; D11, 2098, 1975; D11, 2104, 1975.
6. Bhanot, G.,Creutz, M., Phys. Rev., **D21**, 2892, 1980.
7. Bhanot, G.,Creutz, M., Phys. Rev., **D22**, 3370, 1980.
8. Browler, K.C. *et al*, Phys. Lett., **B104**, 491, 1981.
9. Callaway, D.J.E. and Carson, L.J., Phys. Rev., **D25**, 531,1982.
10. Cline, J.H. and Paban, S., Phys. Lett., **B316**, 158, 1993.
11. Coleman, S. and Weinberg, E., Phys. Rev., **D7**, 1888, 1973.
12. Creutz, M., *Quarks, Gluons and Lattices*, Cambridge University Press, 1985.
13. Creutz, M. and Freedman, B., Annals of Physics, N.Y., **132**, 427, 1981.
14. Creutz, M.,Jacobs, L. and Rebbi, C., Phys. Reports, **95**, 201, 1983.
15. Creutz, M.,Jacobs, L. and Rebbi, C., Phys. Rev. Lett., **21**, 1390, 1979.
16. Creutz, M.,Jacobs, L. and Rebbi, C., Phys. Rev., **D20**, 1915, 1979.
17. Creutz, M., Phys. Rev., **D21**, 199, 1980.
18. Creutz, M., Phys. Rev., **D21**, 2308, 1980.
19. Creutz, M., Phys. Rev. Lett., **43**, 553, 1979.
20. Creutz, M., Phys. Rev., **D21**, 1006, 1980.
21. Dashen, R. and Gross, D.J., Phys. Rev., **D23**, 2340, 1981.
22. DeGrand, T.A. and Toussaint, D., Phys. Rev., **D22**, 2478, 1980.
23. Drouffe, J.M. and Zuber, J.B., Phys. Reports, **102**, 1, 1983.

24. Drouffe, J.M.,Itzykson, C., Phys. Reports, **38**, 133, 1978.

25. Elitzur, S., Phys. Rev., **D12**, 3978, 1975.

26. Elitzur, S.,Pearson, R.,Shigemitsa, J., Phys. Rev., **D19**, 3698, 1979.

27. Fernandez, L.A. *et al*, Phys. Lett., **B267**. 100, 1991.

28. Fradkin, E. and Shenker, S.H., Phys. Rev., **D19**, 3682, 1979.

29. Gerdt, V.P., Ilchev, A.S. and Mitrjushkin, V.K., Jinr Preprint, E2-83-758, 1983.

30. Gerdt, V.P., Ilchev. A.S. and Mitrjushkin, V.K., Jinr Preprint, E2-85-59, 1985.

31. Gerdt, V.P., Ilchev. A.S. and Mitrjushkin, V.K., Soviet J. Nucl. Phys., 43, 468, 1986.

32. Gerdt, V.P. *et al.* Z. Phys., **C29**, 368, 1985.

33. Gerdt, V.P. *et al*, Jinr Preprint, E2-85-103, 1985.

34. Gerdt, V.P. *et al*, Jinr Preprint, E2-85-104, 1985.

35. Gerdt, V.P. *et al*, Nucl. Phys., **B265**, 145, 1986.

36. Gocksch, A. and Shen, Y., Phys. Rev. Lett., **69**, 2747, 1992.

37. Gross, D., Phys. Lett., **B293**, 181, 1992.

38. Guth, A.H., Phys. Rev., **D21**, 2291, 1980.

39. Hammersley, J.M. and Handscomb, D.C., *Monte Carlo Methods*, Chapman and Hill, London, 1964.

40. Harish-Chandra, Amer. J. Math, **79**, 87, 1957.

41. Hasenfrantz, A. and Hasenfrantz, P., Phys. Lett., **93B**, 165, 1980.

42. Hasenfrantz, P. and Montvay, I., Phys. Rev. Lett., **50**, 309, 1983.

43. Ilchev, A.S., Moodely, M. and Welter, A., Phys. Lett., **B332**, 387, 1994

44. Itzykson, C. and Zuber, T.B., J. Math Phys., **21**, 411, 1980.

45. Jansen, J. *et al*, Nucl. Phys., **B258**, 207, 1991,

46. Jongeward G.A. *et al*, Phys. Rev., **D21**, 3360, 1980.

47. Kazakov, V.A. and Migdal, A.A., Nucl. Phys., **B397**, 214, 1993.

48. Kogan, I.I., Semenoff, V.W. and Weiss, N., UBC preprint, UBCTP-92-002, 1992.

49. Korthals-Altes, C.P., *Lectures on Lattice Gauge Theory*, Spain, 1981

50. Korthals-Altes, C.P., Nucl. Phys., **B142**, 315, 1978.

51. Koutsoumbas, G., Phys. Lett., **B140**, 379, 1984.

52. Kuhnelt, H.,Lang, C.B.,Vones, G., Nucl. Phys., **B138**, 171, 1984.

53. Kuti, J., *et al* Phys. Lett., **B98**, 199, 1981.

54. Lang, C.B., Rebbi. C. Virasoro. M., Phys. Lett., **B104**, 294, 1981.

55. Lautrup, B., Cern preprint Ref.TH.3521-CERN, 1983.

56. Lautrup, B. and Nauenberg, M., Phys. Rev. Lett., **45**, 1755, 1980.

57. Lautrup, B. and Nauenberg, M., Phys. Lett., **B95**, 63, 1980.

58. Mack, G., and Petkova, V.B., Ann. Phys., **123**, 442, 1979.

59. McLerran, L.D. *et al*, Phys. Rev., **D24**, 450, 1981.

60. Mehta, M.L., Comm. Math. Phys., **79**, 327, 1981.

61. Metropolis, N *et al*, Chem. Phys., **21**, 1087, 1953.

62. Migdal, A.A., Mod. Phys. Lett., **A8**, 139, 1993.

63. Migdal, A.A., Mod. Phys. Lett., **A8**, 153, 1993.

64. Migdal, A.A., Mod. Phys. Lett., **A8**, 245, 1993.

65. Munehisa, Y., Phys. Rev., **D30**, 1310, 1984.

66. Munehisa, T.,Munehisa, Y., Phys. Lett., **B116**, 353, 1982.

67. Munehisa, T.,Munehisa, Y., Nucl. Phys., **B215**, 508, 1983.

68. Munster, C. and Weisz, P., Phys. Lett., **B96**, 119, 1980.

69. Negele, J.W., *Stochastic evaluations of path integrals in nuclear many-particle systems*, Preceedings of La Rabida International summer school, 1985.

70. Osterwalder, K.,Seiler, E., Annals of Physics, **110**, 440, 1978.

71. Ranft, J., Kripfganz, J., Ranft. G., Phys. Rev., **D28**, 360, 1983.

72. Rothe, H.J., *Lattice Gauge Theories: An Introduction*, World Scientific, Singapore, 1992.

73. Simon, B., *The $P(\phi)_2$ Euclidean (Quantum) Field Theory*, Princeton University Press, Princeton, NJ, 1974.

74. Wegner, F.J., J. Math. Phys., **12**, 2259, 1971.

75. Whightman, A.S., Phys. Rev., **101**, 860, 1956.

76. Wilson, K., Phys. Rev., **D10**, 2445, 1974.

77. Yang, C.N. and Mills, R., Phys. Rev., **96**, 191, 1954.